FOURIER TRANSFORM INFRARED SPECTROMETRIC DETECTION OF CHROMATOGRAPHIC EFFLUENTS -- INSTRUMENTAL AND METHODOLOGICAL IMPROVEMENTS USING A FLOW CELL INTERFACE

by

Charles Clifford Johnson

Dissertation submitted to the Faculty of the Virginia Polytechnic Institute and State University in partial fulfillment of the requirements for the degree of

Doctor of Philosophy

in

Chemistry

APPROVED:

Larry T. Taylor, Chairman

Harry C. Dorn

Harold M. Bell

Jack D. Graybeal

John G. Dillard

Harold M. McNair

April 1985
Blacksburg, Virginia

FOURIER TRANSFORM INFRARED SPECTROMETRIC DETECTION OF CHROMATOGRAPHIC EFFLUENTS -- INSTRUMENTAL AND METHODOLOGICAL IMPROVEMENTS USING A FLOW CELL INTERFACE

by

Charles Clifford Johnson
Dr. L. T. Taylor, Department of Chemistry

(ABSTRACT)

The Fourier Transform Infrared spectrometer (FTIR) has been used increasingly as a detector for various forms of chromatography. Clearly the most established marriage has been that of the Gas Chromatograph (GC) with the FTIR. GC-FTIR has been developed well beyond other forms. The main objective of this thesis, however, is to extend the FTIR as a detector to previously untested forms of chromatography using a flow cell interface. These forms of chromatography include High Performance Liquid Chromatography (HPLC), both normal-phase and reversed-phase, and packed-column Supercritical Fluid Chromatography (SFC).

Normal phase HPLC-FTIR was demonstrated on not only analytical scale columns, but semi-preparative and microbore scales as well. Significant advantages, particularly with respect to the low solvent consumption, were found in the microbore HPLC-FTIR experiment. This led to the development of a chromatographically improved flow cell, the Zero Dead Volume (ZDV) HPLC-FTIR interface. The ZDV cell shows superior chromatographic characteristics and has unique spectrometric characteristics because of its unusual cross-section. Detection limits as low as 40 ng were observed.

Extension to reversed-phase HPLC-FTIR required incorporation of the

Flow Injection Analysis (FIA) technique of low-dispersion flowing extraction. The compounds separated by HPLC are extracted into an infrared-transparent solvent, and the extracted compounds are detected by similar means to normal-phase HPLC-FTIR.

Investigation of SFC-FTIR incorporated a high-pressure, gold-lined lightpipe flow cell to detect the components separated by the supercritical CO_2/packed-column chromatograph. Several unusual spectrometric characteristics were noted. Detection limits as low as 50 ng were observed with SFC-FTIR.

To Mom, Dad and
Their encouragement and prodding
moulded my personal philosophy:

"Success emerges from a long string of failures;
persistence is the key."

ACKNOWLEDGEMENTS

A large number of people influenced my ability to perform the research described in the following pages. Specifically, I'd like to thank Dr. James F. Wolfe who convinced me to attend Virginia Tech. His friendly disposition and fatherly words of encouragement always came at the right time. His ability to make any situation a little brighter will always be appreciated. The sincerity and presence of Dr. John G. Mason is greatly appreciated, and will always be remembered. Dr. Larry T. Taylor's ability to interest a born tinkerer in Analytical Chemistry certainly helped make this work successful.

Numerous people with whom I've worked over the past years have helped immeasurably. I'd like to thank the following individuals from my resarch group: for his continuous skepticism, for this enthusiastic comic relief, for the laughs through thick and thin (FBI and Birmingham?), for educating me on patience, and for friendship and stability near the end. I'd like to thank and for being such good pupils and carrying on the SFC-FTIR research with such enthusiasm. Special thanks to to probably my second closest friend; I already miss the arguments and the mutual dreams.

Other people who have had various degrees of influence on this work include and I'd like to thank Dr. H. C. Dorn, Dr. J. G. Dillard, Dr. J. D. Graybeal, Dr. H. M. Bell, and Dr. H. M. McNair for serving as my Advisory Committee. Thanks also go to for his help on microbore HPLC. The office staff of the Department of Chemistry at Virginia

Tech always made the day a little brighter in spite of the rain. My most sincere gratitude goes to who showed a great deal of patience in typing this dissertaion.

Several individuals from industry deserve a note of thanks; of IBM Instruments, Inc., for his help on microbore modifications, and of Spectra-Tech, Inc., for the loan of an infrared beam condenser, of the Procter and Gamble Company for conceptual inspiration on the RP-HPLC-FTIR work, and of Nicolet Analytical Instruments, Inc., for their help on the SFC-FTIR work, and of Hewlett-Packard for his enthusiastic discussions on SFC. The research described on the following pages was supported in part by grants and fellowships from the Department of Energy, Mobil Oil Corporation, and the Commonwealth of Virginia.

TABLE OF CONTENTS

LIST OF FIGURES

LIST OF TABLES

CHAPTER 1

INTRODUCTION AND HISTORICAL

One of the essential elements in any chromatographic system is the detector. Some characteristics that an "ideal" chromatographic detector (1-3) should possess include high sensitivity with low noise, universal response to analytes, and wide linear range with simple calibration. With great improvements in separation efficiency and column miniaturization being realized, a chromatographic detector should also have a fast response time and low dead volume. From the point-of-view of conclusive analyte identification, either the detector should be non-destructive so that post-chromatographic analysis on the collected analytes can be performed, or the detector should give qualitative, specific information on the detected component directly. And finally from a practical point-of-view, the "ideal" detector should be rugged, reliable, simple, safe to operate, and inexpensive. Although none has fulfilled the requirements of the "ideal" detector, several detection systems are in use that possess many of the "ideal" attributes.

In Gas Chromatography (GC), most commonly employed are the Flame Ionization Detector (FID) and Thermal Conductivity Detectors (TCD). These GC detectors provide nearly universal response with good linearity and good sensitivity. However, they do not provide a great deal of qualitative information. Furthermore, the FID is a destructive detector, and consequently the analyte cannot be further characterized by other analytical techniques without the incorporation of a splitter. In addition, practical limitations on GC column selectivity and

efficiency may result in ambiguous identification of unknowns if the analyst bases his conclusions solely on the retention time information that can be obtained from these detectors (4).

A similar situation is observed in detectors for High Performance Liquid Chromatography (HPLC). Most widely used is the Ultraviolet absorbance (UV) detector. Although this detector is very sensitive at 254 nm, absorbance at this wavelength is somewhat selective for aromatic compounds. A universal detector for HPLC, the differential Refractive Index (RI) detector, suffers from its relatively low sensitivity and inability to operate with solvent gradients. Variable wavelength UV detectors are an improvement over the conventional 254 nm absorbance detector, but perhaps the most impressive gain in this area has been observed for the UV/Visible Photo-Diode Array (PDA) detector (5). The effectiveness of this detector still depends on the analyte having significant UV absorbance between 190 and 600 nm (typically). Unambiguous identification of the analytes from the resulting UV/Visible spectra is difficult at best.

The most recent addition to the list of separation techniques is Supercritical Fluid Chromatography (SFC). Detectors in SFC are normally either modified GC or HPLC detectors. Typically, UV absorbance or flame ionization detection is used in SFC (6,7). As in GC and HPLC, qualitative information is not obtained to an appreciable degree with these detectors.

Various efforts have been made to couple spectrometric detectors to chromatographic systems in order to improve the qualitative

information obtained. The most successful and widely-used marriage (8) is that of the GC with the Mass Spectrometer (GC-MS). The extensive use of the GC-MS has allowed conclusive identification of GC analytes to nearly the 95% confidence level. Attempts at coupling the HPLC to the MS have resulted in various techniques, including the moving belt (9), heated wire (10), direct liquid injection (11,12) and thermospray (13) interfaces. Recently, several preliminary reports on SFC-MS have appeared (14,15).

Although the mass spectrometer has given a great deal of qualitative information on chromatographic analytes, several attributes of this detector are far from "ideal." Particularly non-ideal is the relative expense of a mass spectrometer over conventional detectors. Also, conformational isomer differentiation is difficult if not impossible by MS alone. These factors undoubtedly have helped bring about the motivation for coupling the Fourier Transform Infrared (FTIR) spectrometer to the GC (16). Although the GC-FTIR may have been developed as an affordable alternative to GC-MS, it has become apparent in recent times that the GC-FTIR and GC-MS are quite complementary rather than competitive techniques (4,17). Several significant developments, such as the gold-coated lightpipe flow cell (18), capillary GC interfacing (19), and extensive digital vapor-phase spectral libraries have advanced GC-FTIR to a level of experimental acceptance comparable with GC-MS (20). However, HPLC-FTIR and SFC-FTIR are mere infants with respect to the development level of GC-FTIR (4). The underlying goal of this thesis work is to elevate HPLC-FTIR and SFC-FTIR to a much more refined experimental level.

The FTIR offers several distinct advantages over dispersive infrared instruments as a chromatographic detector (21). Among these are the capability of rapid data acquisition, high infrared signal throughput resulting in low noise spectra, and good long-term instrument stability. These attributes are a direct result of collecting the infrared spectra in the distance domain by using a continuously-scanning, Michaelson interferometer. Previously this has been discussed in detail for GC-FTIR (22). Although the price for an FTIR system was typically well over $100,000 in 1980, a good-quality system capable of chromatographic detection is now available for less than $60,000 (23).

By 1980, the FTIR had been demonstrated as an on-line detector for size exclusion chromatography (24,25). Unfortunately its use had not been extended to the more traditional normal and polar bonded phase liquid chromatographies because of the difficulty in finding elution solvents that had adequate infrared transparency. Griffiths reported a rather elaborate interface based around diffuse reflectance infrared spectrometry (DRIFT) in which the eluent from an HPLC column was deposited into cups containing KCl (26). The HPLC solvent was evaporated with a heat lamp, and the cup containing the KCl and analyte mixture was spectrometrically analyzed by diffuse reflectance. In addition to the appreciable off-line analyte manipulation, the HPLC-DRIFT method is not suitable for volatile analytes or relatively non-volatile eluents. For these reasons, as well as the undesirable instrumental complexity of the HPLC-DRIFT method, the research on HPLC-FTIR and SFC-FTIR described in the following chapters incorporates

the much simpler, in-line flow cell interface.

Reversed-phase HPLC (RP-HPLC) with FTIR detection was, in 1980, out of the question. The aqueous solvent systems ordinarily used for RP-HPLC afforded little or no infrared transparency for flow cell experiments using cell pathlengths appropriate for typical concentrations of analytes at the column outlet (21). The DRIFT interface could not be used because the RP-HPLC mobile phase would simply dissolve the KCl substrate on deposition rendering impossible the diffuse reflectance spectral collection. Skeptics have even placed the idea of RP-HPLC-FTIR experiments in the "impossible" category (17). The development of flow cell RP-HPLC-FTIR is perhaps the most challenging phase of the work described in the following chapters.

Supercritical fluid chromatography had been suggested (4) as a more easily interfaced type of chromatography to the FTIR than HPLC. In late 1983, Shafer and Griffiths demonstrated the SFC-FTIR experiment using capillary columns (27). They concluded from their experiments that SFC using packed HPLC columns (7) was probably a better choice for SFC-FTIR because of the increased mass load possible with packed columns. It was also suggested that a high pressure lightpipe be developed for these experiments. Conveniently, Hewlett-Packard released a commercial supercritical fluid chromatograph that used packed columns in late 1982. No one to date had reported the coupling of packed column SFC to the FTIR. The SFC-FTIR work is, without a doubt, the most exciting area of research in FTIR detection.

The main objective of the research described in the following

chapters is to extend the FTIR as a detector to previously untested forms of chromatography using a flow cell interface. These forms of chromatography will include both normal-phase and reversed-phase HPLC and packed-column SFC. The methodology incorporated in GC-FTIR experiments will be refined to address the attendant problems associated with HPLC- and SFC-FTIR in order to establish these new techniques as viable analytical procedures.

In Chapter 2, FTIR detection of normal-phase HPLC effluents (NP-HPLC-FTIR) is demonstrated. During this part of the work, microbore HPLC columns were being heralded as a new quantum leap in chromatographic efficiency (28). As the success of NP-HPLC-FTIR was realized using standard, analytical-scale columns, it was only appropriate to evaluate the new microbore columns as well as semi-preparative scale columns with regard to NP-HPLC-FTIR. Several unexpected results led to the conclusion that microbore columns have several distinct advantages in NP-HPLC-FTIR using a flow cell interface.

The unanticipated success of microbore NP-HPLC-FTIR led to the development of a new flow cell interface which was designed around the chromatographic constraints of microbore HPLC. The Zero Dead Volume Flow Cell, described in Chapter 3, demonstrates the first multipath-length flow cell interface for FTIR measurements of chromatographic systems. Several unique spectral features were observed as a result of the unconventional cell geometry.

It became apparent during the work that led to Chapter 3 that

the software developed for GC-FTIR, which used a constant sampling rate for collection of each spectrum, was not the optimum methodology for the relatively broad peaks observed in HPLC-FTIR. In the latter case, peak area methodology for quantitation, in which the infrared spectrum obtained is a result of signal-averaging across the peak, was found to be much better in terms of infrared detector sensitivity than using the single scan spectrum at the peak maximum. This methodology as well as the incorporation of the new, long pathlength flow cell resulted in minimum detectable quantities in the tens of nanograms for microbore NP-HPLC-FTIR.

Chapter 4 describes the first demonstration of reversed-phase HPLC-FTIR using a flow cell interface. This approach employs low-dispersion, flowing extraction in a segmented stream (29). The organic solvent used to extract analytes from the RP-HPLC effluent is detected in the ZDV flow cell interface described in the previous chapter.

Packed-column SFC-FTIR using a lightpipe flow cell is demonstrated in Chapter 5. Infrared spectra of analytes separated by supercritical CO_2 using packed HPLC columns are shown for the first time. Detection limits as low as 50 ng have been observed in SFC-FTIR. Several unique spectral features of high-pressure CO_2 are also discussed.

The research presented in the following chapters has opened several avenues of research that should be pursued. The refinements made have brought both HPLC-FTIR and SFC-FTIR to technological levels that should ensure a much broader acceptance of this unusual but information-rich detection system for chromatography.

CHAPTER 2

NORMAL PHASE LIQUID CHROMATOGRAPHY WITH FOURIER TRANSFORM INFRARED SPECTROMETRIC DETECTION FOR ANALYSIS OF NON-POLAR MATERIAL WITH SEMI-PREPARATIVE, ANALYTICAL AND MICROBORE COLUMNS

INTRODUCTION

Identification of non-volatile components in a complex mixture has always been one of the most demanding tasks for the analytical chemist to perform. Approaches to these analyses have been facilitated by the increasing technological level of chromatography. High Performance Liquid Chromatography (HPLC) has been particularly enhanced by the development of more efficient columns and by the employment of a variety of highly specific detectors. Continuing improvement in small-bore column technology may lend itself nicely to those complex separation problems that require very high column efficiency in order to achieve the necessary high resolution (28). Multiple and simultaneous selective detection allows detailed information to be obtained for chromatographically unresolved components (30). Chromatographically unconventional spectrometric detectors can potentially provide highly specific information for less than adequate complex mixture separations (25). The application of infrared (31), nuclear magnetic resonance (32), inductively coupled plasma atomic emission (33), and mass spectrometry (34) to chromatography, however, is not without experimental problems. Compatible spectrometric-chromatographic solvents, minimal dead volume between column and detector, and reasonable detection limits are but a few of these problems.

Even though the information content of Fourier Transform Infrared

spectrometry (FTIR) is great, the state of the art of HPLC-FTIR has not been particularly advanced (17). The problems previously listed no doubt account for the paucity of data. Size exclusion chromatography wherein the elution is isocratic and the elution solvent has few IR absorbing regions has been reported (24). To date, employment of a larger variety of solvents has been accomplished by using a relatively complex interface which eliminates the solvent by evaporation prior to the IR detection (26).

The use of microbore column separations in flow cell HPLC-FTIR may enable a wider range of otherwise uneconomical solvents to be utilized because of the small elution volumes required. In addition, microbore separations should be as amenable to flow cell FTIR detection as other scales of HPLC because of the comparable peak concentrations (35). Several preliminary reports dealing with coupling micro liquid chromatography to IR spectrometry have recently appeared; collection of the eluent on a KBr crystal plate after passage through a UV detector to indicate when a compound was eluting followed by off-line FTIR detection constituted one study (36). On-line FTIR analysis of the exclusion separation of diethylphthalate and p-nitrotoluene with CCl_4 elution using a microbore column has also been reported (37).

In this chapter, the results which have evolved from an evaluation of normal phase HPLC-FTIR employing semi-preparative, analytical and microbore scale separations are presented and discussed. Model mixtures of numerous aliphatic and aromatic hydrocarbons have been separated on silica gel. In an attempt to identify some of the nonpolar constituents

in several coal liquefaction process solvents and jet fuels, normal phase HPLC-FTIR with Freon 113 elution has been employed.

EXPERIMENTAL

Apparatus

Analytical and Semi-preparative Scale HPLC

The chromatographic system employed consisted of the following: Waters Associates M45 pump (Millford, MA), Valco UHP 6-port injector (Houston, TX) with a 50 µL injection loop, Regis (Morton Grove, IL) Spherisorb S5W 5 µm silica gel column (4.6 mm I.D. x 25 cm), Whatman (Clifton, NJ) Partisil Magnum 9 10/25 10 µm silica gel column (9.4 mm I.D. x 25 cm), Nicolet (Madison, WI) FTIR flow cells (1 mm and 0.2 mm pathlengths), and a Waters R401 Differential Refractive Index detector.

Microbore Scale HPLC

The chromatographic system employed for microbore separations consisted of the following: Waters 6000A pump, Waters 660 solvent programmer, Rheodyne (Cotati, CA) 7413 injector, 10 µm Silica Gel 60 (E. Merck, Darmstadt, Germany) microbore column (1 mm I.D. x 50 cm) and a modified LDC (Riviera Beach, FL) Refractomonitor with minimized tubing (38). A Nicolet FTIR flow cell holder was modified with shortened, capillary tubing to minimize the dead volume; the total illuminated volume plus inlet tubing volume was calculated to be ca. 4 µL using a 0.2 mm pathlength cell. Flow rates were controlled by connecting the pump to one channel (A) of the solvent programmer, setting the overall flow (A+B) to 0.1 mL/min, and controlling the output

of the pump by varying the percent composition control. The flow rates were measured by timed displacement measured at the output of the column into a 50 μL GC syringe. The elution solvent in all three scales of chromatography was 1,1,2-trichloro-1,2,2-trifluoroethane -- Freon 113, obtained from Miller-Stephenson (Danbury, CT) under the tradename Freon TF.

FTIR Detection

A Nicolet Model 6000C FTIR equipped with a wide band (5000-400 cm^{-1}) model 7010B mercury cadmium telluride (MCT-B) detector with the formentioned IR flow cell in the sample compartment was used to detect the eluting components from the chromatographic systems. Provisions were made so that the column was physically located within the optical bench in order to minimize the length of required tubing from the column outlet to the flow cell. The injector and pump were located immediately outside the optical bench on a separate table to minimize any external vibration. In all HPLC-FTIR runs, the standard Nicolet FTIR chromatography software was used to collect time-resolved, 4 cm^{-1} infrared spectra.

Samples

Process Solvent

A preparative chromatographic sequence was used to crudely separate coal-derived process solvents into four discrete fractions according to polarity. Twenty grams of process solvent are mixed with 40 mL of heptane to facilitate sample loading onto a 500 g Silica Gel 60 (E.

Merck) column (3.5" I.D. x ca. 2'). The process solvent is sequentially eluted with successive applications of 2 liter amounts of four solvents at a flow rate of 30-40 mL/min; the fractions obtained and the elution solvents are as follows:

1) Nonpolar fraction - 100% heptane
2) Intermediate polar fraction - 80% heptane/20% chloroform
3) Polar fraction - 90% chloroform/10% acetonitrile
4) Very polar fraction - 100% methanol

Fractions are rotary evaporated to remove the elution solvent, and then dried at 40°C (1 torr) for ca. 10 hours.

Two coal recycle process solvents, a hydrotreated solvent (Mobil 92-26-019) and a non-hydrotreated solvent (Mobil 92-03-035), were subjected to the above preparative scheme. The nonpolar fractions were diluted appropriately and injected through a 0.5 μm Swinny filter into the sample injection loop of the chromatographic system. Process solvents were provided by Mobil Research and Development Corporation, Princeton, NJ, and originated at the SRC-I pilot facility in Wilsonville, AL.

Models

Preliminary model compounds (Model I) were mixed as follows:

dodecane 0.10 g	anthracene 0.09 g
cyclohexane 0.08 g	fluorene 0.15 g
decalin 0.14 g	diphenylmethane 0.17 g
benzene 0.08 g	pyrene 0.17 g
tetralin 0.14 g	anisole 0.11 g
naphthalene 0.05 g	nitrobenzene 0.10 g

All of the above were dissolved in 50 mL of Freon 113. The Model I mixture was injected without dilution through a 0.5 μm Swinny filter

into the sample injection loop.

A second model mixture (Model II), which appeared to be more consistent with the observed process solvent's composition, was prepared as follows:

n-pentane	0.13 g	p-diethylbenzene	0.17 g
dodecane	0.15 g	cyclohexylbenzene	0.19 g
isooctane	0.14 g	tetralin	0.19 g
cyclohexane	0.16 g	2,6-dimethylnaphthalene	0.20 g
decalin	0.18 g	1-methylnaphthalene	0.20 g
p-xylene	0.17 g	naphthalene	0.40 g
2-ethyltoluene	0.18 g	4-phenyltoluene	0.20 g
n-butylbenzene	0.17 g	biphenyl	0.40 g
benzene	0.18 g	9,10-dihydrophenanthrene	0.20 g
		fluorene	0.20 g

The combined weights were dissolved in 5 mL of Freon 113. The Model II mixture was diluted appropriately in Freon 113 and injected through a 0.5 μm Swinny filter into the sample injection loop of each chromatographic system.

Jet Fuel

In addition to the coal-derived process solvent and the associated models, a jet fuel (VN-80-72 from the Jet Propulsion Laboratory, Wright Patterson AFB, OH) was also studied via HPLC-FTIR. This sample was diluted appropriately in Freon 113 and injected through a 0.5 μm Swinny filter into the sample injection loop.

RESULTS AND DISCUSSION

The objectives of this study were: (i) to demonstrate the feasibility of on-line HPLC-FTIR employing normal phase chromatography; (ii) to evaluate various chromatographic parameters for data optimization in the HPLC-FTIR mode; and (iii) to apply the HPLC-FTIR

technique to the problem of identification of components in synfuel mixtures. The general class of compounds which one wishes to speciate naturally dictates, in part, certain chromatographic conditions. For this study, the non-polar (hydrocarbon) species in several synfuel materials were singled-out for further chromatographic separation and detection via FTIR. Silica was chosen as the column packing because of its known capability for separating aliphatics, hydroaromatics and aromatics (32). In order to maximize the IR spectral region for observation of the eluting components, Freon 113 was selected as the mobile phase. Freon 113 has been recently demonstrated to have good elution solvent characteristics for normal phase chromatography as well as distinct advantages over commonly used n-alkanes (39). In an effort to understand the separation mechanism and to aid in interpreting the various file spectra taken during the separation, several non-polar model mixtures have been investigated via HPLC-FTIR. Three chromatographic scales have been examined: semi-preparative, analytical and microbore.

Preliminary HPLC separations were performed on the analytical scale column. Initially, the 1 mm pathlength IR flow cell was found to be unsatisfactory for FTIR detection because the broad, solvent bands obscured the absorbance bands of the analytes. In an effort to increase the available IR windows of the Freon 113 elution solvent, a 0.2 mm pathlength flow cell was substituted. The effect of this pathlength change on the available IR windows is shown in Figure 1 along side the vapor phase IR spectrum of Freon 113. The gain in IR window regions,

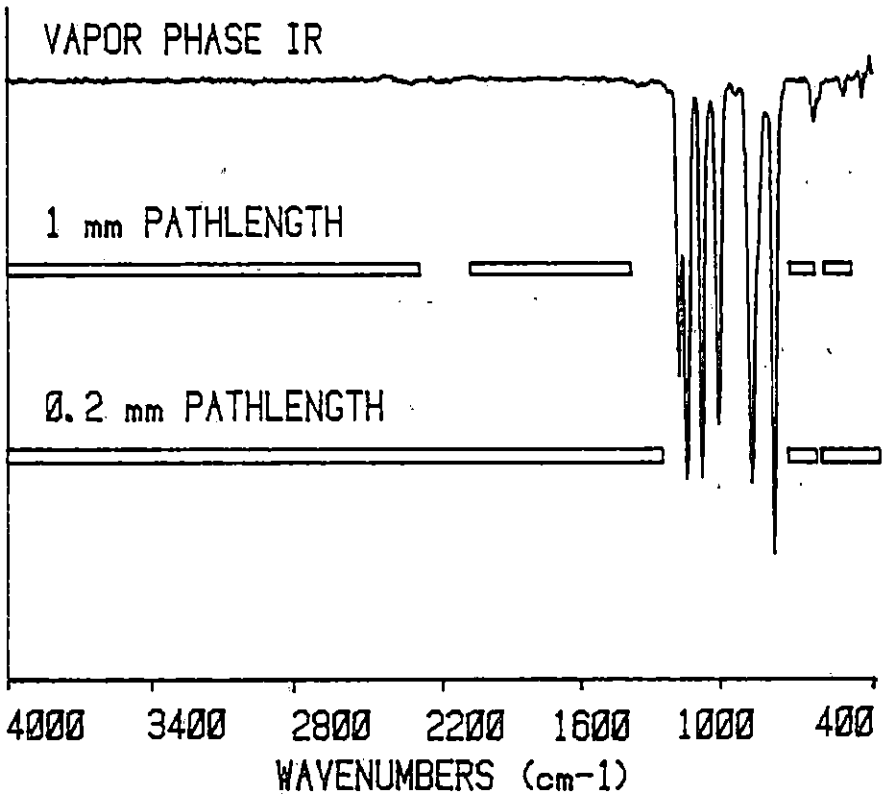

Figure 1. Infrared windows of Freon 113 as an HPLC-FTIR solvent.

however, was not without cost. The increased information available using the 0.2 mm pathlength flow cell was overshadowed by the resultant insensitivity of the FTIR to the eluted components from the analytical scale HPLC column. In order to obtain equivalent IR sensitivity with the enlarged window regions, an attempt was made to increase the concentration of the eluting components according to the following schemes:

1) Increase sample loading on the analytical scale column.

2) Increase column capacity by substituting a semi-preparative column.

3) Increase the eluted peaks' concentrations by using a microbore column.

The results of each approach are presented separately.

Analytical Scale HPLC-FTIR

Sample loading was maximized to a concentration that would not seriously degrade the separation due to column overload. Results from the separation of the Model I mixture using refractive index detection are presented in Figure 2A. The HPLC-FTIR separation of the same mixture was detected using a 1 mm pathlength IR flow cell. The Gram-Schmidt reconstructed chromatogram (40) from FTIR detection (Figure 3A) corresponds peak for peak to the refractive index trace. We have found that the RI detector, under these conditions, appears to have nearly the same detection limits as the HPLC-FTIR detector. Consequently the RI detector has been used for developmental separations prior to HPLC-FTIR experiments.

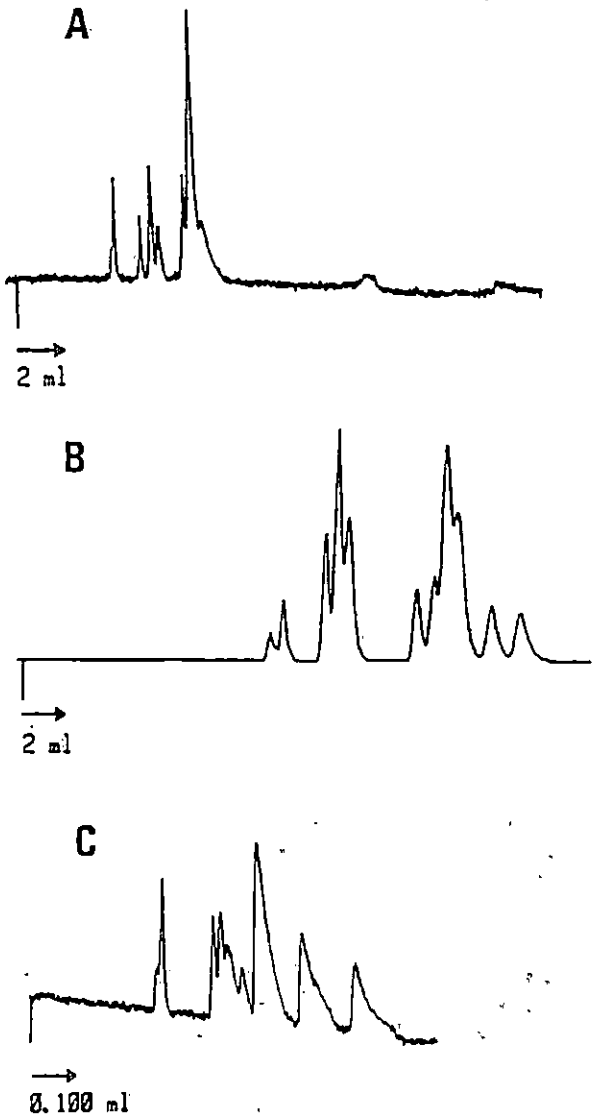

Figure 2. Refractive index traces of Model separations: [2A] Analytical scale separation of Model I, 50 µL injection, 1 mL/min, RI-1x; [2B] Semi-preparative scale separation of Model II, 50 µL injection-50% v/v, 2 mL/min, RI-4x; [2C] Microbore scale separation of Model II, 5 µL injection-25% v/v, 50 µL/min, RI (modified)-1x.

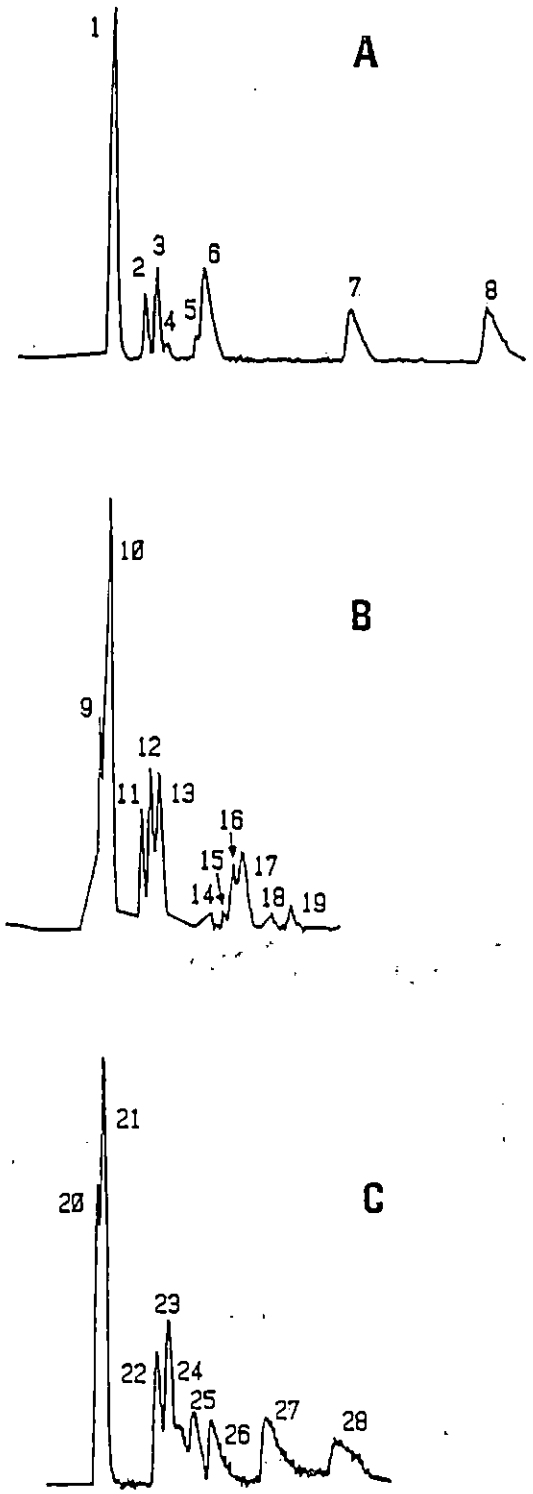

Figure 3. Gram-Schmidt reconstructed chromatograms of Model separations (compare to RI traces in Figure 2); [3A] Analytical scale separation of Model I; [3B] Semi-preparative scale separation of Model II; [3C] Microbore scale separation of Model II. Peak numbers refer to file spectra presented later.

The elution volumes of the model compounds based on single compound injections are presented in Table I. File spectra taken during the chromatographic separation have been used to confirm the assignment of each eluting component. Inspection of file spectra in the C-H stretching region indicates the elution of tetralin between benzene and naphthalene. Figure 4 shows the rise and fall of aliphatic C-H stretching absorption unique to tetralin in the file spectra in the vicinity of peak no. 3.

The front shoulder of the chromatographic peak at an elution volume of 9 mL (Figure 3A, peak no. 5) contains no aliphatic C-H stretch. Single compound injections suggest elution of anthracene rather than pyrene. The heart of this peak contains chromatographically overlapping but spectrally distinguishable diphenylmethane and fluorene under the envelope of peak no. 6. Spectra in the C-H stretch regin (Figure 5) suggest a relative elution order of anthracene, diphenylmethane, fluorene, and pyrene. It is interesting to note that the silica gel/Freon 113 separation gives some class separation according to the degree of aromaticity of the model compounds. In addition, structures having small, permanent dipoles (e.g. fluorene, diphenylmethane) are eluted later than the other two-ring aromatics as would be expected.

In separating the non-polar fraction of the Hydrogenated Process Solvent (HPS) 92-26-019, a similar separation by compound class is observed. The column loading is typically maximized at a 2-3% v/v solution of the non-polar fraction of HPS before significant degradation

TABLE I

Elution Order of Model I

Peak No.	Compound	Retention Volume (mL)
1	Dodecane	2.6
	Cyclohexane, decalin	2.7
2	Benzene	3.4
3	Tetralin	3.6
4	Naphthalene	3.8
5	Anthracene	4.6
6	Fluorene	4.8
	Diphenylmethane	4.9
7	Pyrene	5.0
	Anisole	6.9
8	Nitrobenzene	10.75

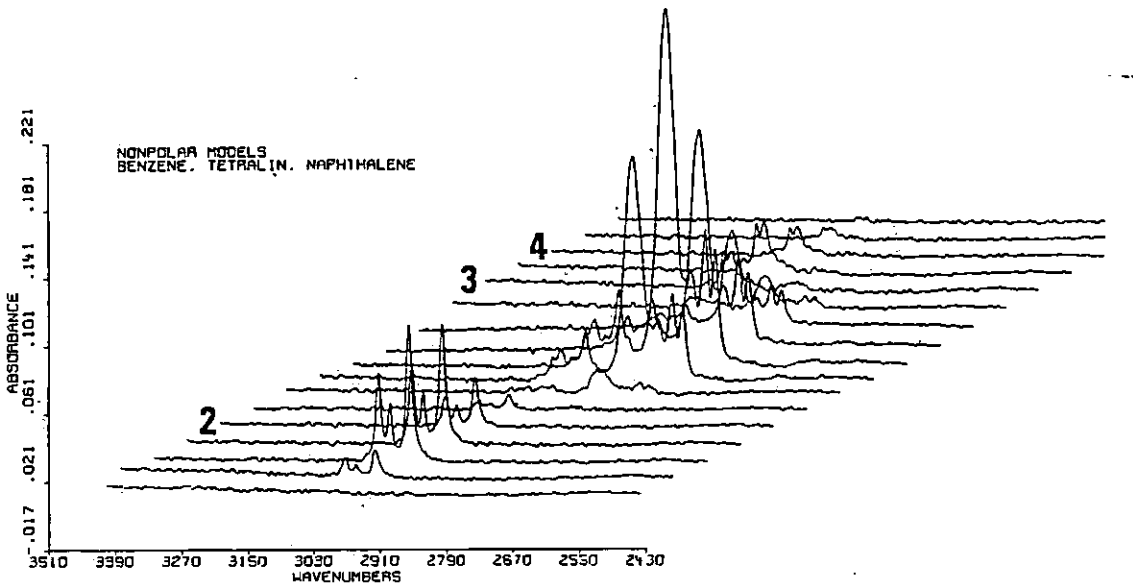

Figure 4. Stacked plots of benzene, tetralin and naphthalene elution (Peaks no. 2, 3 and 4) from the Model I analytical scale separation.

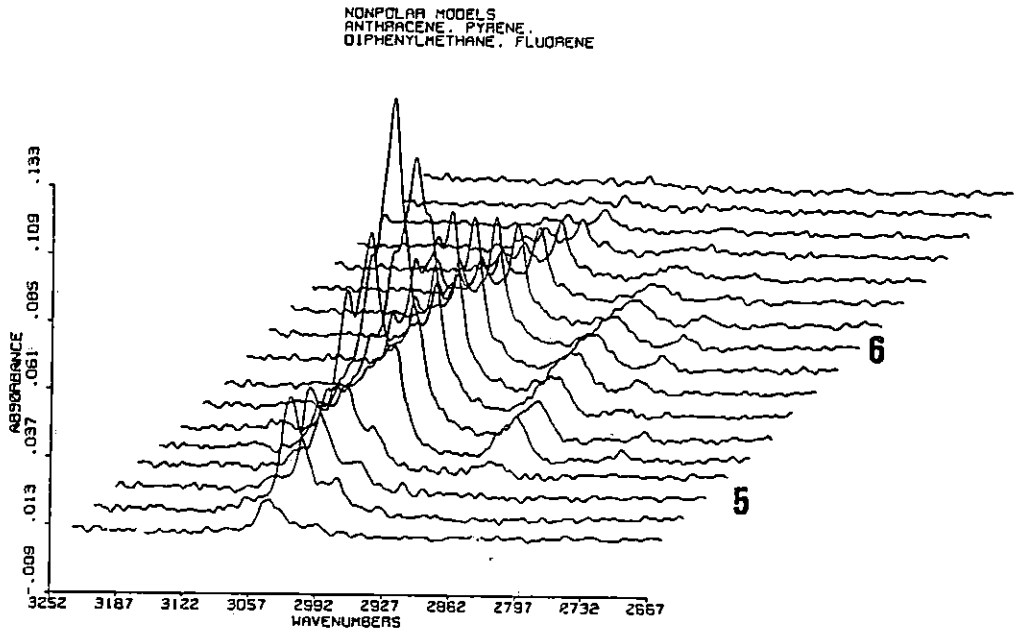

Figure 5. Stacked plots of anthracene (Peak no. 5), diphenylmethane, fluorene and pyrene (Peak no. 6) elution from the Model I analytical scale separation.

of chromatographic resolution is observed. Increasing aromaticity (Figure 6A) is observed with increasing elution volume as confirmed by inspection of the file infrared spectra. Studies of the non-polar fraction of non-hydrogenated Process Solvent (PS) 92-03-035 showed a lower aliphatic character as would be expected (41). Figure 6D illustrates this separation with RI detection. Note the lower intensity of the first peaks at the same attenuation. Gram-Schmidt reconstructed chromatograms for these two non-polar fractions under the same separation conditions duplicate again the RI traces. As indicated previously, the 1 mm pathlength cell restricted the IR window regions. The loading capacity of the column was not sufficiently large to allow increased sample injection without serious degradation of chromatographic resolution. Decreasing the flow cell pathlength to 0.2 mm compromised the IR sensitivity to an unacceptable level.

Semi-Preparative Scale HPLC-FTIR

An improved model mixture (Model II), which contained additional components suggested from the analytical scale work, was used in the semi-preparative scale separation. Figures 2B and 3B illustrate the RI trace and Gram-Schmidt reconstruction, respectively. Peak assignments are listed in Table II based on single injections and infrared file spectra taken during the separation. A class separation similar to the analytical scale separation, is observed. Much better chromatographic resolution is obtained between the monoaromatics (15.0 mL to 16.3 mL) and the polyaromatics (19.7 mL to 25.0 mL) than in the analytical-scale separation. Sample file spectra are shown in Figure 7 to indicate the

TABLE II

Semi-Preparative Scale Elution Order of Model II

Peak No.	Compound	Retention Volume (mL)
9	n-pentane, dodecane, iso-octane	12.3
10	cyclohexane, decalin	13.3
11	p-xylene	15.0
	o-ethyltoluene	15.3
	n-butylbenzene	15.5
12	benzene, p-diethylbenzene	15.7
	cyclohexylbenzene	16.0
13	tetralin	16.3
14	2,6-dimethylnaphthalene	19.7
15	4-phenyltoluene, 1-methylnaphthalene	21.0
16	naphthalene	21.3
17	biphenyl	22.0
18	9,10-dihydrophenanthrene	23.0
19	fluorene	24.8

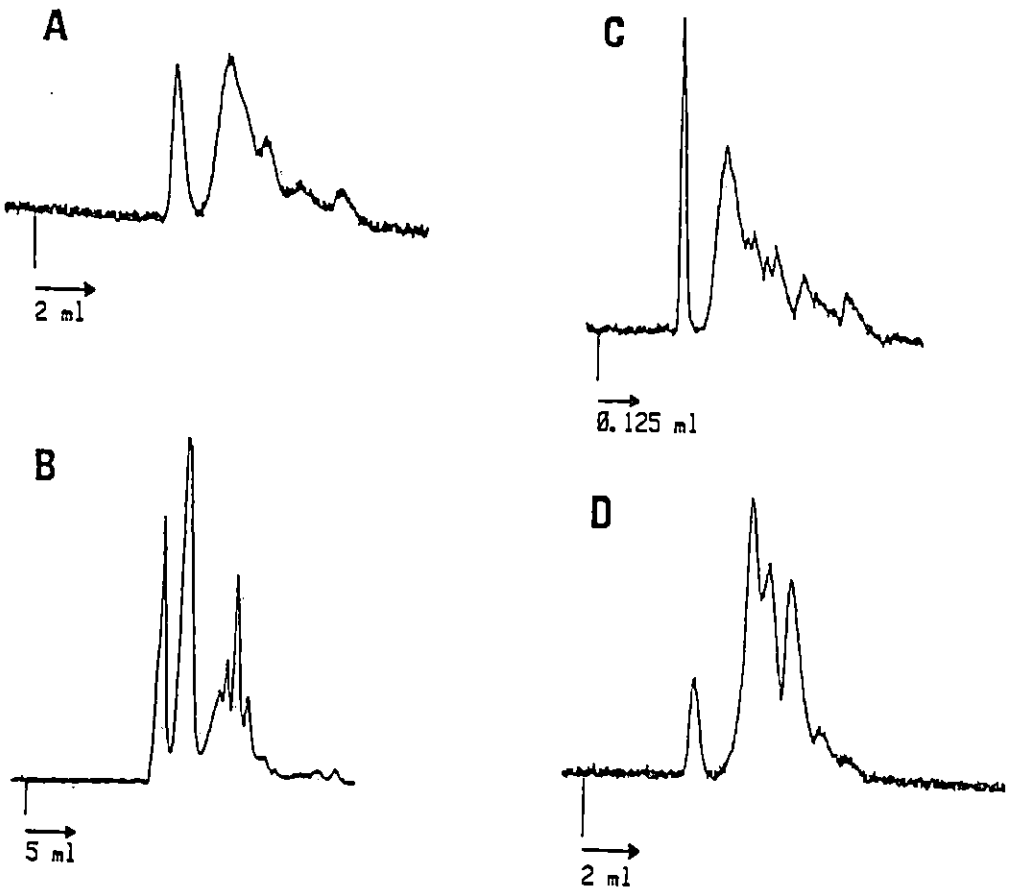

Figure 6. Refractive index traces of Process Solvent separation; [6A] Analytical scale separation of non-polar fraction of Mobil 92-26-019 (HPS), 50 µL injection-5% v/v, 1 mL/min, RI-1x; [6B] Semi-preparative scale separation of non-polar fraction of HPS, 50 µL injection-50% v/v, 2 ml/min, RI-2x; [6C] Microbore scale separation of non-polar fraction of HPS, 5 µL injection-25% v/v, 80 µL/min, RI (modified)-2x; [6D] Analytical scale separation of non-polar fraction of Mobil 92-03-035 (PS), 50 µL injection-5% v/v, 1 mL/min, RI-1x.

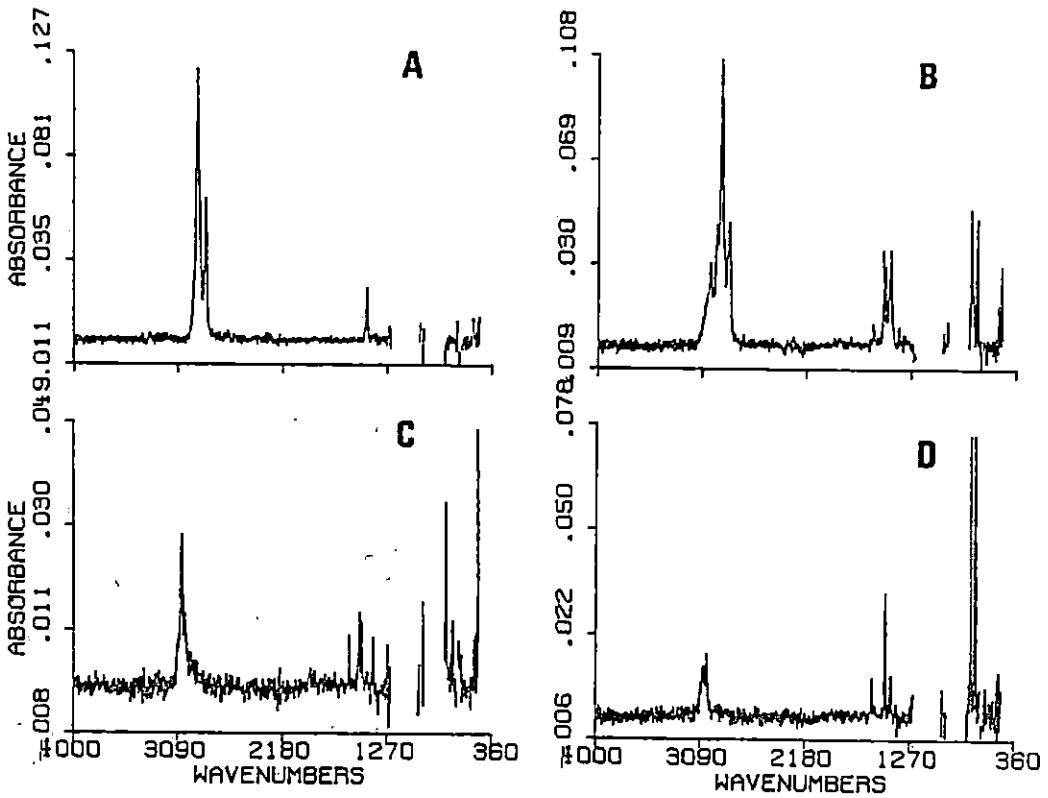

Figure 7. Infrared spectra obtained from the semi-preparative scale separation of Model II; [7A] cycloalkanes (peak no. 10); [7B] p-diethylbenzene (peak no. 12); [7C] naphthalene (peak no. 16); [7D] biphenyl (peak no. 17).

information content possible in this separation mode. Peaks no. 9 and 10 are assigned to linear alkanes and cycloalkanes, respectively. The virtual absence of methyl symmetric and asymmetric C-H stretching modes in the file spectra associated with peak no. 10 suggests the later elution of cycloalkanes (Figure 7A). Peaks no. 11 and 12 show both aromatic and aliphatic C-H stretching modes. Peak no. 12 has been assigned arbitrarily as p-diethylbenzene (Figure 7B). Comparison of file spectra associated with peaks no. 16 and 17 match well with static spectra of naphthalene and biphenyl, respectively.

Separation on a semi-preparative scale of the non-polar fraction of HPS 92-26-019 gave much better chromatographic resolution than the analytical scale as can be seen in Figures 6B and 8. The class separation observed in the model studies appears to hold in the process solvent based on examination of the infrared spectra obtained Figure 9. Peak no. 34 (Figure 8) is assigned as an aliphatic-substituted biphenyl, and has an elution volume of 21.0 mL. This corresponds to the model elution of 4-phenyltoluene. The infrared spectrum of biphenyl, which is similar, is presented in Figure 7D.

The jet fuel VN-80-72 shows a similar class separation, as can be seen in the RI trace (Figure 10). The primary difference between the non-polar fraction of HPS and the jet fuel is the much higher aliphatic content of the jet fuel. In this case the monoaromatics and polyaromatics are very minor components as can be seen by the 8:1 attenuation difference necessary to bring all RI peaks to scale. The non-polar fraction of HPS, on the other hand, gives an RI chromatogram

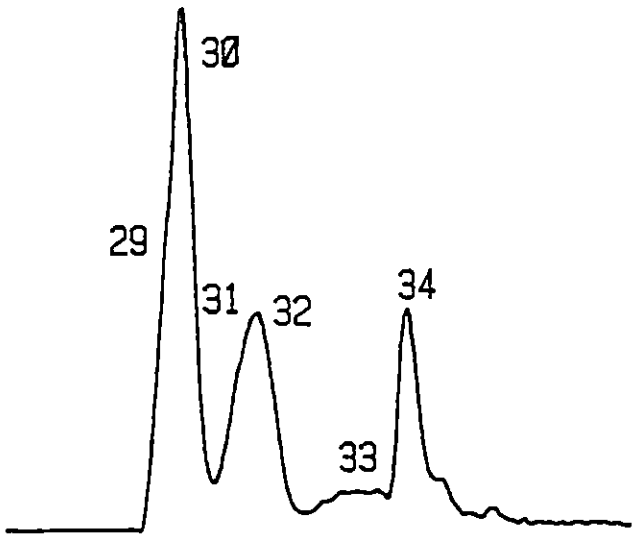

Figure 8. Gram-Schmidt reconstructed chromatogram of semi-preparative scale separation of the non-polar fraction of Mobil 92-026-019 (HPS).

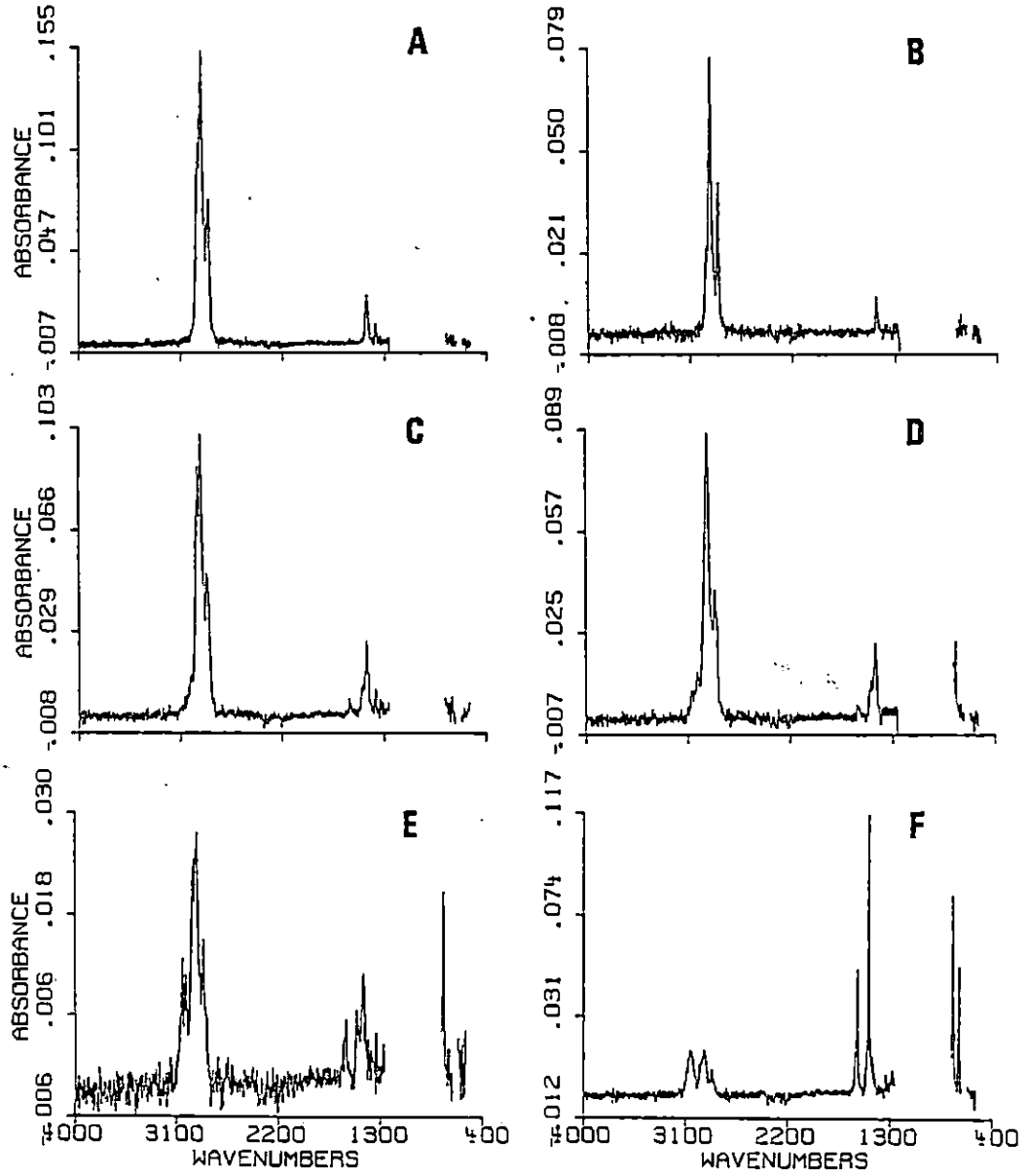

Figure 9. Infrared spectra obtained from the semi-preparative scale separation of the non-polar fraction of Mobil 92-26-019 (HPS); [9A] Peak No. 29; [9B] Peak no. 30; [9C] Peak no. 31; [9D] Peak No. 32; [9E] Peak no. 33; [9F] Peak no. 34.

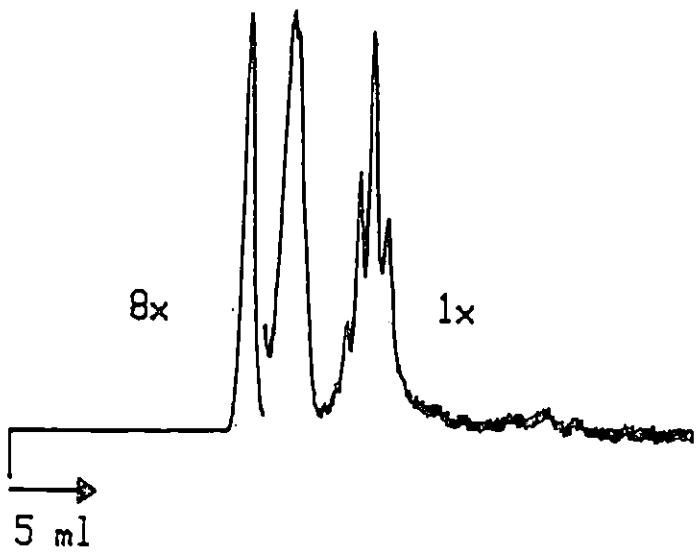

Figure 10. Refractive index trace of the semi-preparative separation of Jet Fuel VN-80-72, 50 µL injection-50% v/v, 2 mL/min, RI-8x/1x.

with detection of all three main groups at the same attenuation. The Model II separation gives a similar RI chromatogram without a change in attenuation. From the known composition of the Model II, the concentration ratio of monoaromatics to aliphatics is nearly 1.5:1. On the basis of peak height measurements of the observed RI trace of both the Model II and the process solvent, it is reasonable to conclude that the concentration ratio of monoaromatics to aliphatics in the non-polar fraction of HPS is at least 1:1. This also would suggest that jet fuel VN-80-72 has a concentration ratio of monoaromatics to aliphatics of ca. 1:8. The concentration ratios of polyaromatics to monoaromatics can be treated similarly. The Model II mixture was approximately 1:1 in polyaromatics to monoaromatics. The process solvent appears to have slightly less polyaromatic material than monoaromatic, perhaps on the order of ca. 0.7:1. The jet fuel is on the order of 1:1, however. The overall approximate concentration ratios are compared below:

Sample	Polyaromatic:Monoaromatic:Aliphatic
Model II	1.5 : 1.5 : 1
Non-polar Fraction of HPS	0.7 : 1 : 1
Jet Fuel VN-80-72	1 : 1 : 8

Detection was achieved in the semi-preparative scale HPLC-FTIR experiments using the 0.2 mm pathlength flow cell. The infrared sensitivity is still quite good in spite of the necessary five-fold decrease in infrared absorptivity. The maximum concentration determined for injection without significant degradation of chromatographic resolution was 50% v/v of the non-polar fraction of HPS -- over twenty

times the maximum amount allowable for the analytical scale separation. This accounts for the comparable infrared sensitivity (analytical vs. semi-preparative) with a wider IR window region. The benefits of the semi-preparative scale separation are not without cost. Rather exotic or unconventional solvents must be used in HPLC-FTIR to provide good infrared spectral window regions. Solvent consumption in the semi-preparative separation is approximately five times that of the analytical-scale separation. Freon 113, a common solvent available in high purity, is not prohibitively expensive. However, other possible solvents, because of their desirable infrared windows, would cost far too much for routine use in semi-preparative scale HPLC-FTIR.

Microbore Scale HPLC-FTIR

Encouraging results were observed using microbore columns with FTIR detection. The RI trace of Model II is shown in Figure 2C. The disparity between this and the semi-preparative RI trace for the microbore separation (Figure 2B) was, at first, rather disappointing. The fact that the Gram-Schmidt reconstructed chromatogram (Figure 3C) followed the RI trace (Figure 2C) peak for peak ruled out a possible post-modification detector anomaly. The minor differences noted in the semi-preparative and microbore chromatograms have since been attributed to activation differences between the two silica columns employed.

Investigation of file spectra (Figure 11) revealed a similar class separation to that observed in both the semi-preparative and analytical scale separations. Inspection of file spectra around peak no. 20 (Figure 11A) reveals primarily linear aliphatics. The absence of methyl

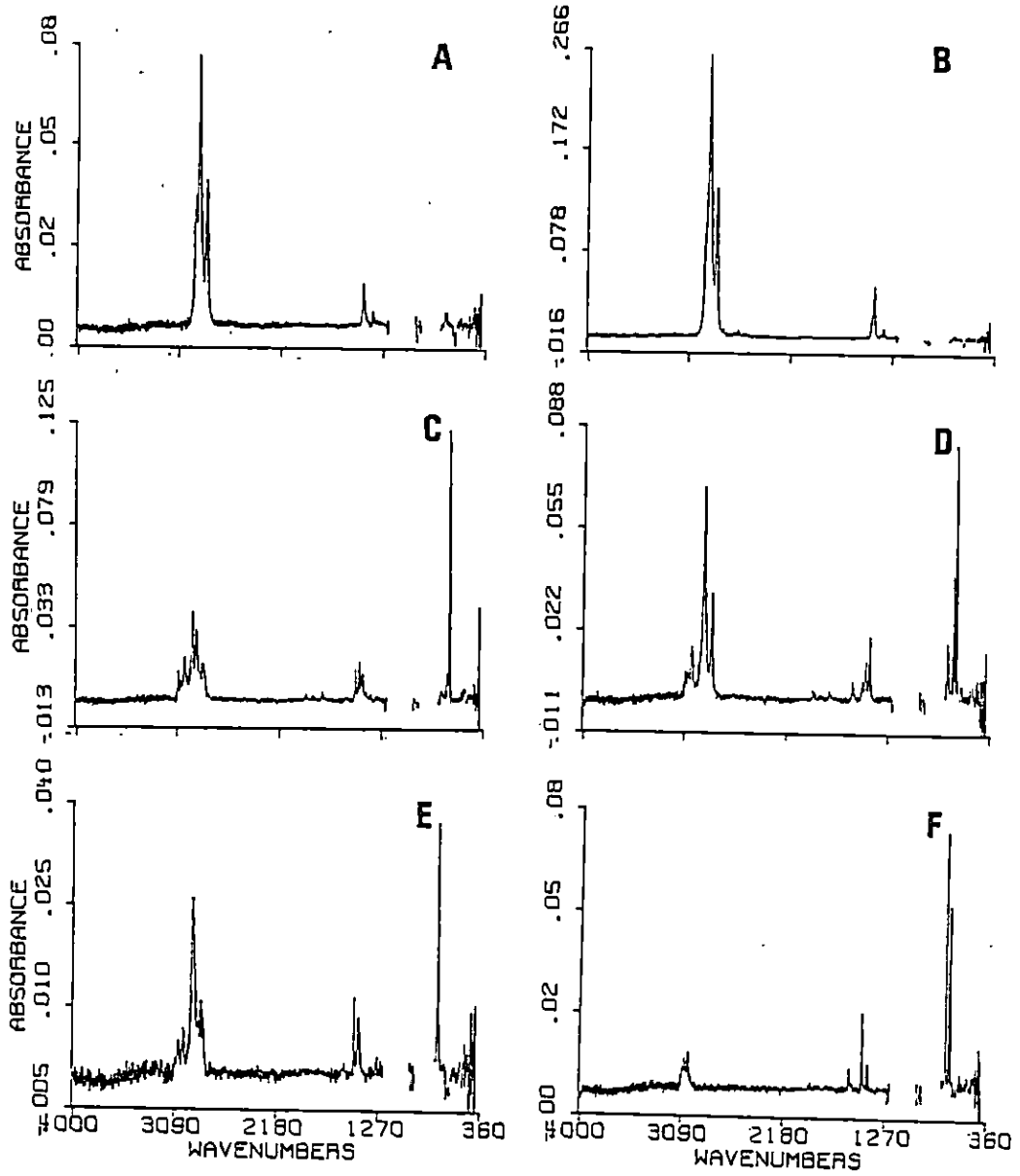

Figure 11. Infrared spectra obtained from the microbore separation of Model II; [11A] Peak no. 20; [11B] Peak no. 21; [11C] Peak no. 23; [11D] Peak no. 24; [11E] Peak no. 26; [11F] Peak no. 27.

group absorbances in peak no. 21 (Figure 11B) suggests that cyclic aliphatics are again retained longer. In addition, aromatic models (peaks no. 22 to 28) appear to be separated comparably by both the semi-preparative and microbore columns. Comparison of file spectra obtained from the semi-preparative (Figure 7) and the microbore (Figure 11) model separations, however, shows that the signal-to-noise in the microbore separation is indeed better. Overtone patterns between 1750 and 2000 cm^{-1} are readily distinguishable (Figure 11C-D) in the microbore HPLC-FTIR experiment. However, these patterns are obscured by noise in the semi-preparative file spectra (Figure 7B-D). The spectrum of biphenyl (Figure 11F) in the microbore separation has much better signal-to-noise than the corresponding spectrum (Figure 7D) in the semi-preparative separation.

The microbore separation of the non-polar fraction of HPS is shown in Figures 6C (RI) and 12 (Reconstructed). The separation of the same fraction in the semi-preparative scale is illustrated in Figure 6B. The presence of a heavy precipitate appeared in this fraction between the time of the semi-preparative and microbore separations. This fact coupled with an analysis of file spectra from both runs has indicated that severe sample aging has taken place. Accordingly, the spectra obtained from the semi-preparative separation are presented (Figure 9) as representative of the non-polar fraction of HPS prior to significant aging.

It is interesting to note that the eluted samples from the microbore column are easily detected by FTIR as can be seen by the good

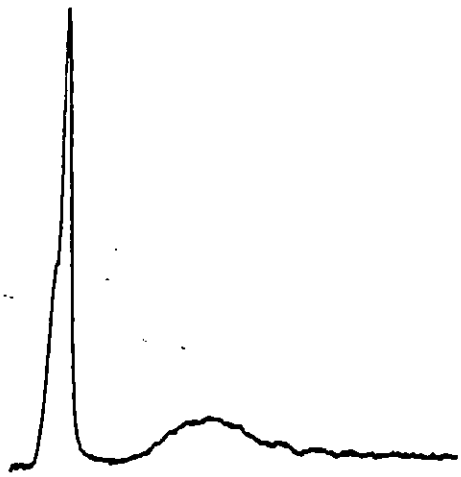

Figure 12. Integrated absorbance reconstructed chromatogram (3300 to 2850 cm-1) of the microbore scale separation of the non-polar fraction of Mobil 92-26-019 (HPS).

signal-to-noise ratio of the file spectra. The solvent consumption is particularly appealing, being less than 1.0 mL per chromatogram. This corresponds to a ten-fold decrease in solvent consumption over the analytical scale, and nearly a fifty-fold decrease over the semi-preparative scale. The actual time of the separation is virtually the same in all cases.

In summary, normal phase HPLC-FTIR has been demonstrated to be a valuable tool in complex mixture analysis. Limitations on solvent windows will always be present in spectral flow cell analyses. This study, however, has shown the feasibility of all scales of normal phase HPLC-FTIR as a routine analytical tool. The use of microbore HPLC-FTIR allows the chromatographer to use relatively expensive solvents with large infrared windows economically without compromising the spectral information obtained.

CHAPTER 3

ZERO DEAD VOLUME FLOW CELL FOR MICROBORE LIQUID CHROMATOGRAPHY WITH FOURIER TRANSFORM INFRARED SPECTROMETRIC DETECTION

INTRODUCTION

The use of a Fourier transform infrared (FTIR) spectrometer as a detector for high performance liquid chromatography (HPLC) has been well documented (21,25,31,42-44). The simplest method of interfacing the HPLC to the FTIR "on-line" has been through the use of a suitable infrared flow cell. Recently, microbore HPLC (μ-HPLC) columns have been incorporated into this hyphenated experiment (44-49). Microbore has been shown to be the most practical mode for FTIR detection because of the low amount of elution solvent used while still maintaining highly efficient separations. Because of the low elution volumes necessary, relatively exotic, high-purity solvents can be used economically in μ-HPLC-FTIR (45). An additional advantage is environmental since the total solvent waste decreases by at least one order of magnitude relative to analytical scale chromatography.

Historically, the design of the μ-HPLC-FTIR flow cell interface has been approached from a spectrometric point-of-view with little emphasis on the chromatographic characteristics (21). Parallel plate alkali halide disks with drilled holes and spacers of different thicknesses have been employed. The flow cell modified in our earlier research is a good example of such a cell (46). The work reported in Chapter 2 suggests that these commercial spectrometric flow cells do not have the necessary chromatographic characteristics for the increasingly efficient

separations available in the μ-HPLC-FTIR experiment. These desirable characteristics include low volume, long pathlength, unencumbered flow geometry to minimize dead volume, and minimal connecting tubing between the column outlet and illuminated region.

Following these design criteria, which approach the flow cell development from a chromatographic point-of-view, a flow cell has been developed for the μ-HPLC-FTIR experiment which is not only chromatographically superior, but also spectrometrically advanced. This Zero Dead Volume Flow Cell is also the first demonstration of a multi-pathlength flow cell for HPLC-FTIR. In addition, improved data manipulation for quantitation has been employed to further enhance the sensitivity of the flow cell experiment.

EXPERIMENTAL

APPARATUS

A Nicolet 6000C FTIR (Madison, WI) equipped with a narrow-band (5000-700 cm^{-1}) Model 7010A mercury-cadmium-telluride detector (MCT-A) was used to monitor the effluents in the flow cell. The standard Nicolet software package was used to collect time resolved, 4 cm^{-1} resolution spectra. The time resolution between each collected interferogram was 0.65 sec. For the data handling, flow, and detection limit experiments, single scan files were stored for post-run data manipulation. For the five-component mixture separation, every four scans were co-added and stored in a file for post-run data manipulation. Interferograms were averaged post-run using the co-addition routine. This routine weights the files that are averaged so that computationally

each interferogram carries equal weight.

An IBM LC/9533 ternary gradient liquid chromatograph (Danbury, CT) was used for solvent delivery. An external electronics module to provide microliter delivery was supplied by IBM. A Rheodyne Model 7413 injector (Cotati, CA) equipped with a 0.5 μL loop was connected for chromatographic studies via a 0.007" ID x 4 cm length of stainless steel tubing to a 1 mm ID x 50 cm microbore column packed with 10 μm Silica Gel 60 (E. Merck, Darmstadt, Germany). The column efficiency was measured at 12,500 plates.

The elution solvent was ethanol-free chloroform (Burdick and Jackson, Muskegon, MI). Model compounds were obtained from Aldrich Chemical Company (Milwaukee, WI) in the following purities: 2,6-di-tert-butylphenol, 99+%; 2-tert-butylphenol, 99%; 2-sec-butylphenol, 98%; o-methoxy-biphenyl, (purity not listed). Cyclohexyl acetate (Eastman Organic Chemicals, Rochester, NY) was also used for both model separations and flow studies.

The flow cell used for this study was developed and manufactured in-house and is schematically represented in Figure 13. The crystal element is a block of either CaF_2 or KBr, approximately 10x10x6 mm, with a 0.75 mm diameter cylindrical hole drilled through it. The crystal is sealed in place using an EM Science (Gibbstown, N.J.) microbore end fitting, which compresses the Teflon gaskets on each end of the crystal. The infrared beam intersects the flow path at a 90° angle; the shape of the spectrometric viewing region is consequently circular in cross-section.

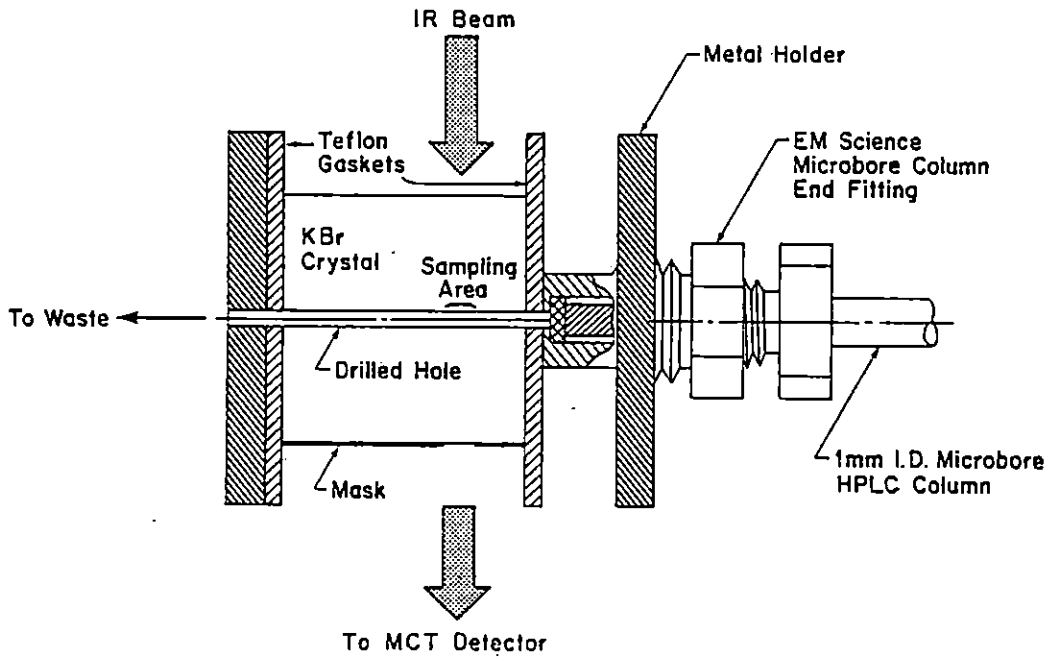

Figure 13. Zero Dead Volume μ-HPLC-FTIR Flow Cell.

Since the focal diameter of the Nicolet 6000C is 3 mm and the hole in the cell is 0.75 mm in diameter, a Barnes Model 600 4x Beam Condenser (Spectra-Tech, Inc., Stamford, CT) was used to reduce the focal diameter to approximately 0.75 mm. With the beam condenser in place, the mask shown in Figure 1 was not used. An aluminum cell holder compatible with the beam condenser was made with provisions for adjusting the cell alignment. Alignment of the cell was facilitated by filling the cell with solvent, and adjusting its location until the observed interferogram showed a minimum signal (peak-to-peak) at the center burst.

RESULTS AND DISCUSSION

The objectives of this work are as follows:

(1) Establish the optimum methodology for obtaining the highest signal-to-noise ratio in the infrared spectrum of a sample whose concentration varies with time according to a Gaussian distribution.

(2) Determine the flow characteristics of the Zero Dead Volume (ZDV) μ-HPLC-FTIR flow cell.

(3) Use this flow cell in a chromatographic separation to determine both its spectrometric and chromatographic performance under typical operating conditions.

(4) Determine detection limits to establish μ-HPLC-FTIR sensitivity, and compare these limits to previously reported values.

Establishing the optimum methodology for obtaining the highest signal-to-noise spectra must be based on several factors. Among these are flow cell volume, spectral collection time, effect of signal-

averaging spectra, typical peak widths and typical peak volumes. We will assume that the flow cell volume is much smaller than the peak volume so that a reliable concentration profile can be obtained. Also, the spectral collection time is adjustable, but must remain fixed throughout the chromatographic run due to software limitations. The effect of signal-averaging spectra will be dealt with later. First, HPLC separations do not have a typical peak width or volume. A compound that is unretained will have a much smaller peak width than one that is retained. The same problem exists in GC, but the chromatographer can use an oven temperature program to effectively eliminate band broadening due to retention. This option is not available for HPLC.

If one assumes that a chromatographic peak has a Gaussian concentration profile and the sampling rate is matched to an unretained peak in a typical HPLC separation (number of plates = 12,500 and the peak width at k'=0 is 10 seconds) so that 88% of the peak elutes during spectral collection, by the time that a peak at k'=5 elutes, only 18% of the peak would be used to collect the spectrum. This is graphically illustrated in Figure 14. The noise contribution should be the same for each spectrum because the FTIR sampling would be the same, but the signal would certainly be diminished in the spectrum of the retained peak for bands with similar molar absorptivities because of the dilution of the retained compound. The sampling width could be enlarged to accommodate the broader peak, but the definition of closely-eluting early peaks would be compromised. Clearly no single sampling rate can be optimal for both early and late eluting compounds. If one bases the

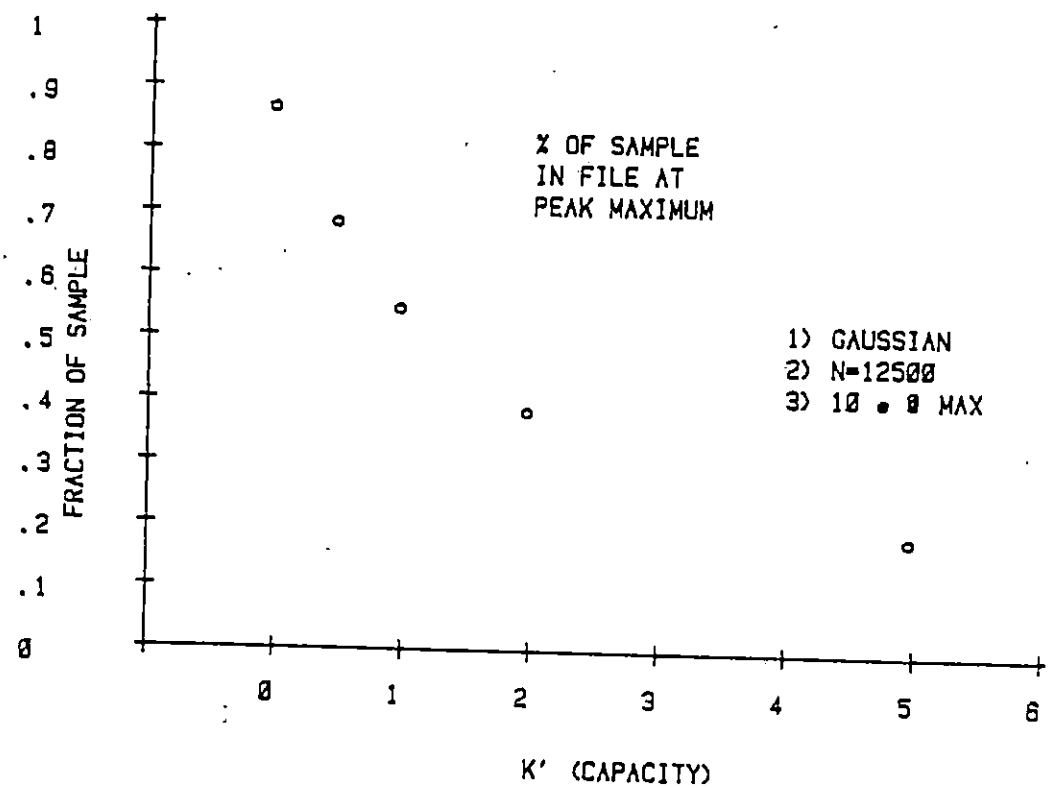

Figure 14. Percent of sample used to collect an infrared spectrum as capacity factor increases.

conditions on the characteristics of each peak, more appropriate sampling conditions can be established.

Establishing a methodology to optimize the signal-to-noise ratio of the infrared spectrum generated for each peak requires the following treatment. If one assumes that a chromatographic peak has a Gaussian concentration profile, then the variation of analyte concentration with time in the chromatographic peak can be described by the normal curve, $\phi(x)$:

$$\phi(x) = \frac{1}{2\pi} e^{-x^2/2}$$

where $x = t/\sigma_t$, $t \equiv$ amount of time from the peak maximum (where t=0), and $\sigma_t \equiv$ standard deviation of the peak. The FTIR can scan with time resolution typically much faster than the chromatographic response time. By saving individual inteferograms, one can obtain a time-resolved histogram of spectra as the peak elutes. If one starts at the chromatographic peak maximum and co-adds spectra symmetrically on either side of the maximum, the co-added file will contain a composite spectrum that will be that of the average concentration (C_{obs}) of analyte over the time interval of co-addition. Expressed mathematically,

$$C_{obs} = \frac{A_x}{2x} = \frac{1}{2x} \int_{-t}^{+t} \phi(x)dx = \frac{1}{x} \int_{0}^{t} \phi(x)dx$$

where $A_x \equiv$ area under the normal curve. The values for this integral are available in tabular form (50).

Incoherent noise contributions to the spectrum can be diminished by

co-addition of repetitive scans; mathematically the noise decreases as the inverse of the square root of the number of scans co-added. Since the signal observed by the infrared at low concentrations is proportional to the observed concentration in the measurement cell, then the signal-to-noise ratio can be described as follows:

$S/N \propto n^{1/2} C_{obs}$, where n ≡ the number of scans coadded.

Intuitively, one would expect that the signal-to-noise ratio would increase as long as the co-addition of scans enhanced the observed concentration and/or diminished the observed noise of the composite spectrum. At some point the co-addition of scans should approach a limiting noise value such that further co-addition of the low concentration spectral scans at the edges of the chromatographic peak simply dilutes the observed analyte concentration. At this point, the signal-to-noise ratio is diminished. This trend is graphically illustrated in Figure 15 using the previous equations. It can be shown that the relative time per scan is irrelevant to the curve maximum at $x = \pm 1.37\sigma$. For practical reasons, the peak should be defined in time resolution where 4σ equals a minimum of ten scans. This would indicate that the maximum signal-to-noise spectrum would be obtained by co-adding seven of these scans which are symmetrical about the peak maximum.

The above theoretical treatment, which approaches the mathematics with chromatography symbolism, is in approximate agreement with that which Griffiths proposed but never tested for GC-FTIR (22). Experimental data to support such a theoretical treatment are presented

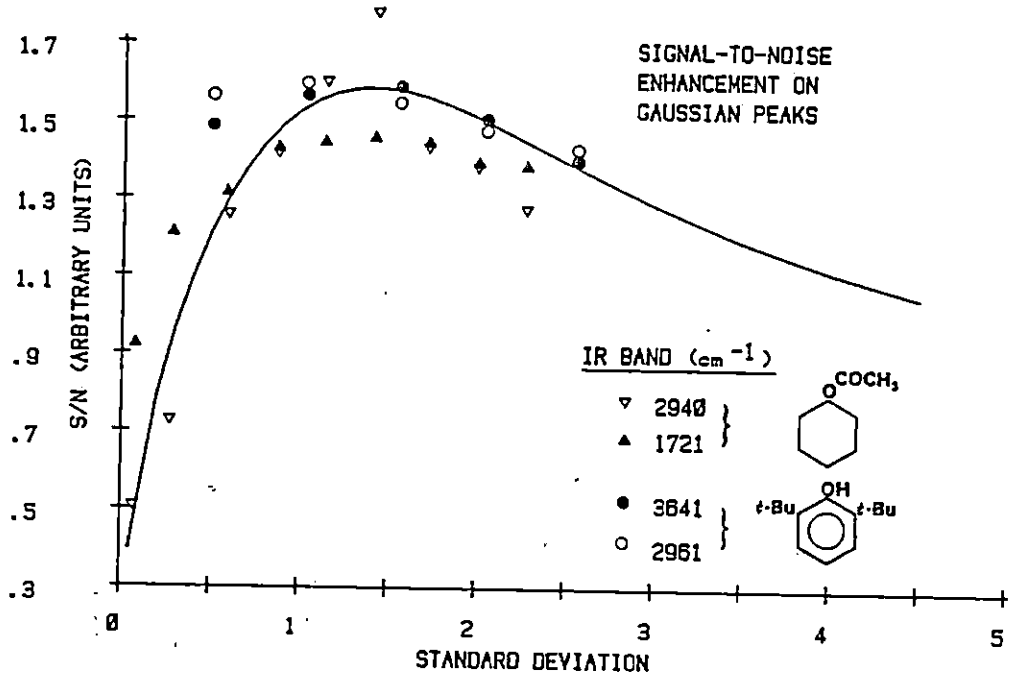

Figure 15. Signal-to-Noise plotted as a function of the amount, $\pm x\sigma$, of a Gaussian peak used for coaddition; (a) Solid Line-Theoretical Curve, (b) Measured S/N (normalized to arbitrary scale) of cyclohexyl acetate and 2,6-di-tert-butylphenol.

here. The elution with chloroform at 45 μL/min of 2,6-di-tert-butylphenol from a microbore silica column was monitored with the FTIR. Co-addition of single-scan files ($\pm 1.37\sigma$) about the peak maximum, which was determined from a Gram-Schmidt reconstructed chromatogram (40), resulted in a series of measured signal-to-noise ratios at 3641 and 2960 cm^{-1}. These ratios were then normalized to an arbitrary S/N scale and superimposed on the theoretical curve in Figure 15.

One would expect better agreement between theory and experiment as the eluted compound is retained longer, which would increase the infrared time resolution. This would increase the confidence in assigning maximum location and the standard deviation of the peak, thereby allowing a more accurate determination of the 1.37σ value in terms of the number of scans to co-add. Additional data points from the 2940 and 1721 cm^{-1} bands of cyclohexyl acetate (Figure 16) were obtained from the flow characteristic study (vide infra). These data appear superimposed on the theoretical signal-to-noise curve in Figure 15 as well. In both cases good agreement between theoretical and experimental signal-to-noise ratios is obtained.

The flow characteristics of the ZDV μ-HPLC-FTIR flow cell were more difficult to determine. One might be tempted to perform a statistical moments treatment to determine the variance contribution of the cell by making injections through a capillary tube directly coupled to the cell. This proved to be quite impractical as the minimum injector volume available, 0.5 μL, was significantly larger than the calculated volume

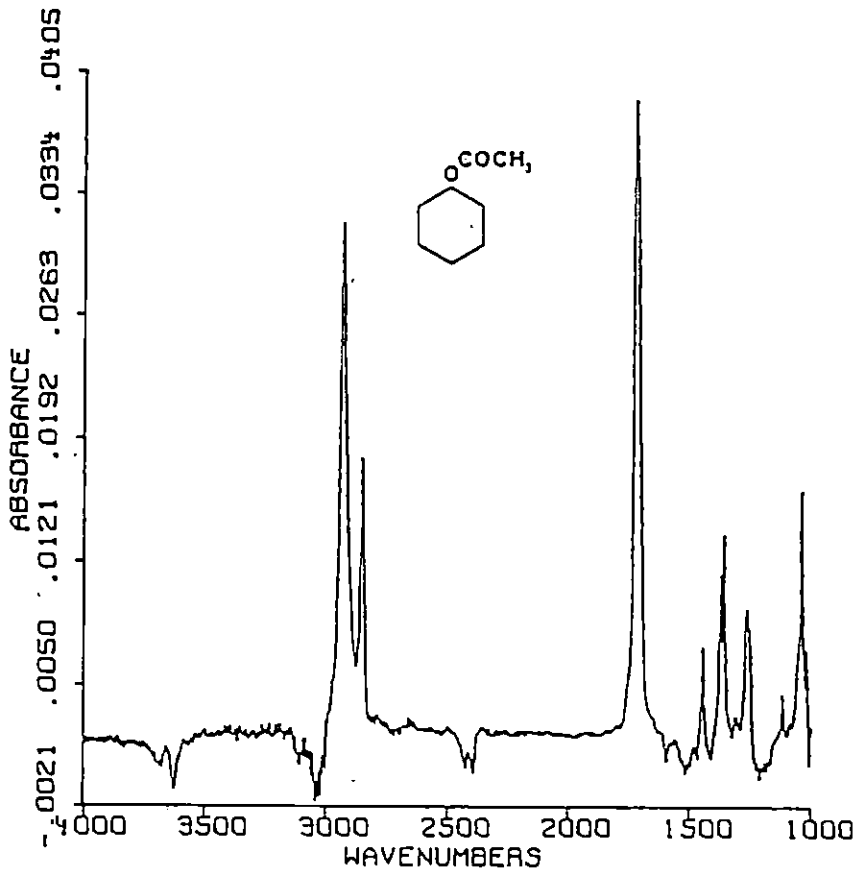

Figure 16. Spectrum of cyclohexyl acetate in chloroform, 5 µg injected into 0.009" ID x 65 cm length tubing, ZDV/CaF_2 flow cell with FTIR detection at 47 µL/min; scans co-added ±1.4σ about peak maximum.

of the cell, 0.33 μL. It has been shown that for a detector cell with such a small volume, the detector variance contribution should be negligible relative to the overall system variance (35).

A comparative approach using the ZDV and previously reported flow cells (46) was chosen. A close-up view of the sealed "ultra-micro" flow cell used in the earlier studies is shown in Figure 17. The major disadvantage of this cell was expected to be the excessive volume created by both the tortuous flow path of the sealed cell and the various gaskets and tubing necessary for connection. This unswept or mixing volume was expected to be observed in the degree to which a sharp, chromatographic peak showed a tailing response. Thus, the peak asymmetry factor, or the distance from the center to the tail of the peak divided by the distance from the center to the front of the peak at 10% of the peak height, was chosen as a comparative measure.

Table III shows the measured characteristics of four flow cells. Several things should be noted. First, cell number I shows significantly more tailing than cell number II despite their identical design. The parallel plate design (Figure 17), which uses a keyhole-shaped spacer to fix the pathlength, requires that the holes drilled in the face of the KBr plate be precisely located at the apex of the slot in the spacer. Cell number II is representative of such a cell. However, the holes drilled in cell number I are considerably off-axis from the desired position. Consequently, a region of dead volume exists in which eddy currents can arise causing peak tailing. Cells number III and IV exhibit consistent flow characteristics,

TABLE III

PEAK ASYMMETRY FOR SEVERAL FLOW CELLS

Cell Number	I	II	III	IV
Type[1]	PP	PP	ZDV	ZDV
Pathlength[2] (mm)	0.2	0.2	0.45	0.45
Material	KBr	KBr	KBr	CaF_2
Volume[3] (μL)	3.2	3.2	0.33	0.33
Peak Asymmetry	1.9	1.3	1.2	1.2
Pathlength/Volume Ratio(mm^{-2})	0.062	0.062	1.36	1.36

[1]PP refers to the "Sealed Ultra-Micro Cell" or Parallel Plate cell; ZDV refers to the Zero Dead Volume cell.

[2]The pathlength for the ZDV Cell is calculated by the ratio of absorbances of a standard solution measured in each cell under the same conditions knowing the pathlength of the PP cell.

[3]Calculated according to geometry from cell inlet to illuminated area.

[4]An injection of 0.5 μL of a standard solution is made into a 0.009" ID x 65 cm length of tubing, which is attached to the flow cell. A flow rate of 45 μL/min of chloroform is used, and the peak shape is followed using single-scan, time-resolved infrared spectra. The peak asymmetry is measured from the Gram-Schmidt reconstructed chromatogram.

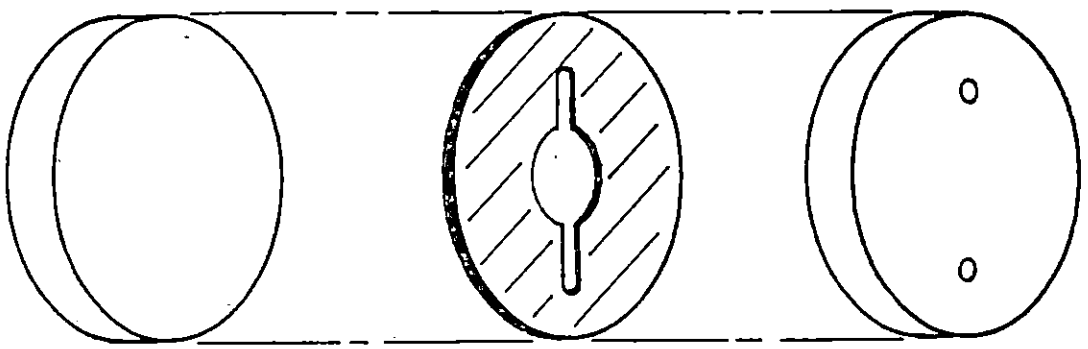

Figure 17. Sealed Ultra-Micro Cell.

probably because of the design simplicity of the ZDV cell. As long as the crystal element is aligned well with the gaskets and microbore column end fitting, a circular flow path is achieved much like that within a tube. Since the infrared viewing area is virtually at the outlet of the column and the end fitting has a 0.75 mm ID, which is the same as that of the flow cell, the volume of the cell is swept cleanly. Thus the asymmetry factor of the ZDV cell is minimal.

The enhanced pathlength/volume ratio should also be noted in the ZDV cell. Not only is the pathlength more than doubled, but the cell volume is decreased by an order of magnitude. Another infrared flow cell used for micro-capillary liquid chromatography with a pathlength of 30 μm and an approximate volume of 54 nL has been reported (49). However, this cell suffers from relatively low sensitivity, attributable to its extremely short pathlength, in spite of its relatively high pathlength/volume ratio of 0.56. The ZDV cell, although currently not applicable to the micro-capillary liquid chromatography/infrared detection experiment, has a higher pathlength/volume ratio (1.36) and has enhanced sensitivity over the parallel plate cell because of its increased effective pathlength.

The ZDV crystal element can be made from a variety of infrared-transparent materials. The two cells listed in the Table were mechanically drilled leaving only a moderately smooth internal surface. This may lead to some scatter of infrared throughput. It has been suggested that ultrasonic drilling may leave a much smoother internal surface (51). Nonetheless, the results presented from the

mechanically-drilled ZDV cell are adequate.

Chromatographically the ZDV cell has been found to perform quite well. A five-component separation of 2,6-di-tert-butylphenol, o-methoxybiphenyl, 2-tert-butylphenol, 2-sec-butylphenol, and cyclohexyl acetate (in order of elution) on silica gel with chloroform elution is shown in Figure 18. This Gram-Schmidt reconstructed chromatogram shows a reasonable signal for all five components, particularly for cyclohexyl acetate. Despite the dilution of this compound at a k' of nearly 3.0, the interferogram has such a distinct change from the baseline interferograms that a very large response is observed. This is probably due to the large absorptivity of the carbonyl stretch. The five-component chromatogram represents an injection of 5 μg of each component in the 0.5 μL injection loop, which is well within the capacity of a 1 mm ID x 50 cm microbore column (52,53).

The file spectra obtained from the five-component separation (co-addition of files ± 1.37σ around each peak maximum) are shown in Figure 19. All have good signal-to-noise ratios, and each contains sufficient information to readily identify the compounds by comparison to library spectra taken in the same solvent. A rather curious feature is absent in these spectra which is quite apparent from spectra obtained with the parallel-plate cell. With a parallel plate-type cell, one observes ratioing errors around regions of total solvent absorbance that graphically give rise to characteristic broad, multiple bands in the spectrum. This annoying feature has been addressed in the Nicolet software by the inclusion of a blanking routine, which causes the

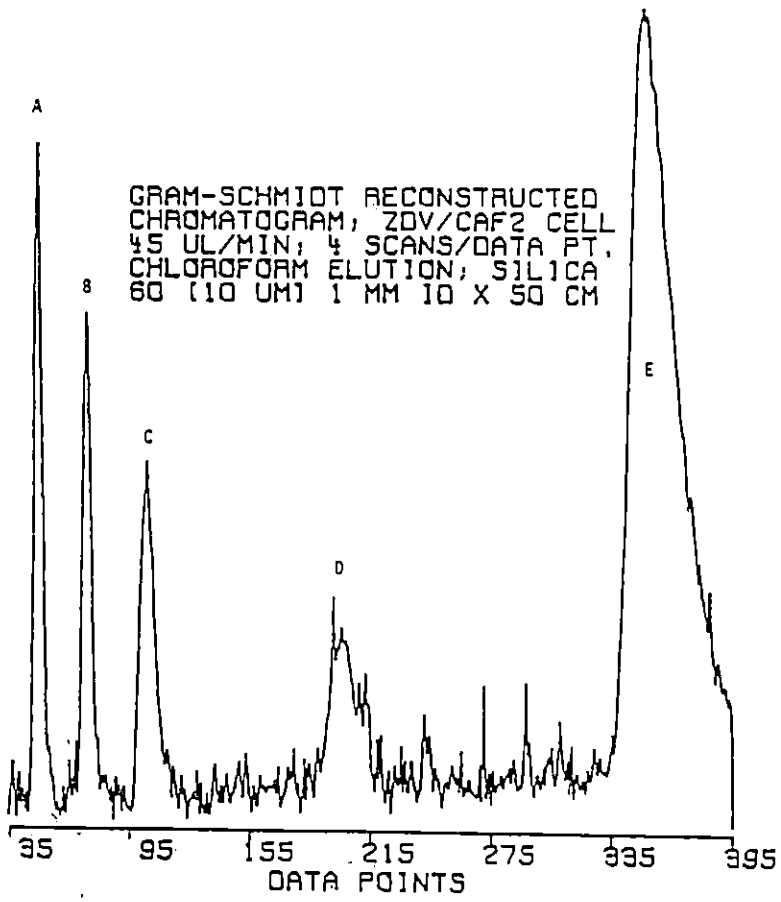

Figure 18. Gram-Schmidt reconstructed chromatogram; ZDV/CaF_2 cell 45 µL/min; 4 scans/data point. Chloroform elution; Silica Gel 60 (10 µm) 1 mm ID x 50 cm.

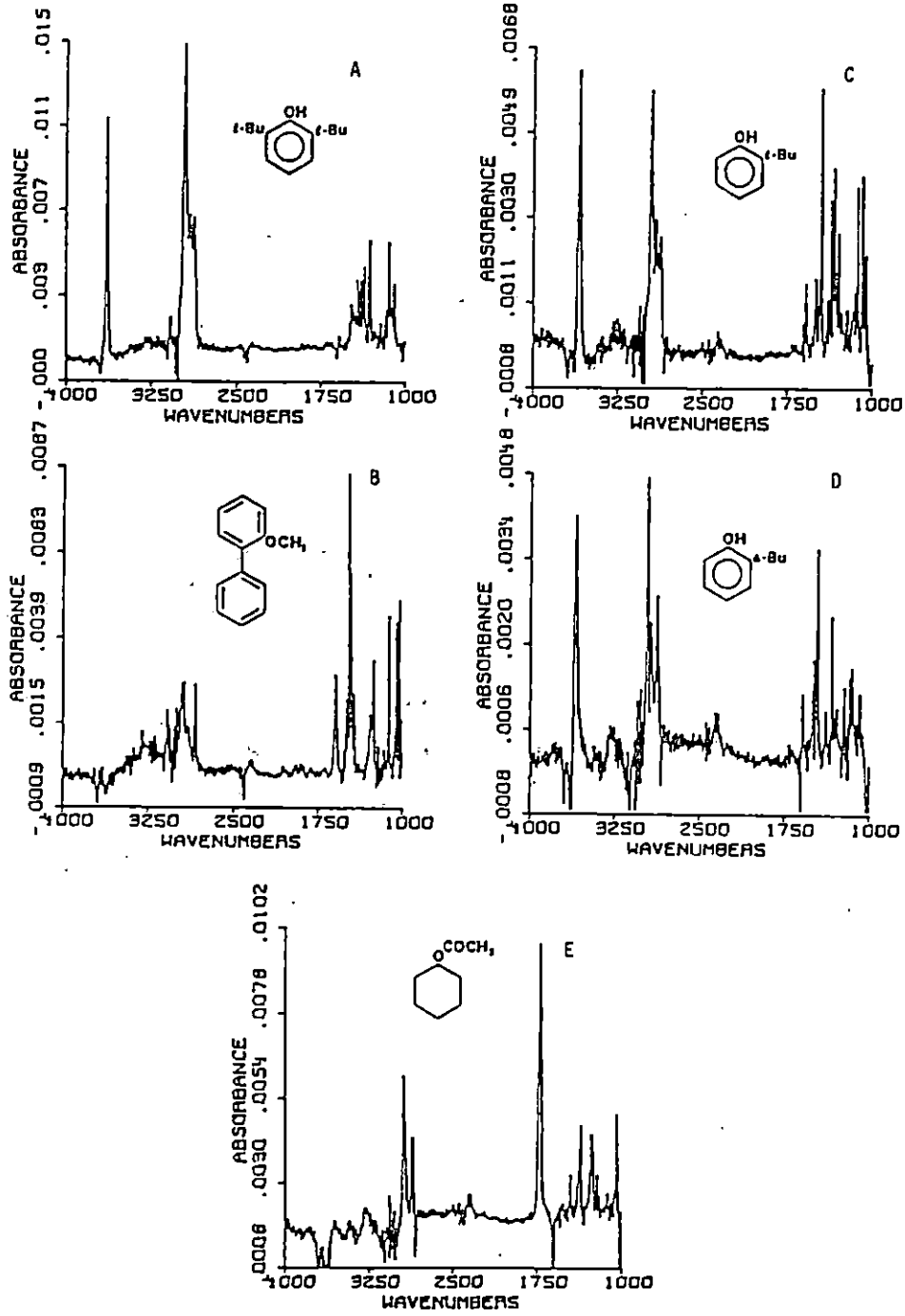

Figure 19. Spectra from separation shown in Figure 18. Co-additon of files across each peak corresponding to limits of $\pm 1.4\sigma$ about the peak maximum was carried out to maximize the signal-to-noise ratio.

display and plotting routines to ignore those regions of the background spectrum whose throughput is below a user-selected threshold. Using the ZDV cell, one does not observe the broad, multiple bands expected at major solvent absorbances, and furthermore no background blanking routine is necessary. Small perturbations in the baseline do occur at those regions where chloroform bands exist, namely 3660-3710 cm^{-1}, 3000-3080 cm^{-1}, 2380-2440 cm^{-1}, 1580-1625 cm^{-1}, 1240-1250 cm^{-1}, 1170-1180 cm^{-1}, and 1020-1000 cm^{-1}. These chloroform bands, considering the pathlength of the cell, are consistent with the "optimal pathlength" diagrams developed by Vidrine (21).

If one considers the origin of the broad, multiple bands observed in the parallel plate cell, the understanding of the ZDV cell performance is facilitated. Operationally, a background spectrum of solvent in the cell is collected as an interferogram in the distance domain and stored. At the appropriate time, a spectrum is collected and stored of both the sample and solvent in the cell. After the chromatographic run is completed, the interferograms are retrieved from the disk and individually Fourier processed by the computer. This includes phase calculation, apodization, Fourier transformation and final phase correction. The result is a single-beam transmission spectrum of each file. Strong solvent bands in the infrared give rise to virtually no throughput; while weaker bands merely attenuate the throughput at each characteristic frequency. Ideally, if the sample spectrum had only solvent in it, the single-beam transmission spectra of the sample and the background would be identical. A normal percent

transmission spectrum could be obtained by dividing each data point in the sample spectrum by the corresponding point in the background spectrum. One would expect the resulting spectrum to be featureless and uniformly exhibit 100% T.

Mathematically, however, regions in which the solvent is opaque to infrared radiation result in response values in the single-beam spectra of zero. Thus, when the %T spectrum is obtained, those IR regions near solvent bands are calculated as a ratio of two numbers very close to zero. Obviously if the numerator is non-zero, division by zero is unattainable. Division of a small number, say 10^{-3} units, by a much smaller number, say 10^{-9}, gives 10^{6} as a result. If the numerator and denominator are interchanged, 10^{-6} is obtained. Slight noise fluctuations causing minor differences such as these around solvent bands can give rise to very large deviations from the 100% T line, both positively and negatively. Consequently, if one plots an infrared spectrum of a strongly IR absorbing solvent, broad, multiple bands, which are essentially amplified noise, are observed in regions of solvent opacity.

The ZDV cell, on the other hand, is cross-sectionally circular. Solvent absorbances in the infrared are not affixed to a single pathlength. On the contrary, the solvent slice at the center of the flow cell gives rise to absorbances characteristic of 0.75 mm pathlength; the slices at the edge of the flow cell give rise to absorbances characteristic of pathlengths approaching zero. Since the infrared beam is not forced using masks or slits to traverse the cell at

only the long pathlength regions, the detector "sees" the average signal across the entire cell. Sufficient throughput is therefore observed at the edges of the cell to add a constant offset to the single-beam spectra.

Using the previous mathematical example, if the offset at a particular solvent band is 10^{-1} units in a single beam spectrum, and we use the values of 10^{-3} for sample and 10^{-9} for background, the ratio of the offset plus sample to offset plus background results in a value of 101%T. If, because of noise variations, the two are switched, a value of 99%T is obtained. Thus, the ZDV cell avoids the problems associated with solvent absorbance while parallel plate cells merely amplify noise contributions in regions of high solvent absorbance. It should be noted that even though these artifacts are not observed, these regions nevertheless remain opaque to dissolved, IR absorbing analytes.

By adding an offset to the single-beam spectra, however, it is evident that Beer's law linearity may be suspect. On the other hand, Hirschfeld has shown that by simultaneously measuring infrared spectra at multiple pathlengths, the dynamic range, particularly at low signal-to-noise regions of the spectrum, is enhanced (54). If the geometry of the ZDV cell were to increase the dynamic range, especially by enhancing the detectability at low concentrations in the μ-HPLC-FTIR experiment, the inconvenience of constructing detailed calibration curves to correct for nonlinearity would be well worth the effort.

A study to determine the detection limits of 2,6-di-tert-butylphenol was undertaken using both the ZDV flow cell and the optimal

peak area co-addition technique previously developed in this paper. A summary of the results for the hydroxyl stretch (3641 cm^{-1}) is given in Table IV. Numerical analysis of the data not only demonstrates excellent linearity (r=0.997), but also gives a detection limit of 40 ng, which is a significant improvement over the previously reported detection (1670 ng) limit for 2,6-di-tert-butylphenol employing this vibrational mode (46). Figure 20 shows a plot of the lowest three amounts injected as well as the spectral features in the hydroxyl stretch region where these measurements were taken. It is apparent that the detection limit is indeed below 50 ng. Significantly lower detection limits are expected using the asymmetric methyl bend at 1426 cm^{-1} (46) where the FTIR detector sensitivity is greater. Unfortunately, the observed asymmetric methyl bend using the ZDV cell is much weaker than that observed with a parallel plate cell of 0.2 mm pathlength. The effective pathlength of the ZDV cell, because of its multiple pathlength geometry, is substantially decreased at 1426 cm^{-1} because the chloroform solvent has a relatively strong overtone band of the carbon-chlorine stretch near that frequency. This makes the long pathlength regions of the ZDV cell opaque, while the short pathlength regions are transparent but attenuated. The result is an effective decrease in pathlength. This phenomenon of variable pathlength in multipath cells has been discussed in detail (55). Consequently, further enhancements in detectability on 2,6-di-tert-butylphenol will have to be made using more transparent solvents in this region of the spectrum.

TABLE IV

Minimum Detectable Quantity Determination of 2,6-di-tert-butylphenol Using ZDV Flow Cell and Peak Area Co-addition of Interferograms.

Amount Injected (ng)	A(3641 cm^{-1})	N_{RMS}(3500-3575 cm^{-1})
50	0.000538	0.000161
200	0.001541	0.000122
500	0.002156	0.000178
1000	0.004049	0.000170
2500	0.01229	0.000170
5000	0.02156	0.000231

$\overline{N}_{RMS}$ = 0.000172

Linear regression analysis:

b (y-intercept) = 0.000358

m (slope) = 4.32x10-6

r = 0.997

[Detection limit taken at $3xN_{RMS}$]

37 ng gives a signal on least squares curve of 0.000518

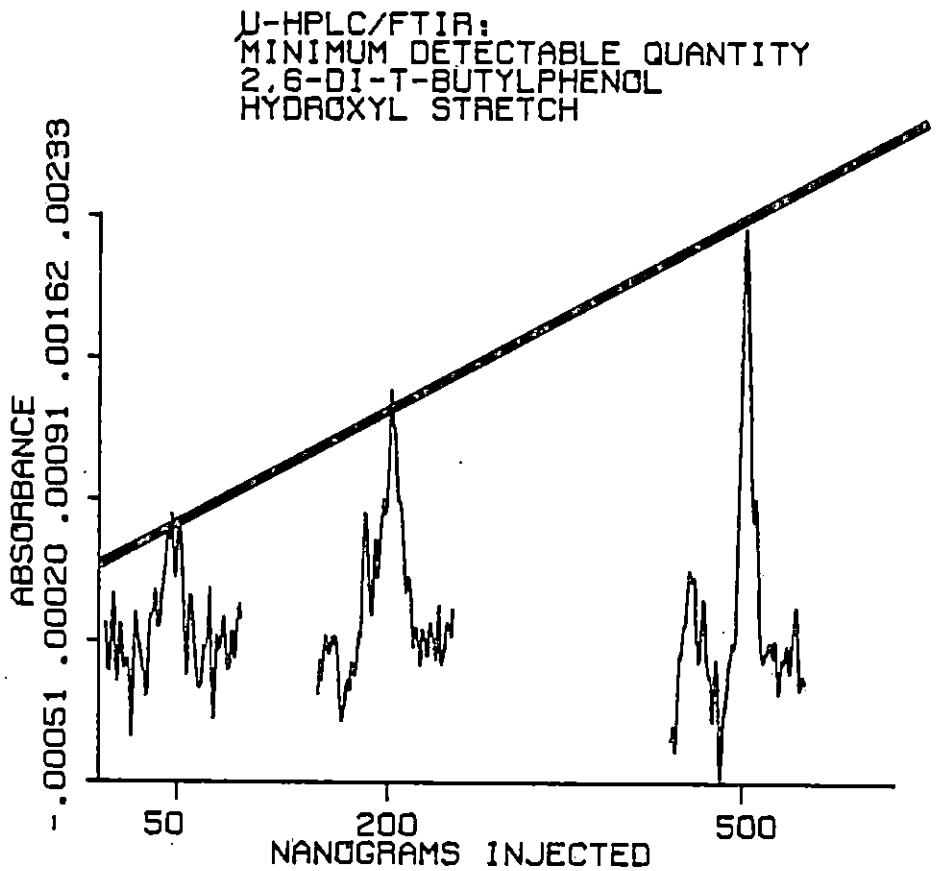

Figure 20. Minimum detectable quantity of 2,6-di-tert-butylphenol using hydroxyl stretch.

CONCLUSIONS

Through this study several conclusions can be drawn. First, it is apparent that although maximum infrared signal at a particular frequency can be obtained in μ-HPLC-FTIR experiments using the infrared scan taken at the chromatographic peak maximum, the maximum signal-to-noise is observed by integrating across the peak to $\pm 1.37\sigma$ from the peak maximum. Second, the FTIR has been shown again to be a concentration-dependent detector for chromatography. Although the early treatment of this matter for GC-FTIR implied that the FTIR has some characteristics of a mass-sensitive detector (22), it has been demonstrated that for the μ-HPLC-FTIR experiment, this is not the case. It is much more beneficial, consequently, to modify optically the infrared beam to fit a suitable chromatographic cell for the μ-HPLC-FTIR experiment than it is to try to force fit the chromatographic system into the existing spectrometric system. Since the concentration profile of a μ-HPLC separation is more closely followed as the detector cell volume decreases, the μ-HPLC-FTIR experiment requires a very-small-volume flow cell. Finally, a multitude of improvements have resulted in enhanced detection limits for μ-HPLC-FTIR. These improvements include the use of a cell with a longer effective pathlength, more sensitive MCT detector, and better data handling methodology. The total of these improvements probably does not enhance the detection limits to the extent observed. It appears that the extended dynamic range expected from a cell with a non-uniform pathlength is the missing contribution to the observed sensitivity enhancement.

CHAPTER 4

REVERSED-PHASE LIQUID CHROMATOGRAPHY WITH FOURIER TRANSFORM INFRARED SPECTROMETRIC DETECTION USING A FLOW CELL INTERFACE

INTRODUCTION

In the previous chapters, several developments involving the Fourier Transform Infrared (FTIR) spectrometer as a detector for normal-phase high performance liquid chromatography (NP-HPLC) employing a flow cell interface (45-48,56) have been described. These developments described the use of semi-preparative, analytical, and microbore scales of NP-HPLC applied to the identification of nonpolar and polar components in various coal-derived products. Earlier work had shown moderate sensitivity for this technique, but a greater problem at the time was the infrared absorbance by the mobile phase (21). The use of chlorinated and deuterated solvents in our work has afforded ample mobile phase transparency for flow cell HPLC-FTIR. Furthermore, various methodological and flow cell improvements have now yielded detection limits below 40 ng of injected material (56).

Aqueous-based, reversed-phase systems are reportedly used in well over 60% of all HPLC separations. Unfortunately the intense infrared bands of water and methanol, and to a lesser degree tetrahydrofuran and acetonitrile, necessitate very short optical pathlengths if adequate infrared transparency is to be observed over a relatively wide range of IR frequencies in flow cell RP-HPLC-FTIR experiments (21,49). This consequent lack of sensitivity has severely limited the utility of reversed-phase systems with infrared detection using flow cells. Several strategies which have been used include nonaqueous reversed

phase separations (57) and monitoring only C-H and C=O absorption regions (58). Even the off-line HPLC-DRIFT (Diffuse Reflectance Infrared Fourier Transform Spectrometry) method has been unsuitable to date for RP-HPLC-FTIR because of the inability of the KCl used for eluent deposit to tolerate even small amounts of water (26,43).

Several approaches to RP-HPLC-FTIR are currently being pursued; all involve removal of water from the HPLC effluent. One approach incorporates the post-column, acid-catalyzed reaction of 2,2-dimethoxypropane with water in the mobile phase to form acetone and methanol (59). The reacted RP-HPLC effluent is then deposited onto KCl substrate for DRIFT detection. The acetone and methanol have sufficient volatility that this approach has had reasonable success. It is not yet clear what classes of compounds can be used with 2,2-dimethoxypropane without sample derivatization occurring.

A less intrusive but slightly more complicated approach to RP-HPLC-FTIR incorporating both DRIFT detection and segmented, flowing extraction has been reported recently (60,61). Briefly, the components in the effluent from the RP-HPLC separation are extracted in a segmented stream (29) into methylene chloride. The two phases are separated by density using a tee in which the similar solvent segments recombine and flow out either of the opposing coaxial ends. The organic stream is then deposited onto the KCl substrate according to the usual DRIFT procedure. The method, however, suffers from several problems. The number of critical instrumental components (i.e. the FTIR system, the HPLC system, the flowing extraction system, plus the DRIFT interface) has become excessively large. The integrity of the KCl substrate for

diffuse reflectance measurements is affected by residual water. Methylene chloride, being slightly soluble in water as well as miscible with methanol, carries a considerable amount of dissolved water with methanol onto the KCl substrate. This inherent drawback may limit the applicability and/or sensitivity of RP-HPLC-FTIR using the DRIFT interface.

The RP-HPLC-FTIR problem is approached using a flow cell interface. In this chapter, preliminary results from experiments which employed (i) flowing extraction of the RP-HPLC effluent, (ii) subsequent separation of the immiscible solvents using a hydrophobic membrane, and (iii) FTIR detection with a flow cell interface are discussed. This approach appears to be a less intrusive but a more pragmatic method for the RP-HPLC-FTIR experiment.

EXPERIMENTAL

A schematic diagram of the entire instrument is shown in Figure 21. The individual components are described below.

HPLC System

An IBM Instruments Model LC/9533 Ternary Gradient Liquid Chromatograph (Danbury, CT), equipped with a Rheodyne Model 7125 Injector (Cotati, CA) and an IBM Instruments Model LC/9522 fixed wavelength (254 nm) UV detector, was used. The fixed injection loop size was 20 μL, although several injections were made with partial loop filling. The HPLC column, an IBM 4.6 mm ID x 25 cm 5 μm octadecyl bonded silica (C18), was employed in all experiments. Model compound mixtures were eluted with 65% HPLC grade methanol (Fisher, Fairlawn,

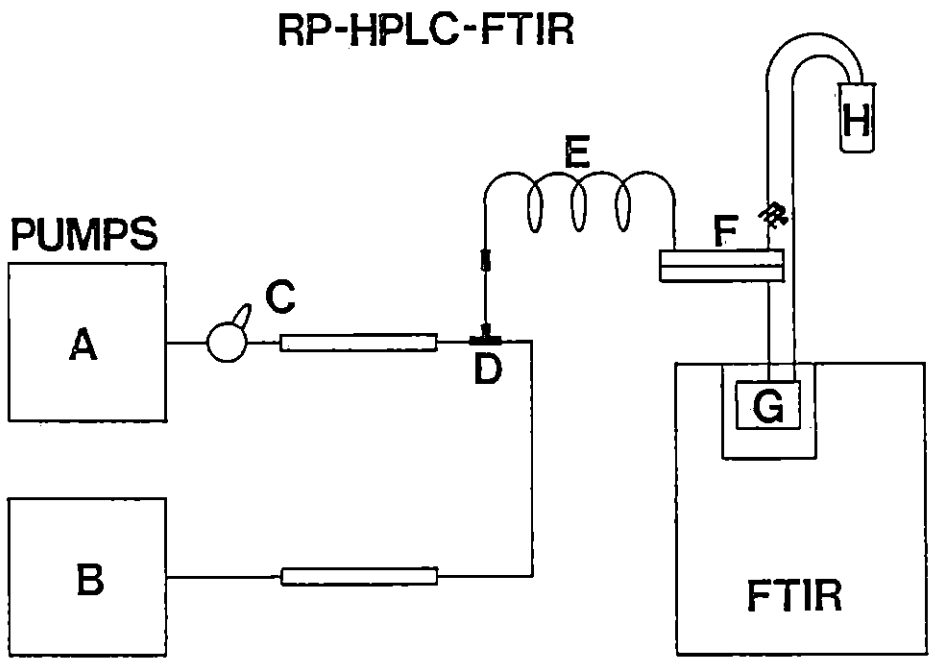

Figure 21. Schematic Diagram of RP-HPLC-FTIR Instrument.
A) Pump delivering methanol/water solution
B) Pump delivering extraction solvent
C) HPLC Injector and C18 column
D) Segmenting Tee
E) Extraction coil
F) Membrane Phase Separator
G) Zero Dead Volume Flow Cell Interface
H) Waste

NJ), 35% water (distilled and deionized in-house) at a flow rate of 0.8 mL/min for all experiments. A Waters Associates Model R401 Refractive Index Detector (Millford, MA) was used for some auxillary experiments.

Extraction System

A second IBM Instruments Model LC/9533 Ternary Gradient Liquid Chromatograph delivered the extraction solvent to the mobile phase at a flow rate of 1.0 mL/min for all experiments. An IBM 4.6 mm ID x 25 cm 5 μm silica column provided back pressure to the pump in order that reliable solvent delivery could be achieved. Extraction solvents were ethanol-free chloroform and carbon tetrachloride (Burdick and Jackson, Muskegon, MI). To create a segmented stream, the extraction solvent and RP-HPLC effluent streams were combined in a standard Swagelok SS-100-3 Tee Union. These streams were connected to the opposing coaxial ports of the tee. A 1 mm ID x 10 cm stainless steel tube was attached to the sidearm to permit proper formation of the exiting segmented extraction stream. A 0.5 mm ID x 1 m length of PTFE tubing, connected to the sidearm tube, provided a residence time for extraction prior to phase separation.

The membrane separator (62), shown in Figure 22, was machined from 316 stainless steel. The connections were made to accommodate standard flanged PTFE connectors. The volume on either side of the membrane was calculated to be 16 μL. The membrane material was an expanded PTFE with 0.2 μm pores (Gore-Tex, W. L. Gore, Elkton, MD). The Gore-Tex membrane, when compressed, provided a seal between the polished faces of the membrane holder. By regulating the differential pressure across the

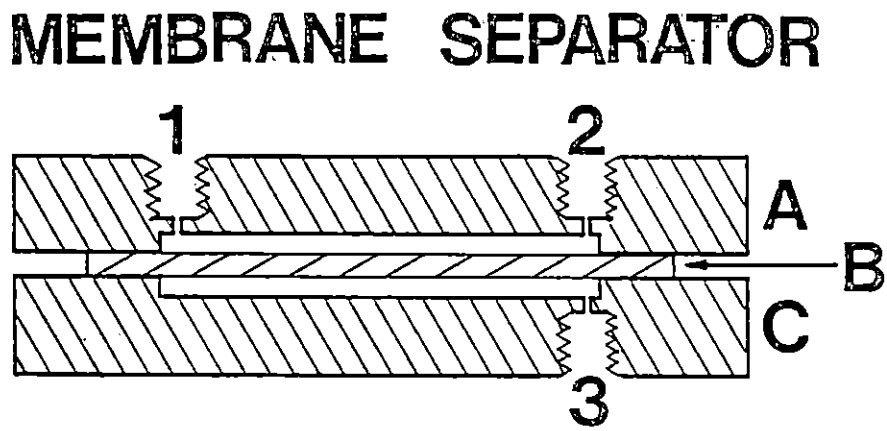

Figure 22. Cross-sectional view of membrane separator.
A) and C) Upper and Lower Stainless Steel membrane holders
B) 0.2 μm Gore-Tex membrane
1) Segmented stream inlet
2) Aqueous waste outlet
3) Organic phase outlet

membrane with a tubing clamp on the segmented stream outlet, the amount of organic solvent that is squeezed through the Gore-Tex membrane can be controlled. A 45 cm length of 0.3 mm ID PTFE tubing was used to connect the outlet of the separator to the FTIR interface.

FTIR System

A Nicolet 6000C FTIR (Madison, WI) equipped with a narrow-band (5000-700 cm^{-1}) Model 7010A Mercury-Cadmium-Telluride (MCT-A) detector was used for these experiments. Time resolved, 4 cm^{-1} resolution spectra were collected with the standard Nicolet software package. In all cases, four interferograms were co-added and stored as a single file, thus giving time resolution between each collected file of ca. 3 seconds. The zero dead volume (ZDV) flow cell interface used for this study has been previously reported (56). The ZDV cell crystal used was drilled from CaF_2, and had an effective pathlength of ca. 0.5 mm. A Barnes Model 600 4x Beam Condenser (Spectra-Tech, Inc., Stamford, CT) was used to reduce the infrared beam focal diameter to ca. 0.75 mm, thereby providing an effective cell volume of 0.33 µL.

Sample Mixtures

A ketone model mixture was prepared by mixing 1.0g of each of the following: cyclohexanone (Eastman Organic Chemicals, Rochester, NY), acetophenone and benzophenone (both Fisher certified, Fairlawn, NJ). This mixture was diluted to 0.5% v/v in the mobile phase (65% methanol/35% water) to provide a stock solution. Another concentrated column test mixture was prepared as follows: 0.16g phenol (J. T. Baker USP grade, Phillipsburg, NJ), 0.16g acetophenone, 0.16g nitrobenzene,

0.16g methyl benzoate (all Fisher certified, Fairlawn, NJ), and 0.16g toluene (Fisher HPLC grade, Fairlawn, NJ) were dissolved in 1.0g of methanol (Fisher HPLC grade, Fairlawn, NJ). This mixture was filtered through a 0.45 μm Swinny filter prior to injection.

RESULTS AND DISCUSSION

The objective of this study was to demonstrate the feasibility of using the FTIR as a detector for reversed-phase HPLC with a flow cell interface. With the use of the post-column flowing extraction method in the interface, two questions need to be addressed: Is the resulting extract sufficiently transparent in the mid-infrared to yield spectra of the eluents; and, does the partitioning between the HPLC solvent system and the organic extraction solvent favor the organic phase for a wide variety of compounds? This discussion concerns the interpretation of current results with respect to these two questions.

Methanol and water both exhibit maximum transparency at approximately 1800 cm^{-1} (21). Even at this maximum, the mid-infrared throughput is extremely low for pure methanol or water. It has been suggested that the longest, practical pathlength for an infrared flow cell directly coupled to a reversed-phase HPLC column is approximately 25 μm. At such a low pathlength, the infrared sensitivity is too low for the FTIR to be practically used as an HPLC detector. It was hoped in this study that the extraction system, which incorporates the membrane phase separator, would greatly reduce the concentration of the water and methanol in the effluent without significantly reducing the analyte concentration.

A separation of a mixture containing three ketones was chosen for the first extraction experiment because of the intense carbonyl stretching vibration that is observed near the frequency of maximum IR throughput in methanol and water. Initial separations without flowing extraction are shown in Figure 23. With UV detection at 254 nm, which is perhaps the most widely used RP-HPLC detector, only benzophenone and acetophenone are detected (Figure 23A) with good sensitivity. If the column loading and attenuation are increased, cyclohexanone is detected as a very weak peak by the UV-254 nm detector (Figure 23B). A further increase in column loading allows the use of a refractive index detector. In this case, only cyclohexanone and acetophenone are detected (Figure 23C) with reasonable sensitivity while benzophenone gave a fairly weak response. In fact, the impurity eluting just after benzophenone shows an equal RI response close to that of benzophenone.

The first solvent extraction attempted was with chloroform since this solvent has relatively good infrared transparency. A Gram-Schmidt reconstructed chromatogram of the separation (i.e. flowing extraction and phase separation) with FTIR detection is shown in Figure 24. Only the first two peaks are detected, and the spectra obtained (Figure 25) are relatively poor. Enough analyte has been extracted to give a good response for the carbonyl stretch, but the concentration of water and methanol in the chloroform is great enough that the regions on either side of the carbonyl are virtually opaque to the infrared. The observed carbonyl stretching frequencies, however, are indicative of each of the two compounds. The third component, benzophenone, is not observed using the FTIR probably because of its low extractability into chloroform

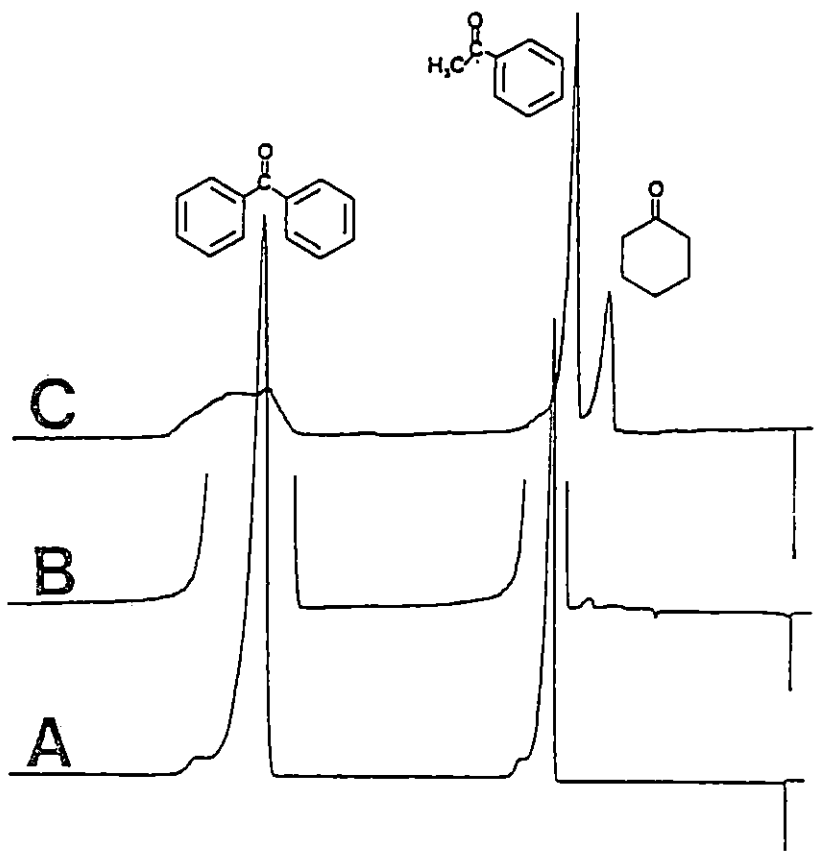

Figure 23. Ketone separation on C18.
A) UV254, 0.500 AUFS, 5 µL Injection of 10% v/v solution
B) UV254, 0.050 AUFS, 20 µL Injection of 10% v/v solution
C) RI, 4x Attenuation, 5 µL Injection of stock solution

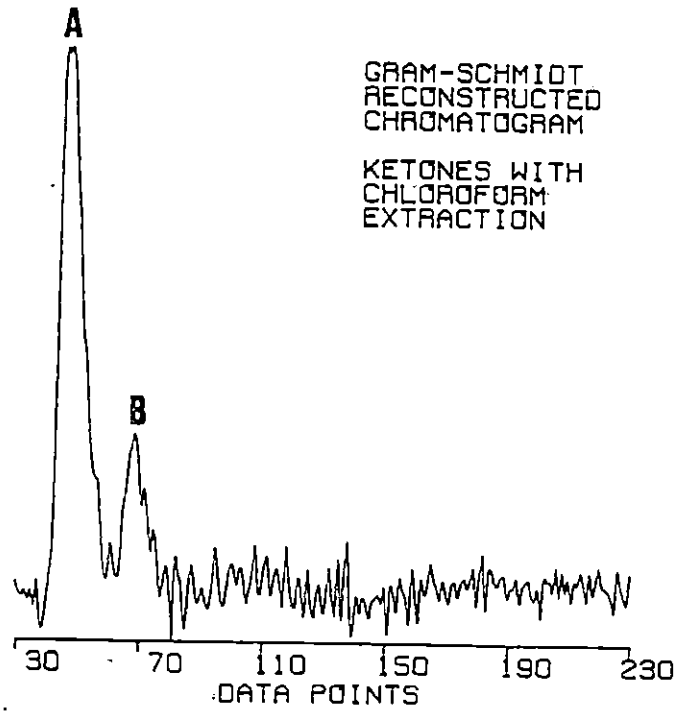

Figure 24. Gram-Schmidt reconstructed chromatogram from FTIR detection of Ketone separation with chloroform extraction. 5 µL of stock solution injected.

A) Cyclohexanone
B) Acetophenone; Benzophenone not detected

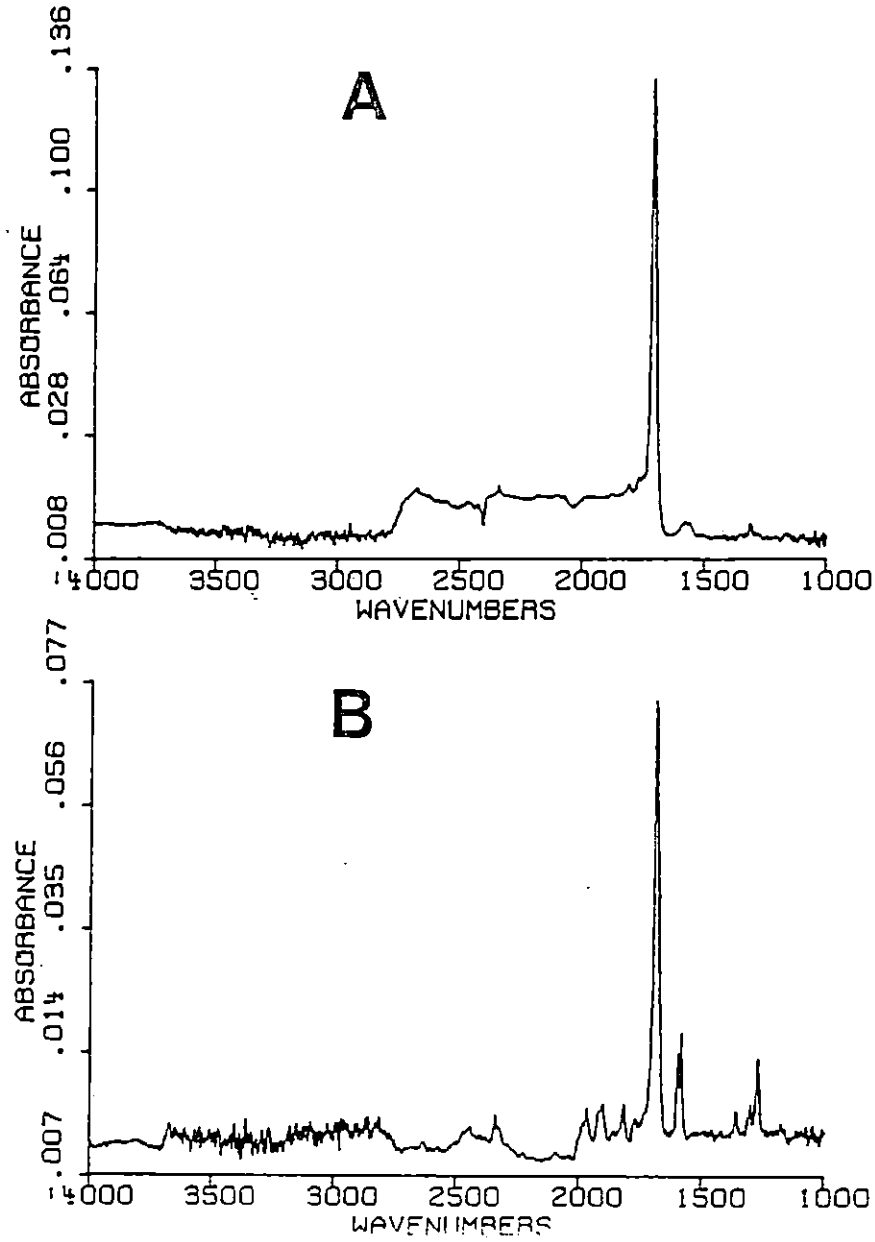

Figure 25. Infrared spectra obtained from Ketone separation with chloroform extraction.

A) Cyclohexanone
B) Acetophenone

under these conditions.

It should be noted that the ZDV cell used in these experiments, because of its multi-pathlength, circular cross-section, does not show solvent bands in the resulting spectra. Although a zero absorbance baseline is observed across strong solvent bands, the solution remains opaque to the infrared in these regions. Consequently, sample spectra are obscured in those regions where strong infrared absorbance due to the solvent are expected. This phenomenon has been previously discussed (56).

Closer inspection of the acetophenone spectrum (Figure 25B) reveals that several bands other than the carbonyl stretch are weakly observed. For example, the substitution overtone bands between 2000 and 1750 cm^{-1} appear to be slightly exaggerated relative to the C=O stretch. This suggests that the intensity of the observed carbonyl stretch is somewhat attenuated because of the reduced throughput at this particular wavenumber resulting from the methanol and water that have dissolved in the chloroform. In any event, the weakly observed bands are not particularly useful for comparison to library spectra because of the intensity distortions that have resulted.

The results from the chloroform extraction experiments nevertheless encouraged further investigation into the development of flow cell RP-HPLC-FTIR. The major problem with the use of chloroform as the extraction solvent appeared to be excessive solubility for the water/methanol mobile phase. Carbon tetrachloride was next investigated as an extraction solvent. Not only does carbon tetrachloride have very good window regions in the mid-infrared, but this non-polar solvent

dissolves a wide variety of compounds as well. Also, the solubility of water in carbon tetrachloride is much less than in chloroform.

An experiment involving a separation of the same three ketones gave greatly improved results when carbon tetrachloride was used as the extraction solvent. The Gram-Schmidt reconstructed chromatogram is shown in Figure 26. Comparison to the reconstructed chromatogram obtained using chloroform as the extraction solvent reveals that not only are all three ketones detected, but also the signal-to-noise ratio is much better using carbon tetrachloride. The corresponding spectra are shown in Figure 27. These spectra also have extremely good signal-to-noise ratios. Furthermore, these spectra match standard, library reference spectra peak for peak, thus allowing conclusive identification.

Inspection of the single-beam spectra (Figure 28) of the background using chloroform and carbon tetrachloride as extraction solvents reveal that carbon tetrachloride extraction has indeed afforded greater IR transparency. The methanol bands, which are quite apparent in the chloroform extraction spectrum, are virtually absent in the carbon tetrachloride extraction spectrum. In addition, the intense, characteristic water absorbances at each end of the mid-infrared spectrum are observed to a much lesser degree when using carbon tetrachloride. Although the absolute amount of water and methanol extracted into the carbon tetrachloride is unknown, the infrared transparency of the solution is more than adequate. This clearly explains the increased quality of IR spectra using carbon tetrachloride.

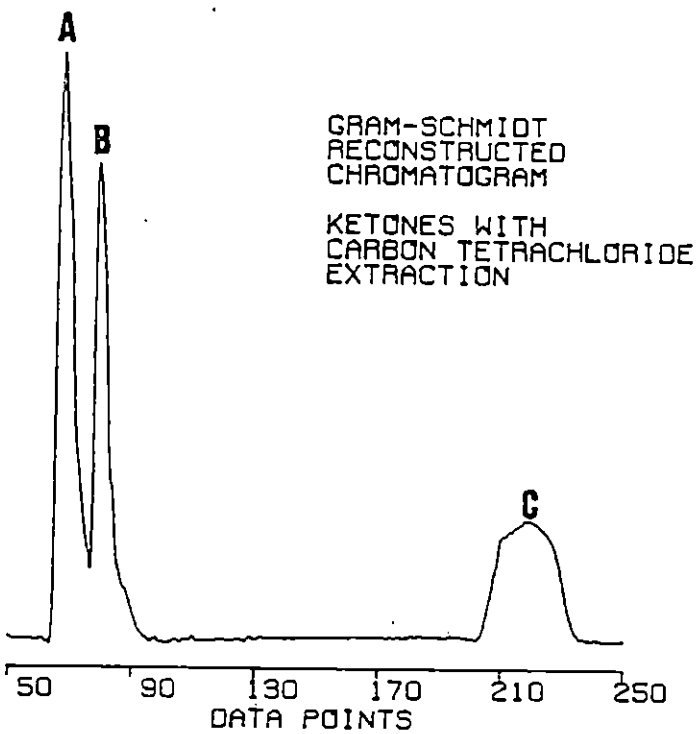

Figure 26. Gram-Schmidt reconstructed chromatogram from FTIR detection of Ketone separation with carbon tetrachloride extraction.

A) Cyclohexanone
B) Acetophenone
C) Benzophenone

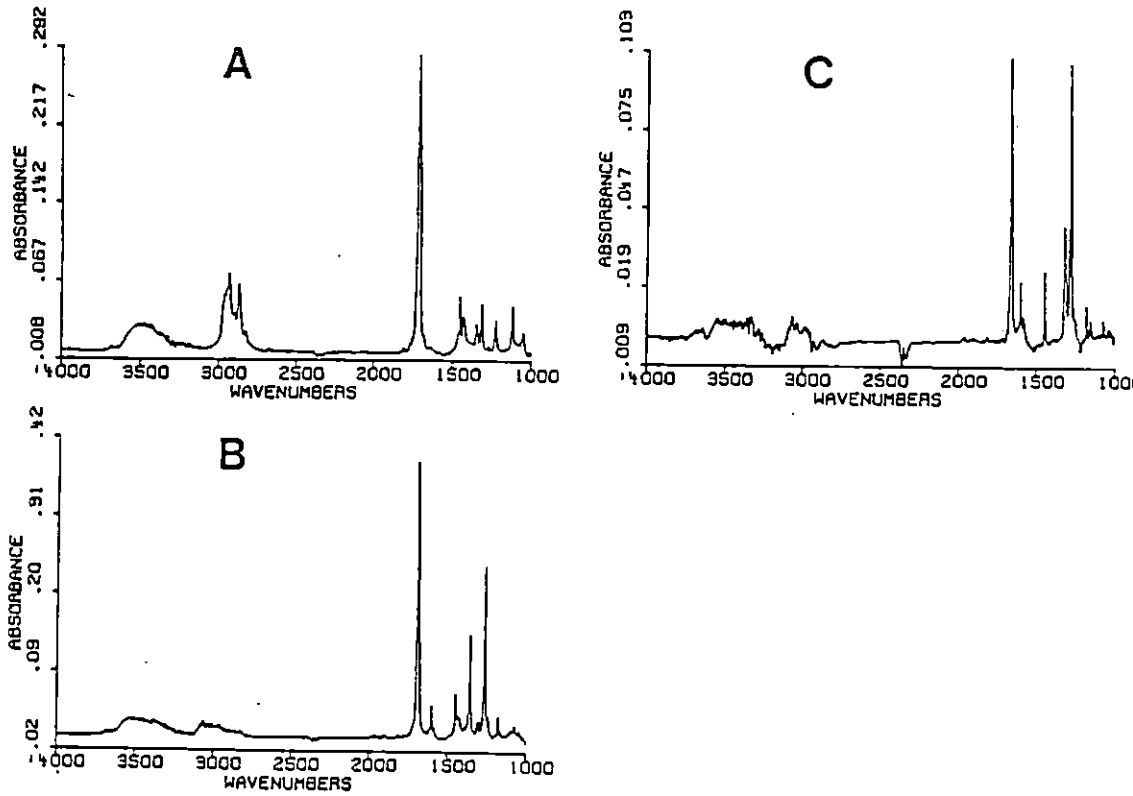

Figure 27. Infrared spectra obtained from Ketone separation with carbon tetrachloride extraction.

A) Cyclohexanone
B) Acetophenone
C) Benzophenone

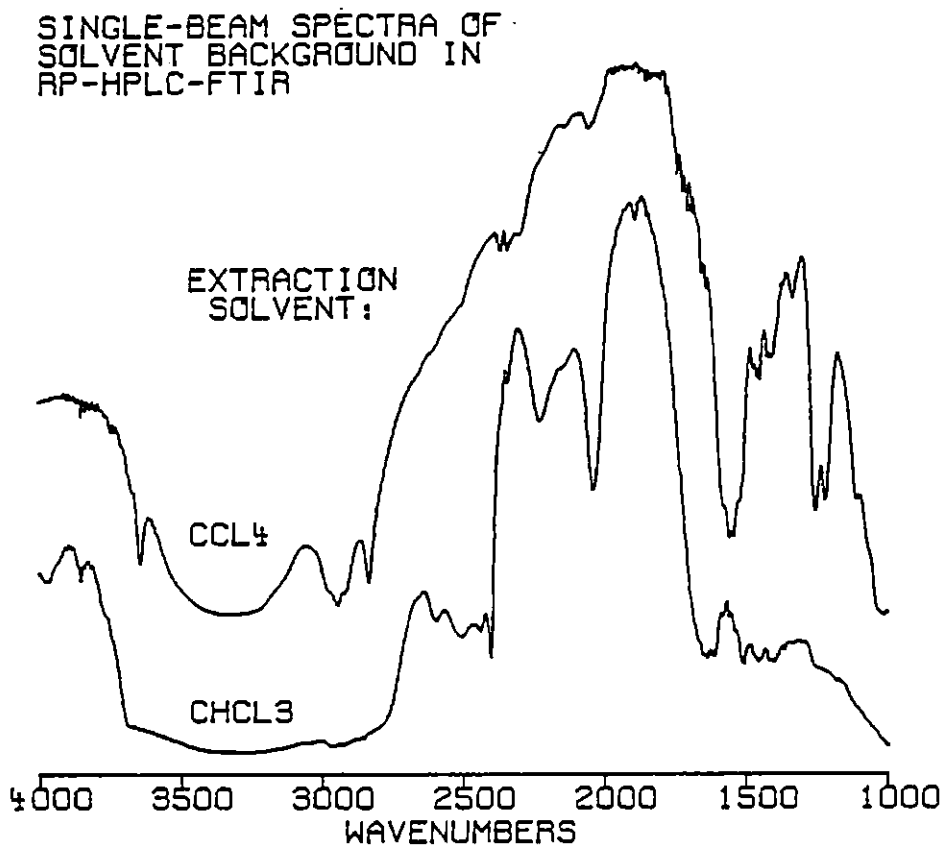

Figure 28. Single-Beam spectra of solvent background in RP-HPLC-FTIR using carbon tetrachloride and chloroform as extraction solvents. The arbitrary y-axis is normalized for each spectrum to the same scale; the CCl_4 spectrum is offset in the y-direction.

The final concern of this preliminary study is whether or not carbon tetrachloride extracts a wide variety of compounds. A five-component test solution in methanol was injected on the RP-HPLC-FTIR system using carbon tetrachloride as the extraction solvent. The resulting Gram-Schmidt reconstructed chromatogram is shown in Figure 29. The five components (i.e. phenol, acetophenone, nitrobenzene, methylbenzoate, toluene), which represent a wide range of polarities, are distinctly detected as well as the solvent front. The corresponding spectra are shown in Figure 30. Again, excellent signal-to-noise is observed in the spectra. Comparison to standard, library reference spectra conclusively identifies each of the five components.

In summary, we have demonstrated for the first time a practical method for flow cell detection of reversed-phase HPLC eluents using the Fourier Transform Infrared spectrometer. No attempt has been made to optimize the extractor/separator portion of this apparatus. In spite of this, readily identifiable, high signal-to-noise, on-line spectra are obtained with less than 300 μg of injected sample. Carbon tetrachloride has been demonstrated to possess all of the necessary characteristics for it to be employed as an infrared-transparent, flowing-extraction solvent. This RP-HPLC-FTIR method shows great promise as the various components in the scheme are optimized.

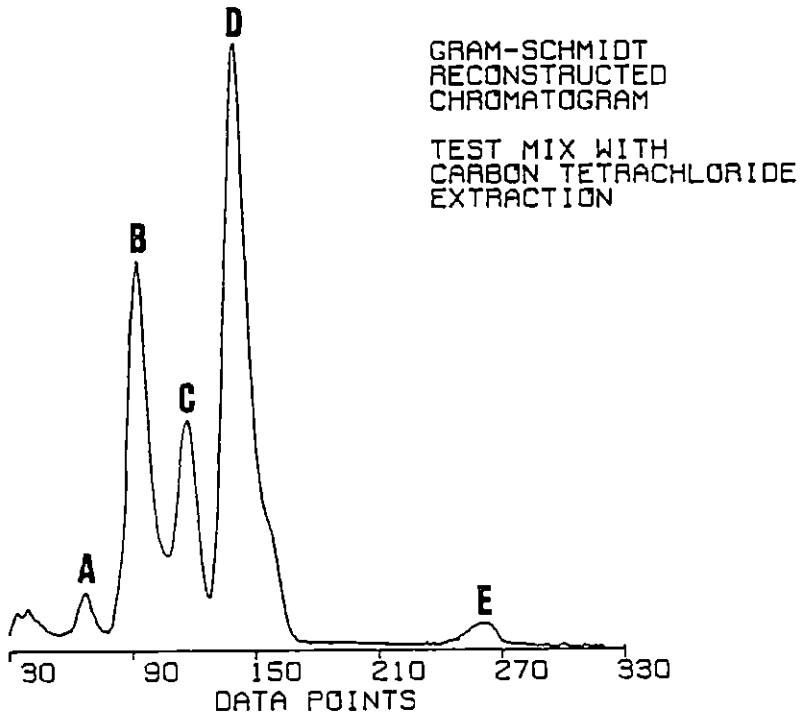

Figure 29. Gram-Schmidt reconstructed chromatogram from FTIR detection of test mixture separation with carbon tetrachloride extraction. 5 µl of stock solution injected (ca. 300 µg of each component).

A) Phenol
B) Acetophenone
C) Nitrobenzene
D) Methyl benzoate
E) Toluene

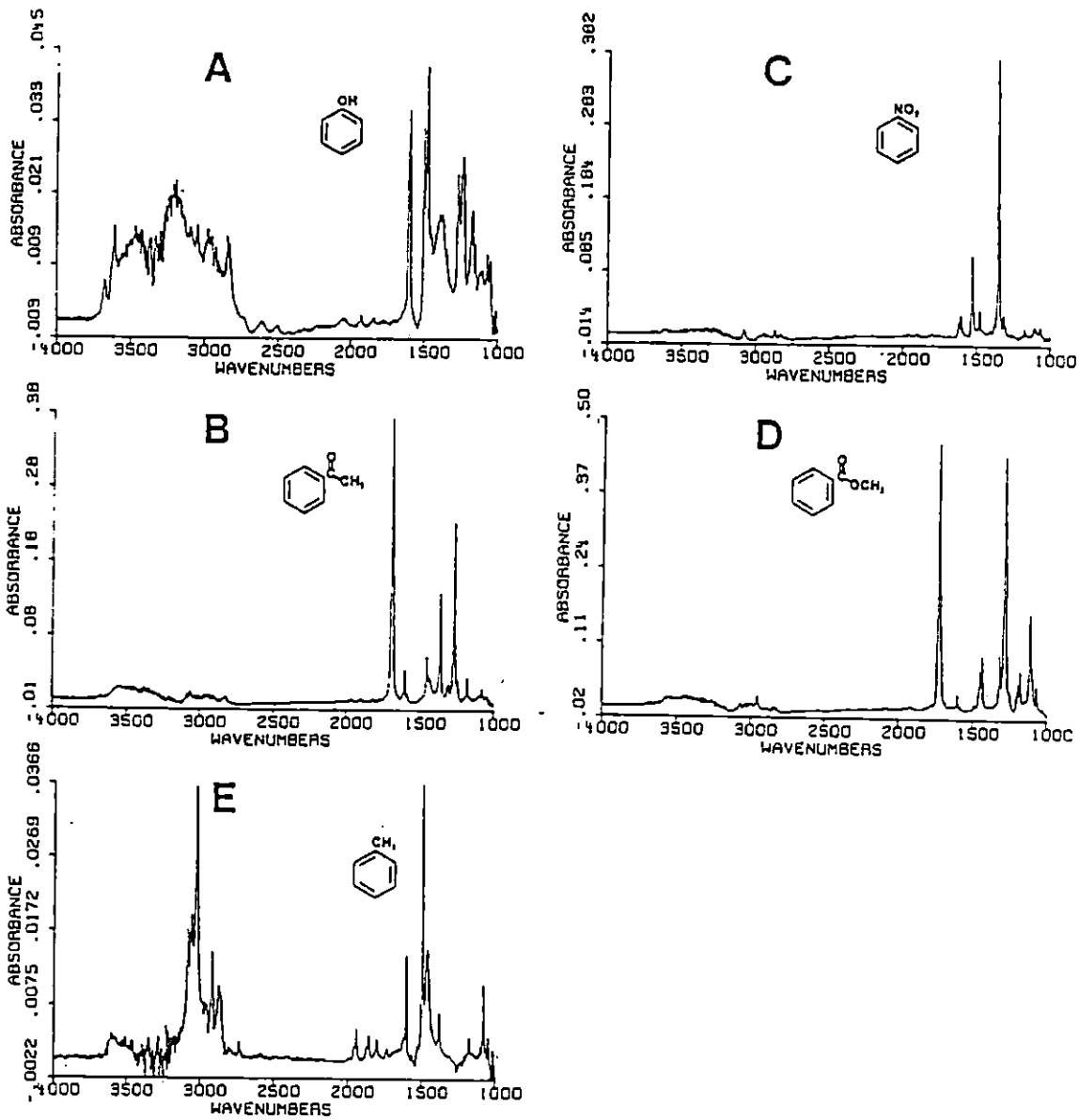

Figure 30. Infrared spectra obtained from test mixture separation with carbon tetrachloride extraction.

A) Phenol
B) Acetophenone
C) Nitrobenzene
D) Methyl benzoate
E) Toluene

CHAPTER 5

SUPERCRITICAL FLUID CHROMATOGRAPHY WITH FOURIER TRANSFORM INFRARED SPECTROMETRIC DETECTION

INTRODUCTION

Supercritical fluid chromatography (SFC) has received a great deal of attention (7,63-65) during the last several years. Supercritical fluids possess many of the attributes necessary for high performance chromatography. Among these include low mobile phase viscosity, high analyte diffusivity, and good solubility for a wide range of analytes (66,67). More importantly, by changing the density of the mobile phase with a change in temperature and/or pressure, one can significantly change the observed chromatographic characteristics in an SFC separation. Thus a single, supercritical mobile phase can be used to afford a wide variety of separations without the time-consuming column equilibration necessary in high-performance liquid chromatography (HPLC) when changing mobile phase composition. Carbon dioxide is by far the most common mobile phase used in SFC. Both packed columns described for use in liquid chromatography and capillary columns initially employed in gas chromatography can be used.

Detection has been one of the major instrumental problems in SFC (68). Conventional HPLC and GC detectors have proven to be compatible with SFC given various modifications. For example, optical detector cell volumes must be fairly small and able to withstand high pressures. Flame detectors must be altered to allow for fluid decompression and expansion into the flame jet. Ultraviolet detection has been the most

popular mode of detection, since many SFC mobile phases are transparent in the UV region and most analytes studied thus far contain one or more UV chromophores. With capillary columns flame ionization and fluorescence detection have proven popular. These systems provide for essentially universal detection rather than specific detection.

The Fourier Transform Infrared (FTIR) Spectrometer can yield both types of detection in real time. Demonstration of this advantage has already been achieved in GC and HPLC with relatively high sensitivity (48). Conventional lightpipes (18) are not suitable for SFC because of the relatively high operating pressures necessary using supercritical carbon dioxide. The potential of SFC-FTIR employing a capillary column and flow cell interface has been reported (27,69). Readily identifiable spectra of three components were obtained for injection of 3 μg each onto the column. The results presented in this chapter include the use of packed columns, beam condensing optics and a new flow cell design.

EXPERIMENTAL

A Hewlett-Packard (Avondale, PA) Model 1082B Liquid Chromatograph modified for supercritical fluid chromatography and equipped with a high-pressure Model 79875A variable wavelength UV absorbance detector was used for these investigations. Anaerobic grade CO_2 (Airco, Bluefield, WV) was used for all experiments. A 4.6 mm ID x 15 cm PRP-1 (polymer reversed phase), 10 μm particle diameter and a 4.5 mm ID x 25 cm C_{18} (octadecyl silica), 5 μm particle diameter packed column was used for all separations. In all experiments the flow rate was set at 2.0

mL/min and the column oven temperature was set at 40°C.

A schematic representation of the lightpipe flow cell is shown in Figure 31. The internal surface of the solid gold insert in the cell is polished longitudinally to give maximum infrared reflectivity. The internal cell dimensions are 1 mm ID x 5 mm pathlength. The cell windows are 13 mm diameter x 2 mm thick ZnSe disks, and are sealed in place with polyperfluorinated elastomer Kalrez O-rings (DuPont). The main body of the flow cell is 304 stainless steel with 0.010" ID x 1/16" OD stainless steel inlet and outlet tubing silver-soldered in place. The cell has been statically tested past 5000 psi of hexane without window or seal failure.

A Nicolet Model 6000C FTIR (Madison, WI) was used to collect time-resolved, 4 cm^{-1} resolution spectra employing the standard gas chromatography software provided by the manufacturer. Each four interferograms were signal-averaged to form a data file on disk with ca. 2.6 second time resolution between files. These files were ratioed against a background file of 32 signal-averaged scans. A Model 7010A (5000-400 cm^{-1}) mercury-cadmium-telluride (MCT-A) detector was used in all experiments. Initially, it was found that the infrared throughput with the specially constructed SFC cell in the standard sample compartment was prohibitively low because of the small internal diameter (1.0 mm) of the SFC lightpipe. To rectify this problem, a Nicolet Model GC-7002C auxiliary lightpipe optics bench was modified as shown in Figure 32. This involved moving the entire refocusing optics and detector such that the off-axis parabolic mirror (9.3" E.F.L.) is 9.3" from the exit window of the flow cell lightpipe. The effective beam

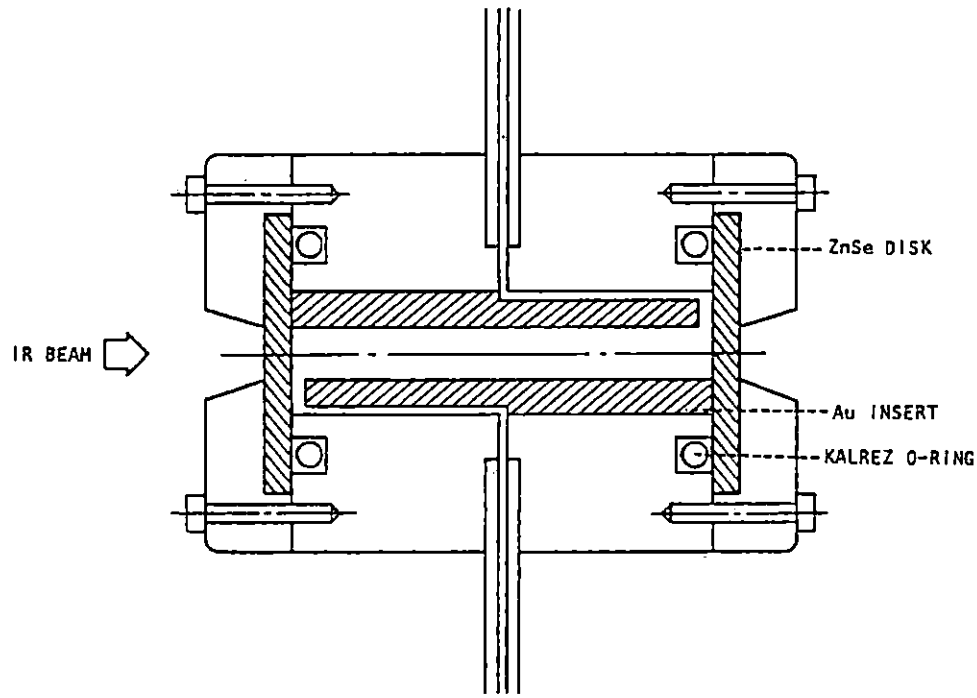

Figure 31. SFC-FTIR lightpipe flow cell.

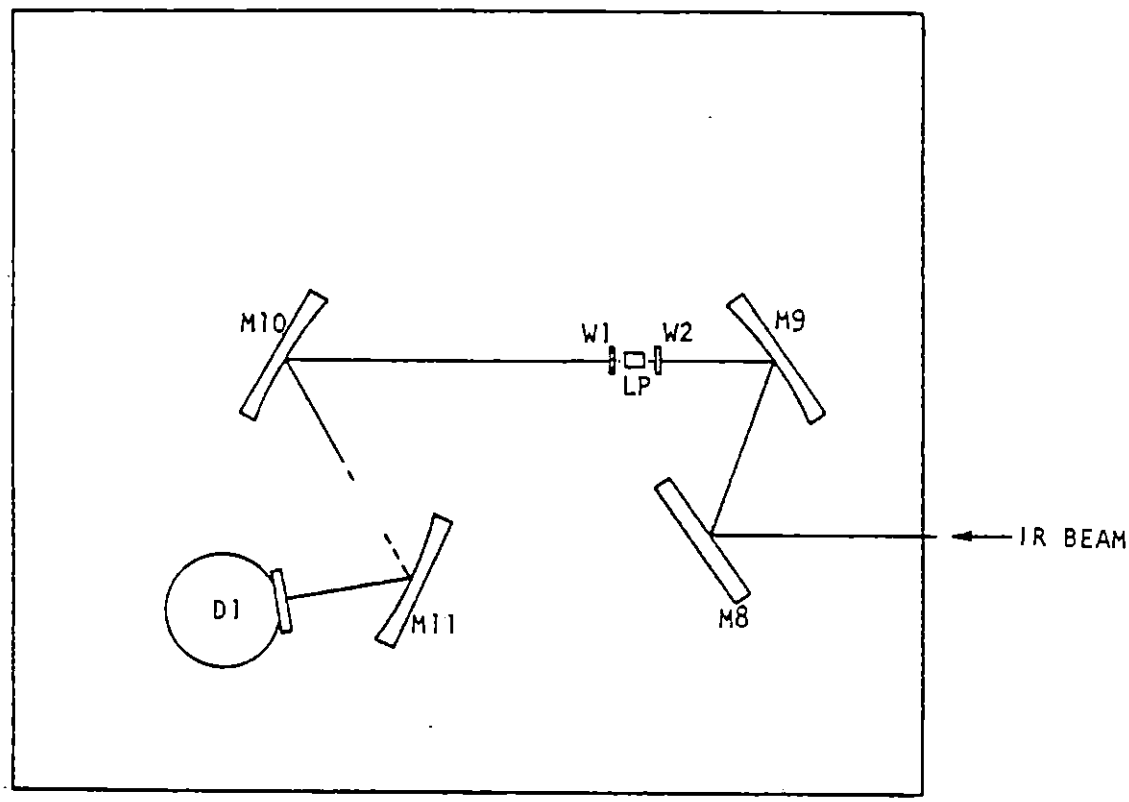

Figure 32. Modified optical arrangement for SFC-FTIR.

D1 - MCT-A Detector
W1,W2 - Lightpipe windows
LP - Lightpipe Flow Cell
Mg, M11 - 70° Off-axis paraboloid,
3.5" effective focal length
M10 - 60° Off-axis paraboloid,
9.33" effective focal length
M8 - Flat mirror

condensing of this optical arrangement is 3x compared to the standard FTIR sample compartment. The observed infrared throughput with the modified arrangement was found to be high, 15-18 volts peak-to-peak at the centerburst of the interferogram with the computer-controlled amplifiers set at unity gain.

The schematic diagram of the entire SFC-FTIR instrument is shown in Figure 33. It should be noted that the FTIR lightpipe flow cell is connected in-line after the Hewlett Packard heat exchanger and before the variable wavelength UV detector with a total of approximately 2 m of 0.010" ID x 1/16" OD SS tubing. Neither the transfer tubing nor the lightpipe flow cell were thermally insulated. The ambient operating temperature in this case was 22°C.

In order to demonstrate the system a concentrated sample mixture was prepared by mixing 1.0g of each of the following: cyclohexanone (Eastman Organic Chemicals, Rochester, NY), acetophenone and benzophenone (both Fisher certified, Fairlawn, NJ). Injections (0.1 µL) of this mixture, which correspond to ca. 33 µg of each component, were made on the SFC-FTIR instrument. A model mixture of benzylethylether, naphthalene, and benzylbenzoate in carbon tetrachloride was also prepared; 6 µL of the dilute solution, which corresponded to ca. 2 µg of each component, was injected on the ODS column. For detection limit studies, a series of of concentrations of acetophenone were prepared in carbon tetrachloride (Fisher HPLC grade, Fairlawn, NJ). In each case, 10 µL of the solution were injected on the SFC-FTIR instrument.

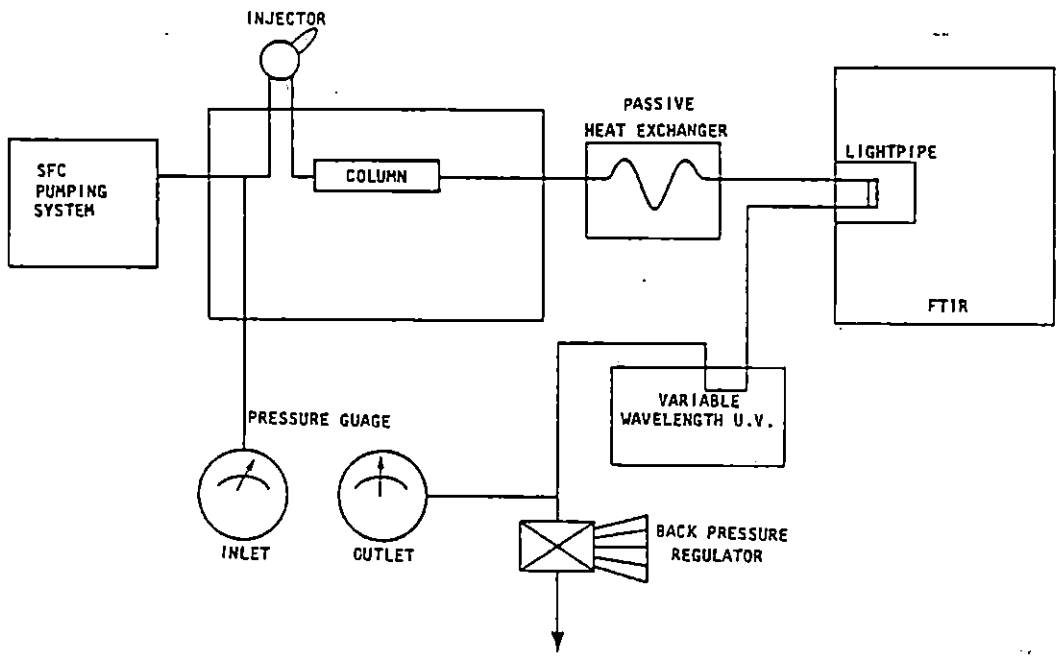

Figure 33. SFC-FTIR Instrument.

RESULTS AND DISCUSSION

The objective of this study was to evaluate the performance of the lightpipe flow cell and associated beam condensing optics for FTIR detection of small particle diameter packed column SFC eluents. One of the primary concerns was the pressure limit of this cell. Although static tests on this cell had been performed past 5000 psi of hexane, it was unclear whether supercritical carbon dioxide would have any adverse effects on the O-ring seal integrity. A second area of concern was the IR transparency of the background at higher pressures. Two pairs of bands (1388, 1286 cm^{-1} and 2064, 1949 cm^{-1}) have been observed in the infrared spectra of CO_2 at pressures greater than 1200 psi (50°C). The lower-frequency bands have been attributed to Fermi resonance between the Raman-active symmetric stretch at 1300 cm^{-1} and the second harmonic of the infrared-active, doubly degenerate bend at 667 cm^{-1}. These Fermi resonance bands appear to increase significantly with increased pressure. Between 1100 psi and 2100 psi these bands were found (27) to increase in intensity by one-tenth of an absorbance unit. Other reports have indicated that these bands also increase significantly with temperature (70). It was hoped that by further increasing the pressure, the observed Fermi resonance bands would not increase to such an extent that these regions of the infrared spectrum would become opaque for SFC-FTIR analysis.

The variation of the Fermi resonance band intensity with a larger range in pressure than earlier demonstrated is shown in Figure 34. At 500 psi column outlet pressure where CO_2 is believed to be gaseous Fermi resonance bands are not present (e.g. CO_2 at 500 psi ratioed to

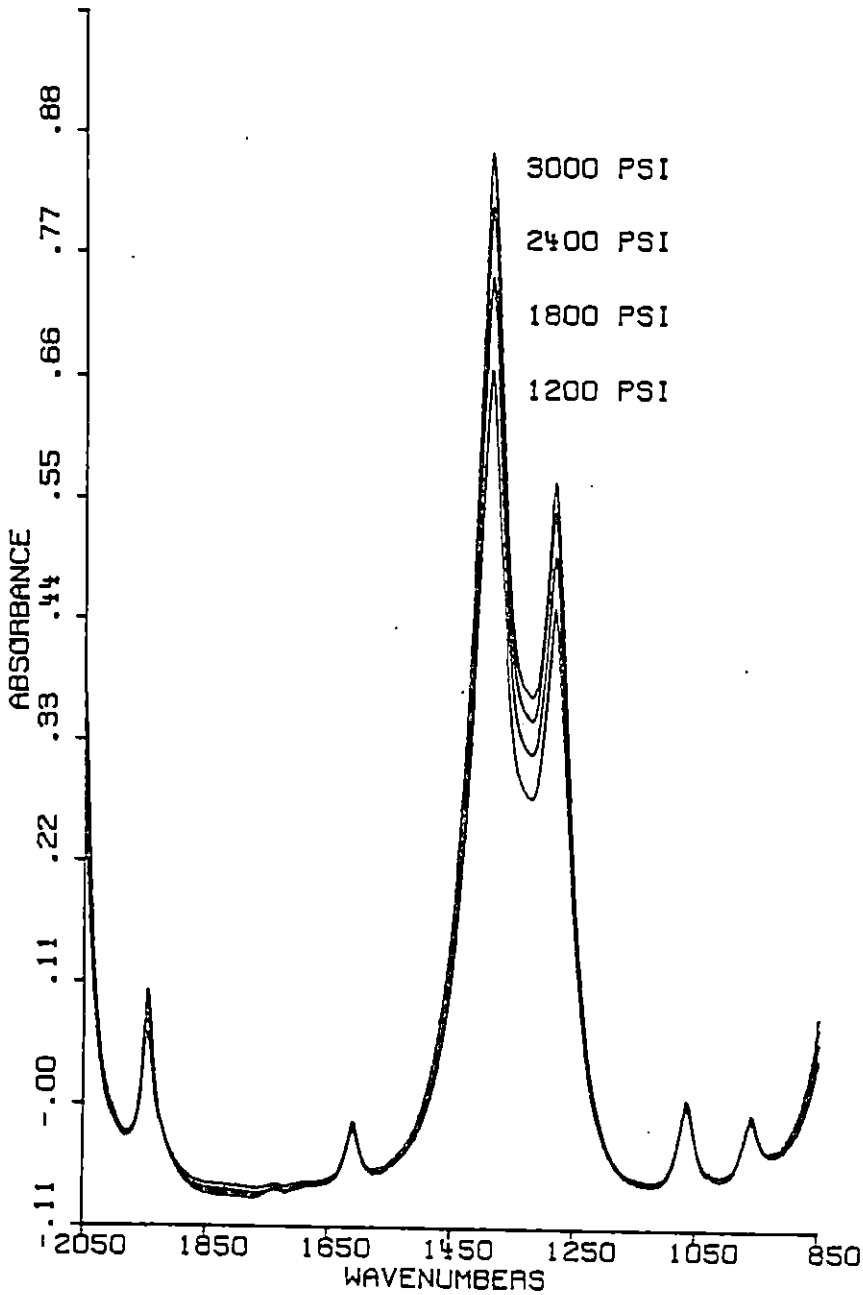

Figure 34. Pressure effect on Fermi resonance bands in spectra of high-pressure carbon dioxide.

CO_2 at ~14 psi). Raising the pressure progressively to 800 psi results in rapidly diminishing IR throughput which may represent the onset of liquid or supercritical conditions. Fermi resonance bands first appear around 1000 psi accompanied by much greater IR throughput. Further increases in pressure cause the Fermi resonance bands to increase in absorbance. The appearance of these bands may not be exclusive to supercritical conditions. No care was taken to heat or insulate the FTIR lightpipe nor the transfer tubing from column to detector. The column was at 40°C for the above experiment; however, the flow cell was ambient (22°C) which is below the critical temperature (31.3°C). Therefore, the CO_2 in the flow cell is not supercritical in these studies. Earlier experiments by Shafer and Griffiths with a flow cell thermostated at 50°C revealed the onset of Fermi bands only above 1100 psi. Their parameters obviously reflect supercritical conditions. The spectra in this study however, are in agreement with Shafer and Griffiths (27). Conceiveably liquid CO_2 may exhibit the same spectral behavior as supercritical CO_2. As evidence for this, the spectrum of CO_2 at 25°C and 2000 psi was measured (Figure 35) and was found to be identical to the spectrum of CO_2 at 70°C and 2000 psi.

Numerical analysis of 1388 cm^{-1} band absorbance variation with pressure indicates that a logarithmic equation best fits the data. When absorbance is plotted versus density, minor exponential curvature is also observed. The density values for the various pressures of CO_2 were determined assuming ambient temperature. This curvature increases if one uses a higher cell temperature. This suggests that pressure not only changes density, but it also changes molecular interactions that

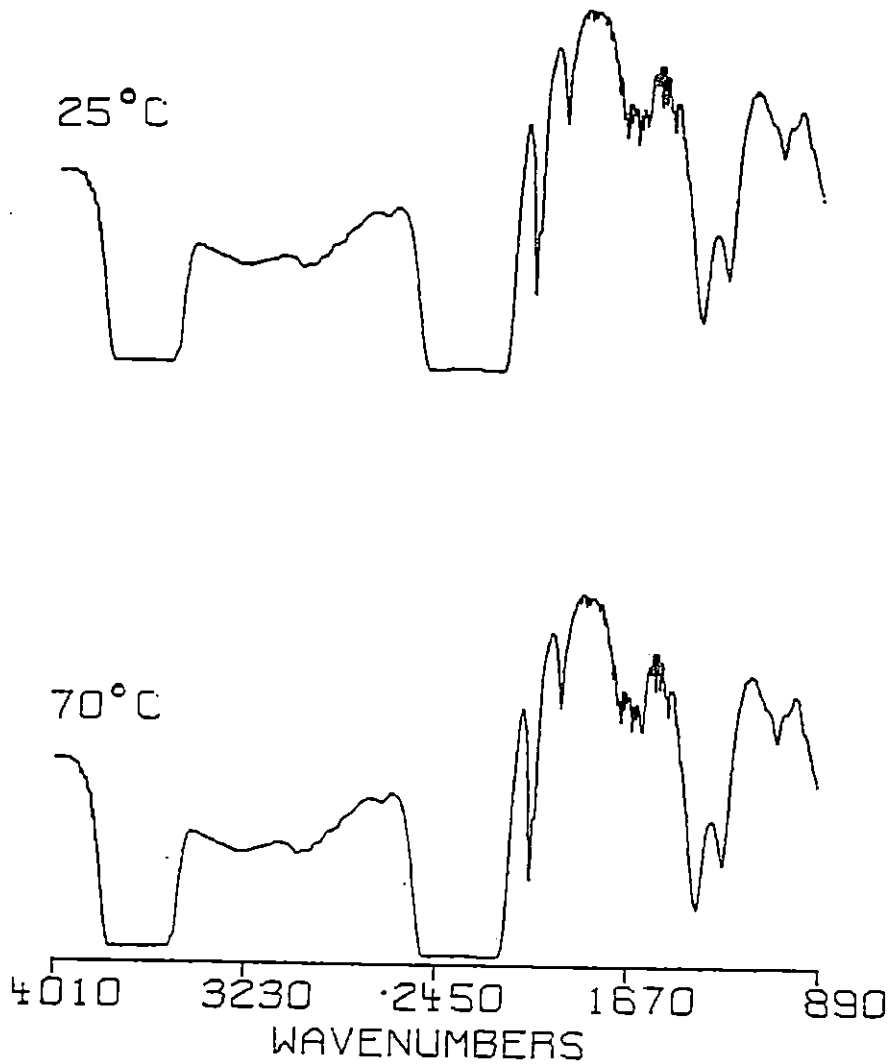

Figure 35. Single-beam spectra of CO_2 at 2000 psi; 25°C (liquid) and 70°C (supercritical fluid).

result in the observation of the Raman-active band. The best numerical fit in both cases, based on the f-test, is the exponential (Table V). Mathematical relationships derived from the above data concerning absorbance and pressure (density) are:

$$A = -0.779 + 0.123 \ln P_{psi}$$

$$A = 0.123 \exp (2.149\rho)$$

In spite of an IR absorbance dependence on pressure between 1200 and 1900 cm^{-1}, enough throughput is realized to allow meaningful data to be obtained with the flow cell at moderate pressures. With longer pathlengths these regions may become obscured.

In order to demonstrate the system a synthetic mixture of cyclohexanone, acetophenone and benzophenone was separated and detected with both FTIR and UV-254 nm. Injection of 33 µg/each component yielded the Gram-Schmidt reconstructed chromatogram (40) shown in Figure 36. All three ketones are easily detected in contrast to UV-254 nm detection (Figure 37) which did not give a response for cyclohexanone. Insignificant band broadening appears to have occurred between the packed column exit and the two detectors (e.g. the trace provided by the UV-254 nm detector which is in-line after the FTIR exhibits comparably sharp peaks). This would be expected as the flow profile of supercritical CO_2 has been described as turbulent in nature (71).

Inspection of the infrared spectra (Figure 38) obtained from the SFC separation using the previously described lightpipe flow cell reveals excellent signal-to-noise. Each spectrum corresponds to the file closest to the maximum in the Gram-Schmidt reconstruction. All three of the ketone spectra obtained match standard, reference library

Table V

Dependence of Fermi Resonance Band Absorbance on Pressure and Density in CO_2

Pressure[1](psi)	Density[2](g/mL)	Absorbance[3] at 1388 cm-1
1200	0.829	0.7310
1800	0.880	0.8130
2400	0.914	0.8760
3000	0.939	0.9260

Regression Analysis

Absorbance versus Pressure

Type	R^2	f
Linear	0.988	162.9
Logrithmic	0.999	999.9

$A = -0.779 + 0.213 \ln P_{psi}$

Absorbance versus Density

Type	R^2	f
Linear	0.998	799.1
Exponential	0.999	999.9

$A = 0.123 \exp (2.149\ \rho)$

[1]Measured at back pressure regulator (See Figure 32).

[2]Interpolated from CO_2 phase diagram; page 17, H-P SFC Manual Supplement.

[3]Measured from peak height to extrapolated zero-absorbance line.

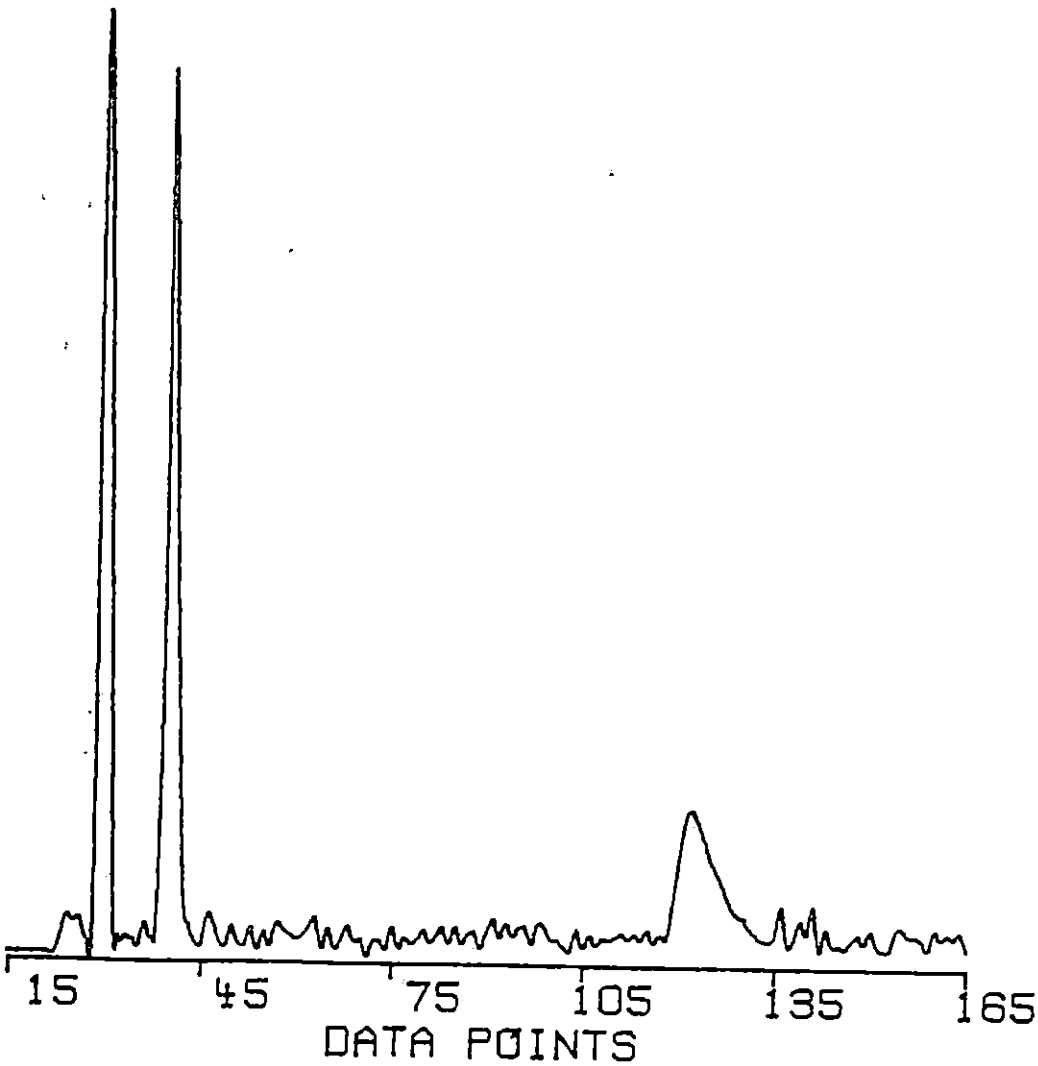

Figure 36. Gram-Schmidt reconstructed chromatogram of SFC-FTIR separation of Ketone mixture: Cyclohexanone, Acetophenone, Benzophenone at 33 µg each (in elution order).

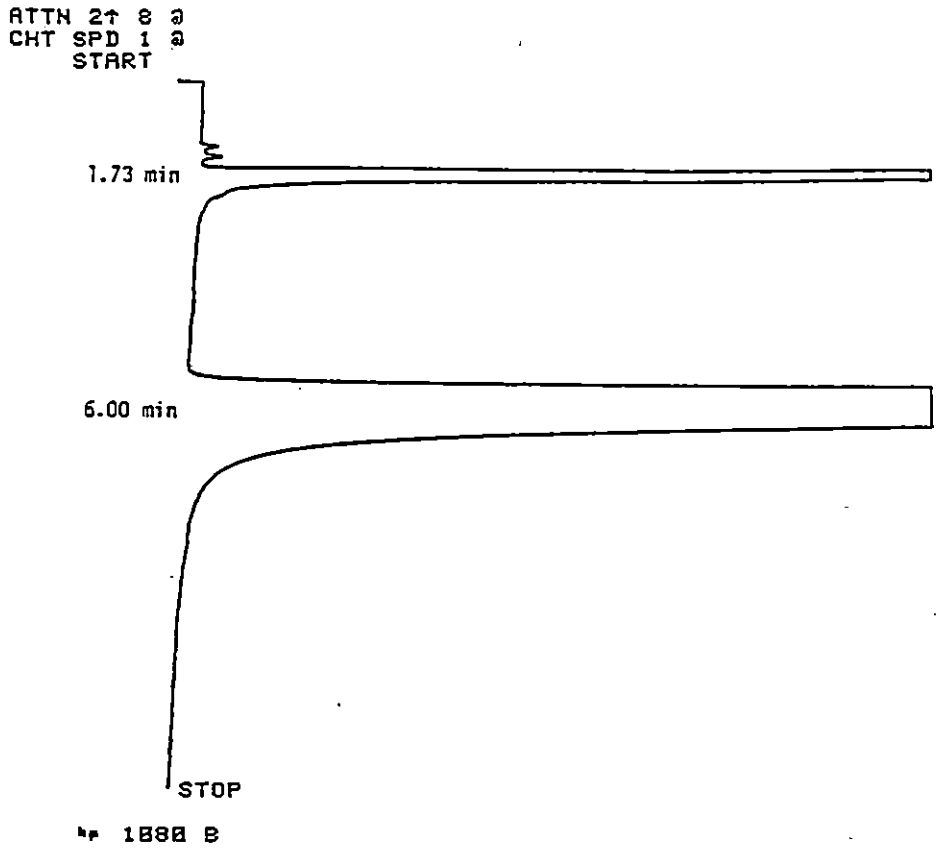

Figure 37. SFC-UV254 chromatogram of ketone mixture: cyclohexane, acetophenone, and benzophenone at 33 µg each.

spectra peak-for-peak. These spectra, in which the SFC separation was run at an outlet pressure of 2000 psi (inlet pressure of 2300 psi), show no signs of opacity due to the Fermi bands. The regions around 2350 cm^{-1} and 3650 cm^{-1} are opaque, as expected, and are consequently blanked in the spectra in Figure 38. Otherwise the remainder of the mid-IR region is transparent being limited only by the IR cutoff of the ZnSe windows in the lightpipe. Each of these spectra correspond to ca. 33 μg of injected material, which is well within the mass loading capacity of the packed column.

A series of dilute solutions of acetophenone was injected to determine the minimum detectable quantity (i.e. 3X beam condensing optics, narrow band MCT detector, 5 mm pathlength lightpipe, PRP-1 column [10 μm]). Acetophenone is a strong IR absorber and should yield relatively low detection limits. Data in Table VI support this opinion if the carbon-oxygen stretching vibrational band (1700 cm^{-1}) is used to determine the minimum detectable quantity. Under the same conditions, the methyl bend (1250 cm^{-1}) would lend itself to a larger minimum detectable quantity. Detection limits (defined as 3X the root mean square noise on a least squares line) of 50 ng and 220 ng respectively have been measured. This number could be further improved with the current flow cell by increasing the mirror velocity (0.748 cm/sec was used) which would enhance the signal-to-noise ratio by increasing the number of interferograms collected per second, thus increasing the number of scans which may be averaged per file. Decreasing the flow rate of the SFC would also lower detection limits by allowing a greater number of scans to be averaged per file (2 mL/min, 4 scans/file were

Table VI

Minimum Detectable Quantity of Acetophenone in SFC-FTIR

Amount Injected(ng)	Absorbance[a] 1700 cm^{-1}	Absorbance[a] 1250 cm^{-1}
10,000	0.0491	0.0387
5,000	0.0260	0.0206
3,000	0.0154	0.0123
1,500	0.0078	0.0069
1,000	0.0047	0.0034
500	0.0027	0.0022

[a]Root mean square noise for 1700 cm^{-1} band = 0.00020; 1250 cm^{-1} band = 0.00037.

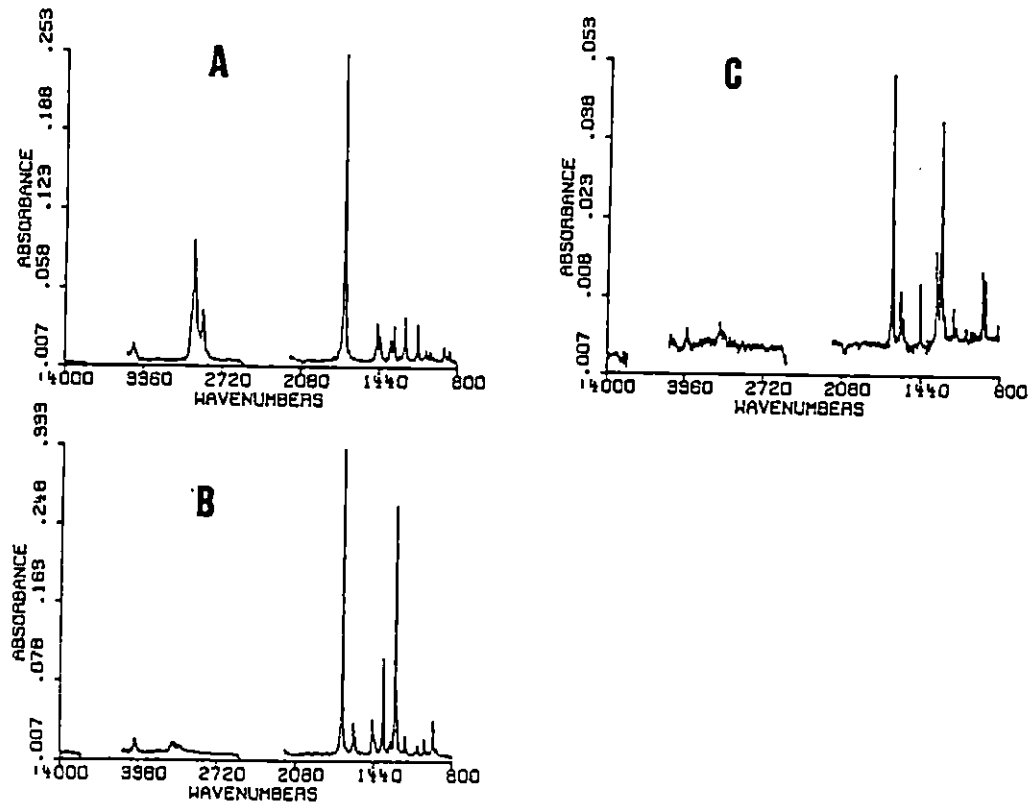

Figure 38. Infrared spectra obtained from SFC-FTIR separation of Ketone mixture.

A) Cyclohexanone
B) Acetophenone
C) Benzophenone

used). The 2 mL/min flow rate used in this study represents a practical compromise flow rate for SFC-FTIR experiments with packed columns, although flow rates as high as 5 mL/min are not uncommon (72).

The UV-254 nm chromatogram from the SFC separation of the second model mixture, separated at 1300 psi outlet pressure (1400 psi inlet pressure) on an ODS column at 1 mL/min, is shown in Figure 39. Inspection of the corresponding Gram-Schmidt reconstructed chromatogram (Figure 40) reveals significantly different peak area ratios. These differences would be expected for the following reasons. The first peak at 1.15 min is the carbon tetrachloride solvent. At 254 nm, carbon tetrachloride has an extremely low extinction coefficient. The UV trace shows a rather small peak, but the infrared chromatogram is more representative of the actual concentration. Benzyl ethyl ether (1.67 min) and benzyl benzoate (3.28 min) give good response in both UV and IR chromatograms. Naphthalene, however, has extremely good UV absorbance at 254 nm because of its aromaticity. The mid-infrared spectrum of naphthalene has a series of particularly weak absorbances, and consequently the IR chromatogram shows a weak response.

Inspection of the corresponding spectra (Figure 41) reinforces this point. The carbon tetrachloride spectrum (Figure 41A) shows very good signal-to-noise as it is the most concentrated peak. The spectrum of benzyl ethyl ether (Figure 41B) is relatively noisy, but this spectrum has more than enough information for conclusive identification. Naphthalene (Figure 41C), while giving the lowest signal-to-noise spectrum, is still identifiable. The spectrum of benzyl benzoate (Figure 41D) has a good signal-to-noise ratio, as would be expected from

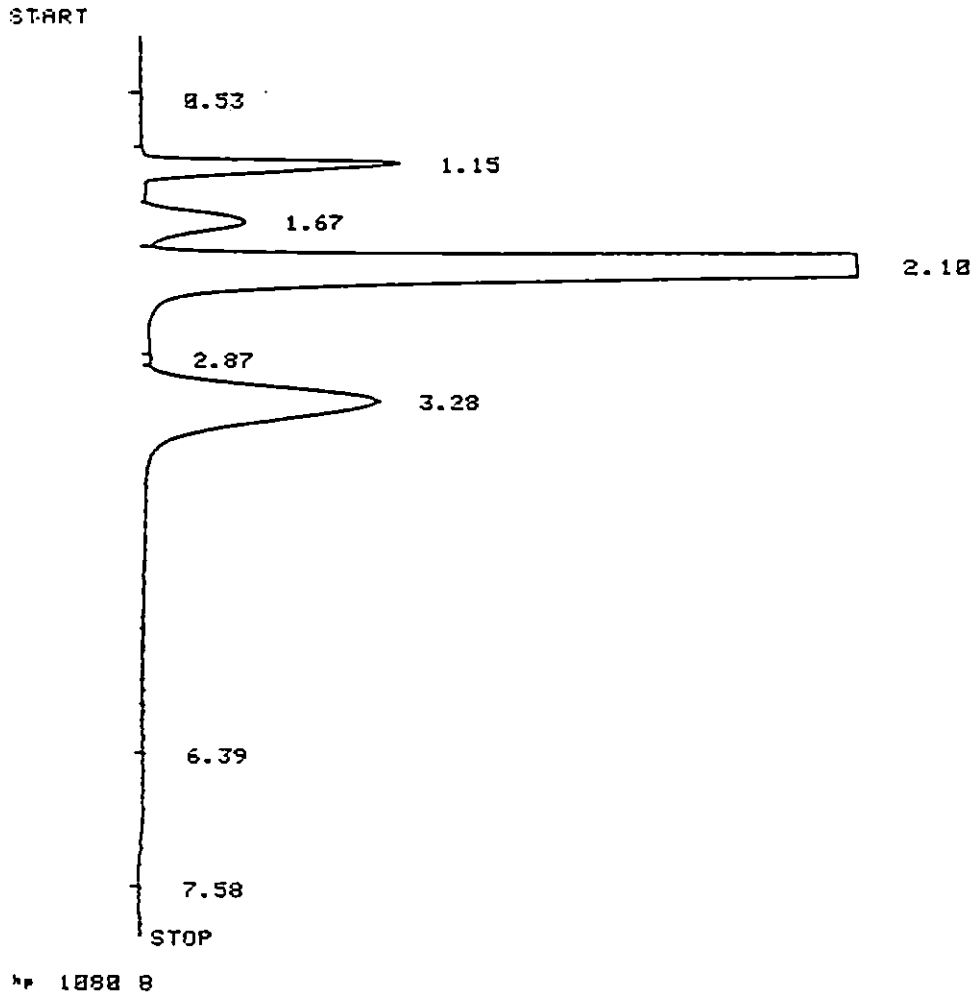

Figure 39. SFC-UV254 chromatogram of dilute model mixture: carbon tetrachloride (Solvent), benzylethylether, naphthalene, and benzylbenzoate at ca. 2 µg each.

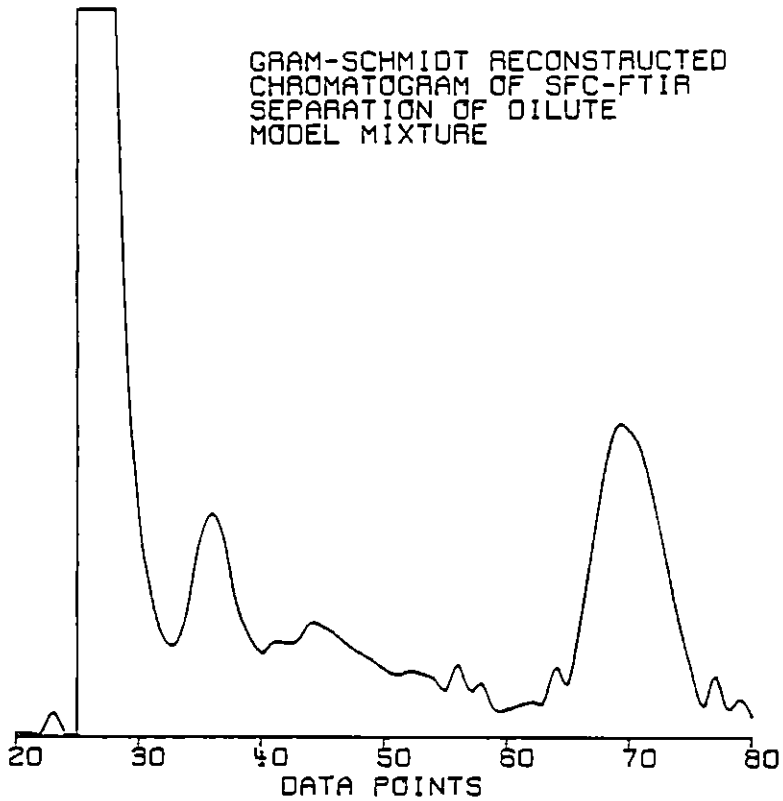

Figure 40. Gram-Schmidt reconstructed chromatogram of SFC-FTIR separation of dilute model mixture: carbon tetrachloride (solvent), benzylethylether, naphthalene, and benzylbenzoate at ca. 2 µg each.

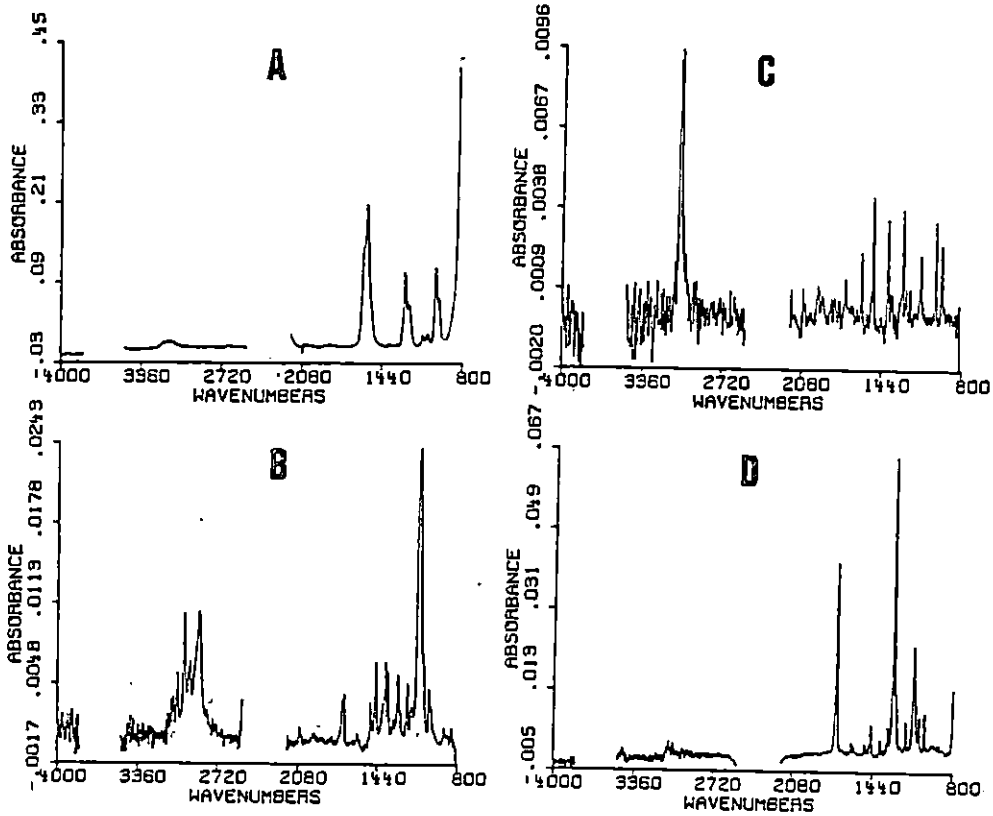

Figure 41. Infrared spectra obtained from SFC-FTIR separation of dilute model mixture.

A) Carbon tetrachloride
B) Benzylethylether
C) Naphthalene
D) Benzyl benzoate

a strongly-absorbing ester. All spectra match well to any standard, reference library spectra, gas or condensed phase.

In summary, the lightpipe flow cell has been demonstrated as an improved interface between the SFC and the FTIR. Used in conjunction with beam condensing optics, this flow cell yields high signal-to-noise spectra from an otherwise standard, commercially-available SFC instrument. The high infrared throughput, which can be directly attributed to the polished gold insert of the flow cell and the associated beam condensing optics, is perhaps the most important feature in obtaining the quality spectra shown. Detection of a variety of compounds has been demonstrated with packed column SFC-FTIR using a lightpipe flow cell.

CHAPTER 6

CONCLUSIONS AND FUTURE WORK

The objectives of this thesis have been to extend the capabilities of the FTIR as a chromatographic detector to encompass HPLC, both normal and reversed phase, and SFC. The extension to HPLC and SFC means that the detector capabilities of the FTIR now cover the most common forms of elution chromatography. Although the new techniques demonstrated in the previous chapters are not fully optimized, this thesis has explored several fundamental concepts to bring these viable techniques to the forefront of analytical hyphenated methods.

In summary, the highlights of this resarch have included the demonstration and comparison of normal phase HPLC with FTIR detection not only with analytical scale chromatography, but with semi-preparative and microbore scales as well. Although all three scales were found to be adequate, the microbore scale HPLC-FTIR experiment proved to have significant advantages. These include low solvent consumption without a sensitivity compromise. The low solvent consumption allows economical use of otherwise non-classical elution solvents that have broad window regions in the infrared. Also, the small quantities of packing material needed for microbore HPLC allows economical use of a variety of otherwise expensive packing materials. One disadvantage of the work in Chapter 2 with microbore HPLC-FTIR was that the flow cell interface used was found to be excessive in dead volume. These results were published in Analytical Chemistry (45).

The solution to the excessive dead volume problem was addressed

through the development of the Zero Dead Volume flow cell in Chapter 3. The flow characteristics of this unconventional spectrometric flow cell were demonstrated to be quite superior. In addition, the spectrometric characteristics of this design demonstrated the first application of Hirschfeld's multipathlength cell concept to a chromatographic system. The sensitivity was demonstrated to be far superior to the conventional flow cells, and the unusual spectrometric characteristics have been found to be beneficial. This work has appeared in Analytical Chemistry (56), Barnes' Scan Time, and a patent application has been filed with the U.S. Patent Office by the Department of Energy for the ZDV cell.

Concurrently in Chapter 3 it was demonstrated that the infrared sampling methodology developed for GC-FTIR was unsuitable for HPLC-FTIR. The sampling must be based on the width of the individual peaks, not on a convenient, fixed sampling rate. Enhancements in the spectral signal-to-noise ratios and consequently the sensitivity can be thus realized. If one were to relate this to quantitation methods used in GC, one would call this a peak area method as opposed to a peak height method. The "peak area" spectrum from an HPLC-FTIR experiment results in the highest signal-to-noise spectrum.

Reversed phase HPLC-FTIR must become a viable technique for HPLC-FTIR to gain widespread acceptance. Several techniques have been attempted, but none with the initial success of the technique demonstrated in Chapter 4. The low-dispersion, flowing extraction technique borrowed from Flow Injection Analysis coupled with the membrane separator has provided the basis for an elegant but simple approach to reversed-phase HPLC-FTIR. This approach may prove to be widely accepted

for routine FTIR detection of reversed-phase HPLC, the most widely-used form of liquid chromatography. This work was published recently in Analytical Chemistry (73).

Supercritical Fluid Chromatography has provided an interesting set of problems with which one must deal to effectively couple the FTIR as a detector. These problems, which include high pressure and rapid mobile phase velocity have been addressed in Chapter 5. The most significant improvement has been the development of the high-pressure lightpipe flow cell for SFC-FTIR. Excellent infrared throughput was observed, and the resulting spectra are high-quality as well. FTIR detection limits using a packed-column SFC are on the order of the best observed with HPLC-FTIR. This area of research may hold the most excitement of all in the near future.

The work in this thesis has answered many questions, but it has raised at least an equal number. These questions could provide the basis for a great deal of further experimentation. Some areas that deserve attention follow.

Normal-phase HPLC-FTIR is rather well developed at this point. However, several questions have emerged. Is any Beer's Law deviation observed using the ZDV flow cell? None was seen at low concentration, but Hirschfeld predicted curvature at high concentration. Can the ZDV cell or concept be applied to smaller, micro liquid chromatographic systems? Can an algorithm be developed and incorporated into the commercial FTIR software packages to "properly" set the sampling rates to correspond to the ideal for each peak? And the most difficult, can a

method for using gradient elution be developed?

Reversed-phase HPLC-FTIR with the current scheme has opened up a larger number of questions. Can the Flow Injection Analysis portion, both hardware and flows, be optimized to produce the most efficient extraction possible? What would be the effect of entraining a salt solution to drive the eluents into the extraction solvent? Could a better extraction solvent be chosen? Can microbore reversed-phase HPLC-FTIR be demonstrated? Apffel, et. al., have recently demonstrated the extraction portion of this experiment (74). Can a gradient elution scheme be developed by entraining an opposing gradient into the stream post-column so that a constant composition of effluent can be extracted?

Supercritical Fluid Chromatography with FTIR detection has generated an equal number of questions as well. Can polar modifiers be used, such as methanol? Can pressure programming be used? Can spectra be searched against condensed or vapor phase libraries? Which is more appropriate? Are the lightpipe dimensions optimal? Can the lightpipe be used for capillary SFC-FTIR? Can a more rapid FTIR be used to enhance detection limits?

These questions plus many more must be construed as a successful accomplishment of the initial goals of this thesis -- to extend the capabilities of the FTIR as a chromatographic detector to new forms of chromatography. Clearly the potential has been demonstrated, and the new forms of chromatography are now detectable by FTIR. The questions raised are simply the logical progression of technology; now that it works, how can it be improved further?

REFERENCES

1. McNair, H. M.; Bonelli, E. J. "Basic Gas Chromatography", 5th ed.; Consolidated Printers: Berkeley, 1969.

2. Snyder, L. R.; Kirkland, J. J. "Introduction to Modern Liquid Chromatography", 2nd ed.; Wiley-Interscience: New York, 1979.

3. Pecsok, R. L.; Shields, L. D.; Cairns, T.; McWilliam, I. G. "Modern Methods of Chemical Analysis", 2nd ed.; Wiley: New York, 1976.

4. Hirschfeld, T.; Anal. Chem. 1980, 52, 298A.

5. Borman, S. A.; Anal. Chem. 1983, 55, 836A.

6. Novotny, M.; Springston, S. R.; Peadon, P. A.; Fjeldsted, J. C.; Lee, M. L.; Anal. Chem. 1981, 53, 407A.

7. Gere, D. R.; Science 1983, 222, 253.

8. Watson, J. T. "Auxiliary Techniques of Gas Chromatography", L. S. Ettre, W. H. McFadden, eds.; Wiley-Interscience: New York, 1969.

9. Eckers, C.; Games, D. E.; Lewis, E.; Nagaraja Rao, K. R.; Rossiter, M.; Weerasinghe, N. C. A.; Adv. Mass. Spectrom. 1980, 88, 1396.

10. Christensen, R. G.; Hertz, H. S.; Meiselman, S.; White, E.; Anal. Chem. 1981, 53, 171.

11. Arpino, P. J.; Guiochon, G.; J. Chromatogr. 1982, 251, 153.

12. Majors, R. E.; LC 1983, 1, 488.

13. Carmody, J. J.; Blakely, C. R.; Vestal, M. J.; J. Amer. Chem. Soc. 1980, 102, 5931.

14. Smith, R. D.; Udseth, H. R.; Anal. Chem. 1983, 55, 2266.

15. Brown, R. S.; Shafer, K. H., Griffiths, P. R.; Wilkins, C. L.; Paper no. 275; Pittsburgh Conference on Analytical Chemistry and Applied Spectroscopy; Atlantic City (March 1984).

16. Low, M. J. D.; Freeman, S. K.; Anal. Chem. 1967, 39, 194.

17. Borman, S. A.; Anal. Chem. 1982, 54, 901A.

18. Azzaraga, L. V.; Appl. Spectrosc. 1980, 34, 224.

19. Rossiter, V.; Am. Lab. 1982, 71.

20. Shafer, K. H.; Cooke, M.; DeRoos, F.; Jakobsen, R. J.; Rosanio, O.; Mulik, J. D.; Appl. Spectrosc. 1981, 35, 469.

21. Vidrine, D. W. in "Fourier Transform Infrared Spectroscopy"; Ferraro, J. R.; Basile, L. J.; eds.; Academic Press: New York, 1979; Vol. 2; pp. 129.

22. Griffiths, P. R. in "Fourier Transform Infrared Spectroscopy"; Ferraro, J. R.; Basile, L. J.; eds.; Academic Press: New York, 1978; Vol. 1; pp. 143.

23. Meyers, M.; Nicolet Analytical Instruments, private communication, 1984.

24. Shafer, K. H.; Lucas, S. V.; Jakobsen, R. J.; J. Chromatogr. Sci. 1979, 17, 464.

25. Vidrine, D. W.; J. Chromatogr. Sci. 1979, 17, 477.

26. Kuehl, D. T.; Griffiths, P. R.; Anal. Chem. 1980, 52, 1394.

27. Shafer, K. H.; Griffiths, P. R.; Anal. Chem. 1983, 55, 1939.

28. Scott, R. P. W.; Kucera, R.; J. Chromatogr. 1979, 169, 51.

29. Karlberg, B.; Thelander, S.; Anal. Chim. Acta 1978, 98, 1.

30. Sepaniak, M. J.; Yeung, E. S.; J. Chromatogr. 1981, 211, 95.

31. Brown, R. S.; Hausler, D. W.; Taylor, L. T.; Carter, R. C.; Anal. Chem. 1981, 53, 197.

32. Haw, J. F.; Glass, T. E.; Hausler, D. W.; Motell, E.; Dorn, H. C.; Anal. Chem. 1980, 52, 1135.

33. Hausler, D. W.; Taylor, L. T.; Anal. Chem. 1981, 53, 1227.

34. Henion, J. D.; Wachs, T.; Anal. Chem. 1981, 53, 1963.

35. Bowermaster, J.; McNair, H. M.; J. Chromatogr. 1983, 279, 431.

36. Jinno, K.; Fujimoto, C.; J. High Res. Chrom. Commun. 1981, 532.

37. Teramae, N.; Tanaka, S.; Spectroscopy Lett. 1980, 13, 117.

38. Johnson, C. C.; Taylor, L. T.; See Appendix I.

39. Glajch, J. L.; Kirkland, J. J.; Schindel, W. G.; Anal. Chem. 1982, 54, 1276.

40. deHaseth, J. A.; Isenhour, T. L.; Anal. Chem. 1977, 49, 1977.

41. Rudnick, L. R.; Whitehurst, D. D.; ACS Symp. Ser. 1981, 169, 153.

42. Vidrine, D. W.; Mattson, D. R.; Appl. Spectros. 1979, 32, 502.

43. Kuehl, D. T.; Griffiths, P. R.; J. Chromatogr. Sci. 1979, 17, 471.

44. Combellas, C.; Bayart, H.; Jasse, B.; Caude, M.; Rosset, R.; J. Chromatogr. 1983, 259, 211.

45. Johnson, C. C.; Taylor, L. T.; Anal. Chem. 1983, 55, 436.

46. Brown, R. S.; Taylor, L. T.; Anal. Chem. 1983, 55, 1492.

47. Brown, R. S.; Amateis, P. G.; Taylor, L. T.; Chromatographia 1984, 8, 396.

48. Amateis, P. G.; Taylor, L. T.; Anal. Chem. 1984, 56, 966.

49. Jinno, K.; Fujimoto, C.; Chromatographia 1983, 17, 259.

50. "CRC Standard Mathematical Tables, 26th Edition"; CRC Press, Inc. Boca Raton, 1981.

51. Sebes, B.; Spectra-Tech Inc., private communication, 1984.

52. Baker, D. R.; LC 1984, 2, 38.

53. Amateis, P. G.; Ph.D Dissertation, VPI & SU, 1984.

54. Hirschfeld, T.; Anal. Chem. 1978, 50, 1225.

55. Dasgupta, P. K.; Anal. Chem. 1984, 56, 1401.

56. Johnson, C. C.; Taylor, L. T.; Anal. Chem. 1984, 56, 2642.

57. Parris, N. A.; J. Chromatogr. Sci., 1979, 17, 541.

58. Jinno, K.; Fujimoto, C.; Uematsu, G.; Am. Lab., 1983, 39.

59. Kalasinsky, K. S.; McDonald, J. T., Jr.; Kalasinsky, V. F.; FT-IR Spectral Lines 1983, 5, 14.

60. Duff, P. J.; Conroy, C. M.; Griffiths, P. R.; Karger, B. L.; Vouros, P.; Kirby, D. P.; Proc. Soc. Photo-Opt. Instrum. Eng. 1981, 289, 53.

61. Conroy, C. M.; Griffiths, P. R.; Duff, P. J.; Azzaraga, L. V.; Anal. Chem. 1984, 56, 2636.

62. Nord, L.; Karlberg,B.; Anal. Chim. Acta 1980, 118, 285.

63. Gere, D. R.; Board, R.; McManigill, D.; Anal. Chem. 1982, 54, 736.

64. Novotny, M.; Springston, S. R.; Peaden, P.A.; Fjeldsted, J. C.; Lee, M. L.; Anal. Chem. 1981, 53, 407A.

65. Grob, K.; JHRC&CC 1983, 6, 178.

66. Lauer, H. H.; McManigill, D.; Board, R. D.; Anal. Chem. 1983, 55, 1370.

67. Peaden, P. A.; Lee, M. L.; J. Liquid Chromatogr. 1982, 5 (Suppl. 2), 179.

68. Fjeldsted, J. C.; Lee, M. L.; Anal. Chem., 1984, 56, 619A.

69. Hughes, M. E.; Brown, C. W.; Fasching, J. L.; Paper No. 661, Pittsburgh Conf. Anal. Chem. Appl. Spectrosc., Atlantic City, NJ (March 1984).

70. Orchin, M.; Jaffe, H. H. "Symmetry, Orbitals, and Spectra"; Wiley-Interscience: New York, 1971.

71. Jentoft, R. E.; Gouw, T. H.; J. Chromatogr. Sci. 1970, 138.

72. Gere, D. R.; private communication, 1984.

73. Johnson, C. C.; Hellgeth, J. W.; Taylor, L.T.; Anal. Chem. 1985, 57, 610.

74. Apffel, J. A.; Brinkman, U.A. Th.; Frei, R. W.; Chromatographia 1984, 18, 5.

APPENDIX I

MODIFICATION OF A FRESNEL-TYPE REFRACTIVE INDEX DETECTOR FOR USE WITH MICROBORE HIGH-PERFORMANCE LIQUID CHROMATOGRAPHY

The refractive index detector used in Chapter 1 for microbore HPLC is a modified LDC/Milton Roy Refractometer. This detector is a Fresnel-type differential refractive index detector, which is ideally suited for microbore work because of its low internal volume. In order that the Refractometer could be used, however, steps to eliminate the excessive flow volume within the heat exchanger were taken. Since a great deal of tubing was used inside the heat exchanger, the heat exchanger was eliminated consequently eliminating the excess connection volume. The column connects directly to short, 0.007" i.d. tubing leading to the 0.5 μL flow cell.

Figure 42 illustrates the prism holder used for these experiments. The block was machined from 316 stainless steel, and the tubes were silver-soldered in place. To ensure that the solder flowed evenly around the tube, the holes were bored oversize on the backside of the holder. To avoid the tubes filling with solder, fine piano wire was inserted into the bore of the tubes. As the assembly cooled, the piano wire was moved back and forth so that no solder could harden in the tubing. The face of the holder was polished to a mirror-like finish.

This modification was not found to affect the performance of the detector in any way except with respect to baseline drift. This is illustrated in the traces in Figures 2 and 6 (Chapter 2). This drift is presumably due to thermal effects that are observed when the heat exchanger is eliminated. Further improvements may include a heat

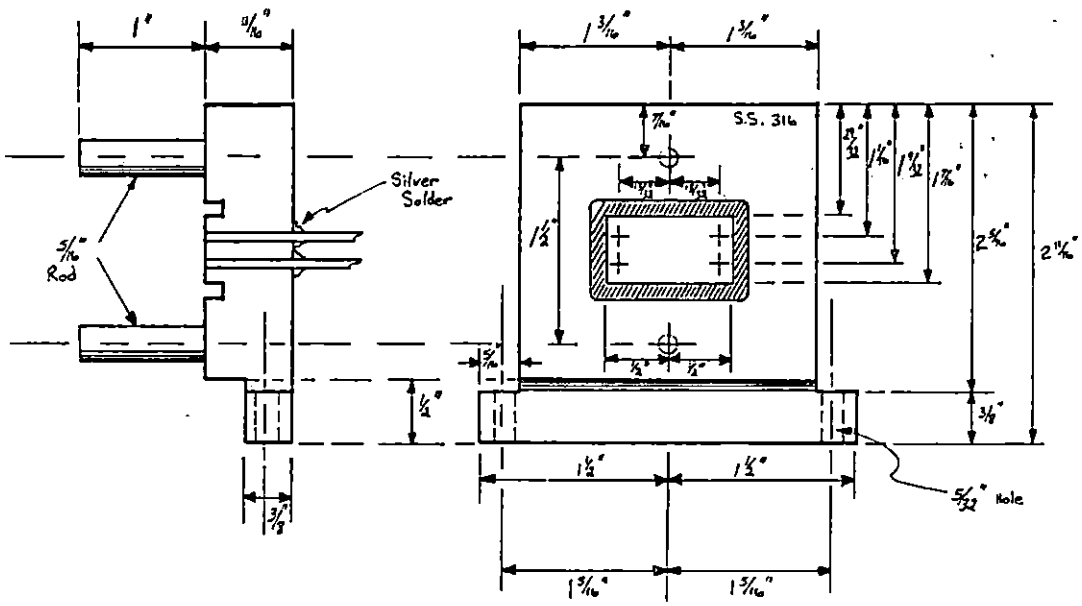

Figure 42. Detailed measurements of the microbore differential refractive index prism holder.

exchanger on the entire microbore column and prism holder. This would certainly eliminate the observed drift. Also the volume of the current connection tubing, which is calculated at 0.75 μL, could be reduced by machining a female, ZDV compression fitting into the back of the prism holder. Then the total detector volume would be less than 0.6 μL from column outlet to detector cell outlet.

APPENDIX II

CONSTRUCTION DETAILS OF ZERO DEAD VOLUME FLOW CELL

The Zero Dead Volume (ZDV) flow cell described in Chapter 3 is essentially an alkali halide crystal with a hole drilled in it. In practice, additionally it consists of an aluminum holder, a pair of Teflon gaskets, a small compression screw, a length of flanged PTFE tubing, and a microbore HPLC column with an EM Science microbore end fitting. This assembly fits into the Barnes Model 600 Beam Condenser without blocking the complex infrared beam path used to reduce the focal diameter of the spectrometer. This cell is schematically shown in Figure 13 (page 40).

The alkali halide portion of the assembly is mechanically drilled, but precautions must be taken to ensure that the crystal does not disintegrate from the stress of drilling. The most successful procedure for preparing the crystal is as follows:

1) The edge of a flat crystal plate (6 mm thick) is drilled carefully with a sharp, 0.75 mm (no. 56) drill bit. Lubrication with methanol, ethanol or isopropanol has been found to be beneficial.

2) The drilling should proceed slowly, and the drill bit tip should be cleaned frequently.

3) The hole should be drilled approximately 12 mm deep, but care should be taken not to drill through the crystal. On exiting the opposite side of the crystal, the stress released will cause the crystal to crack severely.

4) The crystal with the hole drilled into it should then be cleaved with a sharp razor so that two parallel edges (10 mm apart) that are perpendicular to the 0.75 mm hole in the crystal should be polished so that a good seal can be made with the Teflon gaskets.

5) The inner bore of water-soluble crystals may be polished by rinsing the bore with a 20% solution of water in methanol. The resulting bore should be smooth and well-defined. Too much rinsing will destroy the crystal, however.

The aluminum holder is machined according to the detail in Figure 43. The ZDV flow cell is assembled using the drill bit as an alignment arbor. A lone EM Science microbore column end fitting is gently tightened against the Teflon gasket with the arbor in place. The gaskets and crystal are clamped with a pair of small wire ties, and the microbore end fitting and arbor are removed. An appropriate microbore column with an EM Science microbore and fitting is tightened against the Teflon gasket to hold the assembly together. The wire ties may be removed if desired.

The outlet tube is flanged 3/32" o.d. PTFE tubing. This tube is attached with a small compression screw to the top of the ZDV cell holder. This design avoids trapping any air bubbles due to mobile phase outgassing. If additional back pressure is necessary in the ZDV cell, simply clamping the PTFE tube to form a slight restriction is quite effective.

Alignment of the ZDV cell is straightforward once the Barnes Model 600 Beam Condenser is aligned. The ZDV cell should be filled with solvent. The spectrometer focal point should be located as close to the column outlet as possible. This is most easily determined by first adjusting the height of the ZDV cell with the provided adjustment screw until the peak-to-peak voltage of the inteferogram is minimized (maximum absorbance). Then the adjusting screw on the beam condenser is rotated so that the focus is as close to the outlet of the column without

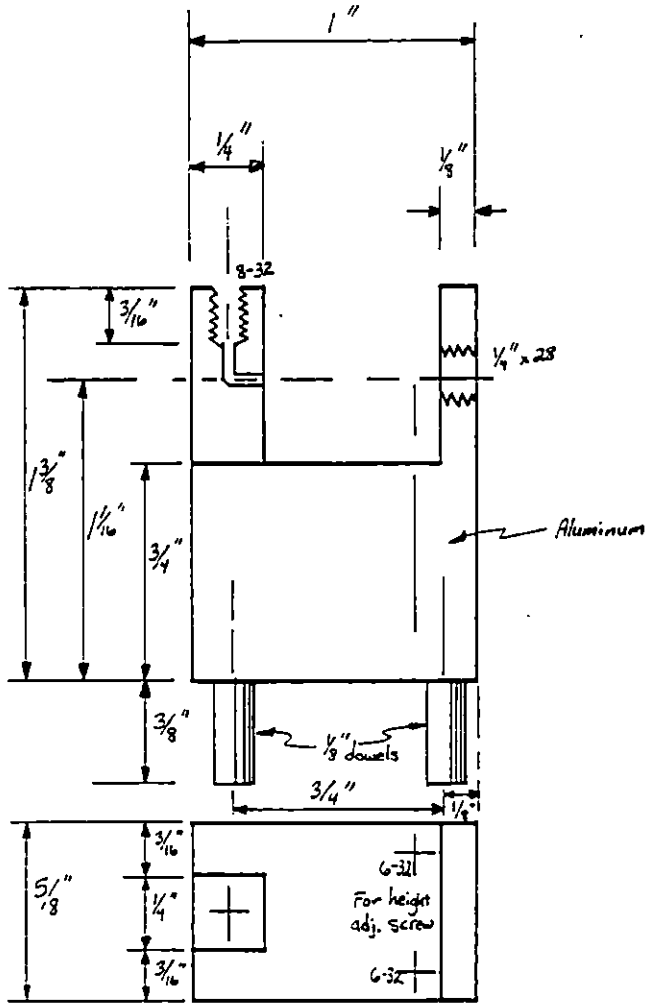

Figure 43. Detailed measurements of ZDV flow cell holder.

further minimizing the signal. At this point, the system is ready for use.

APPENDIX III

CONSTRUCTION DETAILS OF MEMBRANE SEPARATOR

The membrane separator is a borrowed design from flow injection analysis. Nord and Karlberg (62) optimized the chamber dimensions in an FIA system that used a Teflon block to hold the membrane. Comparable dimensions were incorporated here, as can be seen in Figure 44. The mating faces of the two 316 stainless steel halves are polished to a mirror-like finish. The halves are indexed with dowel pins so that the upper and lower chamber will align perfectly. The six bolts should be tightened evenly, as in tightening a gasoline engine cylinder head, to avoid leaks and warps.

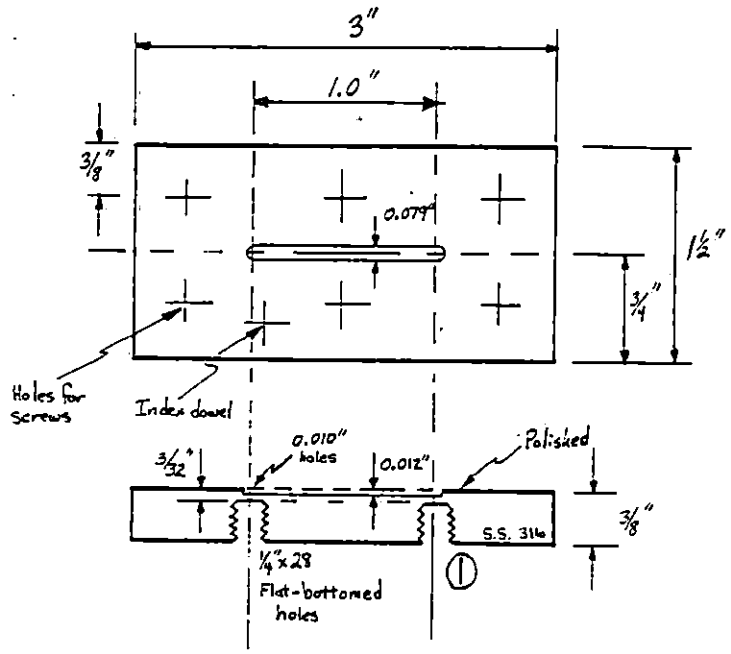

① Top piece does not have this hole.
Bottom piece shown above.

Figure 44. Detailed measurements of the membrane separator used for RP-HPLC-FTIR.

The vita has been removed from the scanned document